

UNCLASSIFIED

AD NUMBER

**AD268411**

NEW LIMITATION CHANGE

TO

**Approved for public release, distribution  
unlimited**

FROM

**Distribution authorized to U.S. Gov't.  
agencies and their contractors;  
Administrative/Operational Use; NOV 1961.  
Other requests shall be referred to Army  
Corps of Engineers, Washington, DC 20310.**

AUTHORITY

**wes d/a ltr, 11 jul 1975**

THIS PAGE IS UNCLASSIFIED

THIS REPORT HAS BEEN DELIMITED  
AND CLEARED FOR PUBLIC RELEASE  
UNDER DOD DIRECTIVE 5200.2J AND  
NO RESTRICTIONS ARE IMPOSED UPON  
ITS USE AND DISCLOSURE.

DISTRIBUTION STATEMENT A

APPROVED FOR PUBLIC RELEASE;  
DISTRIBUTION UNLIMITED.

**UNCLASSIFIED**

---

---

**AD 268 411**

*Reproduced  
by the*

**ARMED SERVICES TECHNICAL INFORMATION AGENCY  
ARLINGTON HALL STATION  
ARLINGTON 12, VIRGINIA**



---

---

**UNCLASSIFIED**

NOTICE: When government or other drawings, specifications or other data are used for any purpose other than in connection with a definitely related government procurement operation, the U. S. Government thereby incurs no responsibility, nor any obligation whatsoever; and the fact that the Government may have formulated, furnished, or in any way supplied the said drawings, specifications, or other data is not to be regarded by implication or otherwise as in any manner licensing the holder or any other person or corporation, or conveying any rights or permission to manufacture, use or sell any patented invention that may in any way be related thereto.

268411

# FLOODS RESULTING FROM SUDDENLY BREACHED DAMS CONDITIONS OF HIGH RESISTANCE

Hydraulic Model Investigation



MISCELLANEOUS PAPER NO. 2-374

2

November 1961

U. S. Army Engineer Waterways Experiment Station  
CORPS OF ENGINEERS  
Vicksburg, Mississippi

**Best  
Available  
Copy**

In this study, the effect of a floor position from which to descend, was to obtain higher reliability scores for the subjects both at and above the mean of the subjects' recorded data. The tests were conducted at the same altitude, and under similar conditions, as those described in the first test series. A single subject was added to the first floor and ceiling, giving a discontinuous sequence of several different times that used in the second series of tests. In the first test series, observations of time versus time were made for several test conditions, as indicated statistically above from the raw data. In the second series, time versus time changes were made of recording start and stop times from the three records, discharge times of discharge points were taken and time versus time through the breach and at the end stations.

Reference documents:

Report No. 1  
Report No. 2

U.S. Bureau of Mines  
Report No. 1  
Report No. 2

.....

.....

.....

.....

.....

.....

.....

.....

.....

.....

.....

.....

.....

.....

.....

.....

# FLOODS RESULTING FROM SUDDENLY BREACHED DAMS CONDITIONS OF HIGH RESISTANCE

Hydraulic Model Investigation



MISCELLANEOUS PAPER NO. 2-374

Report 2

November 1961

U. S. Army Engineer Waterways Experiment Station  
CORPS OF ENGINEERS  
Vicksburg, Mississippi

ARMY-MRC VICKSBURG, MISS.

## Preface

This is the second interim report published by the U. S. Army Engineer Waterways Experiment Station on the study, Floods Resulting from Suddenly Breached Dams; it describes briefly the test procedures and summarizes the test results obtained from breaching (to various degrees) simulated dams that were situated at mid-length of a 400-ft flume. For these tests, artificial roughness was added to the sides and bottom of the flume to achieve a high resistance to flow.

The tests reported herein were conducted during the period July to December 1958, under the general supervision of Messrs. E. P. Fortson, Jr., and F. R. Brown. Mr. G. L. Arbuthnot, Jr., assisted by Mr. J. N. Strange, was directly in charge of the study. Operation of the model, data analysis, and correlation of the test results were accomplished by the following personnel: SP-4 T. Schmidgall, SP-4 N. J. Ferrell, SP-5 R. P. Andrew, Mr. S. H. Halper, and Mr. G. A. Wilkerson. This report was prepared by SP-4 Schmidgall and Mr. Strange.

The consultative services of Drs. G. H. Keulegan, R. F. Dressler, H. Rouse, and A. T. Ippen, and Messrs. R. L. Irwin and F. B. Barkalow are gratefully acknowledged.

Colonels A. P. Rollins, Jr., CE, and Edmund H. Lang, CE, were Directors of the Waterways Experiment Station during the testing phase and during the preparation of this report. Mr. J. B. Tiffany was Technical Director.

Contents

	<u>Page</u>
Preface . . . . .	iii
Notations . . . . .	vii
Summary . . . . .	ix
The Problem . . . . .	1
Purpose and Scope of Investigation . . . . .	1
Adjustment and Calibration of Flume . . . . .	1
Revision of model dams . . . . .	1
Slope and alignment of flume . . . . .	2
Calibration of roughness . . . . .	3
Test Conditions . . . . .	3
Nonbase-flow tests . . . . .	3
Base-flow tests . . . . .	4
Changes in Methods of Recording Stage Versus Time Data . . . . .	6
Determining the Discharge-Time Hydrographs . . . . .	7
At the dam . . . . .	7
Downstream from the dam . . . . .	7
Test Results and Discussion . . . . .	10
Stage-time hydrographs, nonbase-flow tests . . . . .	10
Stage-time hydrographs, base-flow tests . . . . .	12
Discharge-time hydrographs at the dam . . . . .	13
Discharge-time hydrographs, downstream from dam . . . . .	17
Upstream negative wave . . . . .	18
Downstream positive wave (flood wave) . . . . .	19
Conclusions . . . . .	19
Improvements in test procedure . . . . .	19
Stage-time measurements . . . . .	20
Discharge-time measurements . . . . .	20
Propagation of the negative wave . . . . .	21
Propagation of the downstream flood wave . . . . .	21
Applications to Prototype Situations . . . . .	21
Recommendation . . . . .	22
List of References . . . . .	23
Tables 1-16	
Plates 1-77	

Notation

- Area of flow, sq ft
- $b_b$  Vertical distance from original water surface to bottom of breach (depth of breach), ft
- $g$  Acceleration of gravity, 32.2 ft/sec<sup>2</sup>
- $n$  Manning's coefficient of roughness, sec/ft<sup>1/3</sup>
- $Q$  Discharge at dam, cu ft/sec
- $Q_b$  Base flow discharge, cu ft/sec
- $Q_d$  Discharge at station downstream of dam, cu ft/sec
- $Q_{max}$  Maximum discharge at dam, cu ft/sec
- $t$  Time after breach, sec
- $t_a$  Arrival time of negative or positive wave, sec
- $v$  Velocity of flow (average), ft/sec
- $V_{+b}$  Volume of reservoir above breach level, cu ft
- $w_b$  Width of breach at original water surface, ft
- $w_d$  Width of dam at original water surface, ft
- $x_d$  Distance downstream from dam, ft
- $x_u$  Distance upstream from dam, ft
- $y$  Depth of water, ft
- $y_d$  Depth of water (stage) downstream from dam, ft
- $y_o$  Depth of water at the dam before breach, ft

### Summary

The purpose of this study, the second dealing with floods resulting from suddenly breached dams, was to obtain experimentally stage and discharge hydrographs both at and downstream of simulated, suddenly breached dams. It is planned to use this information, along with the results reported in the first report of this series, to publish a final report which will extend current theoretical approaches and will also assess the reliability of analytical methods which have been developed to predict the magnitude of dam-breach floods under full-scale conditions.

The experimental tests were conducted in the 400-ft-long rectangular flume already described in the first report. Aluminum strips were added to the flume floor and sides to provide a considerably rougher channel than that used in the first series of tests (Manning's "n" varied from 0.04 for a uniform depth of flow equal to 0.7 ft to 0.12 for a uniform depth of flow equal to 0.15 ft in the second series compared to  $n \approx 0.009$  in the first series). An experimental program was conducted under conditions of zero base flow, involving 8 of the 12 test conditions used in the first test series. Five test conditions, having the same breach sizes as in the first test series, were tested using the same two base flows used in the first test series.

As in the first test series, observations of stage versus time were made for each test condition at recording stations upstream from the dam, at the dam, and downstream from the dam. Velocity versus time observations were made at recording stations downstream from the dam. From these records, discharge-time hydrographs were calculated for flow through the breach and at selected stations downstream.

Several changes made in the methods of obtaining test data proved advantageous over the methods used previously in the first test series.

As a result of these tests, conclusions were reached regarding the maximum flow through a given breach, the maximum stage at the breach and at stations downstream from the dam, the propagation of the negative wave up the reservoir, and the shape, velocity, and propagation of the positive flood wave downstream for a channel of high resistance to flow. These results are discussed in the narration and are compared in many of the data plots with the results previously reported in the first report.

## FLOODS RESULTING FROM SUDDENLY BREACHED DAMS

### CONDITIONS OF HYDRO RESISTANCE

#### Hydraulic Model Investigation

##### The Problem\*

1. The flood-wave damage resulting from the deliberate breachings of the Mohne and Eder Dams during World War II demonstrates the tremendous destructive forces of a suddenly released, uncontrollable flood wave. Pertinent dimensions of these artificially created floods are given in table 16. If a method of estimating the depth, duration, and magnitude of such flood waves could be developed, it might be possible to initiate countermeasures to alleviate or obviate some of the damaging effects.

##### Purpose and Scope of Investigation\*

2. The purpose of this, the second series of model tests on floods resulting from suddenly breached dams, was to provide quantitative data for determining the change in magnitude and character of the flood wave with the roughness of the channel substantially increased above that used in the first test series where  $n \approx 0.009$ . To accomplish this purpose, stage and discharge hydrographs were determined at selected stations above, at, and below the breached model dam. From interpretation of these data, an evaluation of the flood wave as a function of time was possible.

##### Adjustment and Calibration of Flume\*

##### Revision of model dams

3. Because of the difficulty encountered in maintaining a watertight seal at the dam during the first series of tests and also the difficulty of maintaining true position of the remaining portions of the dam after breach,

---

\* For a more detailed description of the history, purpose, scope, test facilities, and procedures, please refer to Report No. 1 (reference 15).

the dam seating section was redesigned. Aluminum angles and plates were used to form a narrow grooved section across the flume bottom as well as up the flume sides. An aluminum-plate tongue, attached to the upstream face of the dam, fitted smoothly into the groove without altering the hydraulic characteristics of the breach. Fig. 1 shows the section and the model dam used in simulating a total breach (removal of entire dam, test condition 1.2). Other than for the revision just described, the test facilities during this series of tests were the same as for the first test series.<sup>15\*</sup>



Fig. 1. Flume at sta 200 (location of simulated dam) showing roughness strips in place

Slope and alignment of flume

4. Before the second test series was begun, the slope of the bottom

---

\* Raised numerals refer to similarly numbered items in the List of References.

and alignment of the sidewalls were checked. Levels were taken at 4-ft intervals along the entire length of the flume at the base of each sidewall and along the center line.

Periodic checks of the slope and alignment were continued during the testing operations to ensure that both were within the permissible tolerances established previously.<sup>15</sup>

#### Calibration of roughness

5. The first series of tests<sup>15</sup> represented the smoothest flow conditions that were easily attainable (Manning's  $n \approx 0.009$ ). For the tests reported herein, roughness was added to the bottom and sides of the flume. After experimenting with several schemes of roughening the flume, aluminum angles ( $3/4$  by  $3/4$  in.) with one leg tacked to the

flume floor and side were found to be acceptable. The other leg of the angle extended into the flow region, providing the resistance to flow. The angles were cut and shaped from 22-gage aluminum sheets and were fastened at 6-in. intervals across the bottom and 1 ft up each flume wall. Fig. 1 shows the roughness strips in place. Fig. 2 shows how the flume roughness and discharge varied with depth of flow (these curves were obtained under conditions of uniform flow).

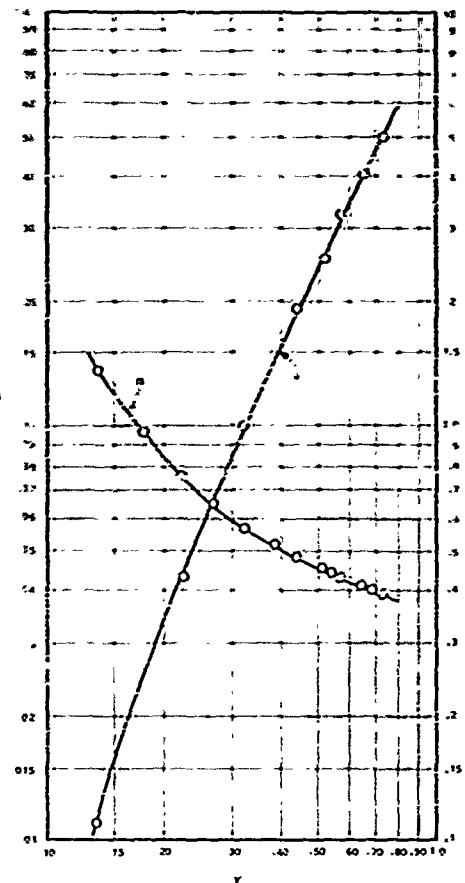


Fig. 2. Variation of Manning's  $n$  and discharge with depth of flow

#### Test Conditions

##### Nonbase-flow tests

6. A review of the nonbase-flow test results obtained in the first test series revealed that the two smallest partial width-full depth test

conditions and the two smallest partial depth-full width test conditions could be omitted without jeopardizing or substantially decreasing the value of the test results. Consequently these four test conditions were omitted from the second test series; the remaining eight conditions are described below. In the first column of the tabulation, the whole number refers to the test condition (breach pattern and orientation), which is the same as similarly numbered tests of the first series, while the decimal refers to the number of the test series and/or the roughness condition.

#### Nonbase-Flow Test Conditions

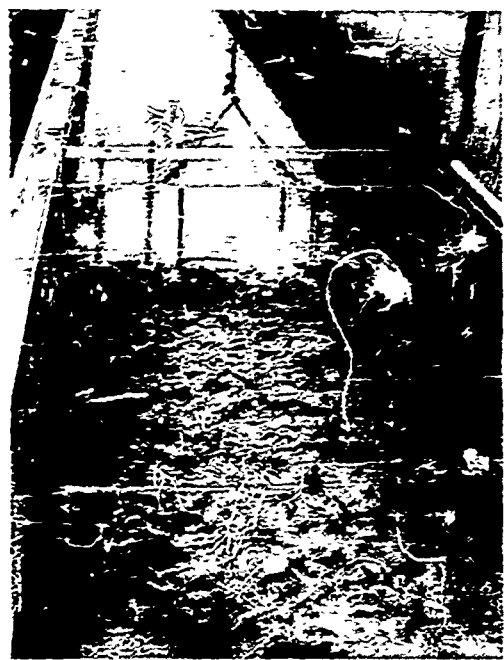
<u>Test Condition No.</u>	<u>Width of Breach, ft</u>	<u>Depth of Breach, ft</u>	$\frac{Y_b}{W_d}$	$\frac{n_o}{Y_o}$	$\frac{W_b}{W_d} \times \frac{D_b}{Y_o}$
1.2	4.00	1.00	1.00	1.00	1.00
2.2	2.40	1.00	0.60	1.00	0.60
3.2	1.20	1.00	0.30	1.00	0.30
4.2	0.60	1.00	0.15	1.00	0.15
7.2	4.00	0.60	1.00	0.60	0.60
8.2	4.00	0.30	1.00	0.30	0.30
11.2	2.40	0.60	0.60	0.60	0.36
12.2	1.20	0.30	0.30	0.30	0.09

#### Base-flow tests

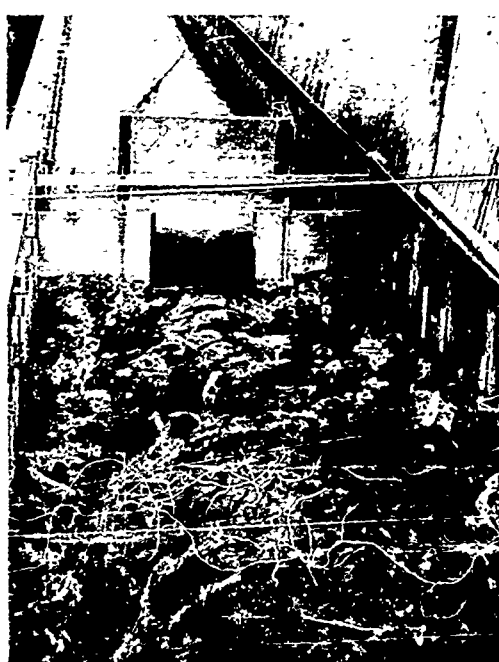
7. The base-flow test conditions including base-flow discharges for the tests described in this report were the same as those used in the first series. The added roughness, however, increased the base-flow depth from 0.1 to 0.32 ft for the 1.0-cu-ft-per-sec discharge and from 0.2 to 0.56 ft for the 3.07-cu-ft-per-sec discharge. The five base-flow test conditions were therefore designated as follows: 1.2(32), 1.2(56), 2.2(32), 2.2(56), and 3.2(32). Fig. 3 pertains to test condition 3.2(32). Fig. 3a shows the model dam in place (except for breach section). Note that space is provided beneath the dam to permit passage of the base flow. The flow conditions before breach are shown in fig. 3b, and those shortly after breach in fig. 3c.



a. Dam in place (except for  
breach section)



b. Base flow before breach



c. Flow conditions shortly  
after breach

Fig. 3. Breach pattern for test condition 3.2 (32)

Changes in Methods of Recording Stage Versus Time Data

8. The measurements of stage versus time were obtained in essentially the same manner as in the first series of tests; however, several innovations were adopted to improve and accelerate the data-recording process. First, a standard set of recording stations along the flume was adopted for all test conditions, namely: stations 40, 70, 100, 120, 140, 150, 160, 172, 180, 186, 190, 194, 196, 198, 199, 200, 225, 280, and 350. Second, the number of motion picture cameras in operation during testing was increased from four to six. With this increase, only three or four test runs were required to complete testing of a given test condition. Third, a standard designed staff gage was used for all stage measurements. These gages were mounted on individual wooden beams which rested on the sidewalls of the flume, making them easily portable from station to station. Fourth, notches were cut through the sidewalls of the flume at the

stations farthest upstream from the dam in order to place the cameras nearer the staff gages. The closer exposure permitted more accurate interpretation of the stage records. Fig. 4 shows the improved method of camera stationing. Finally, Kodachrome color film was used in the cameras to provide a sharper definition on the water surface. This reduced significantly the time involved in reading the film record from each of the recording stations.



Fig. 4. Camera, staffs, and clock arrangement for recording stage versus time

### Determining the Discharge-Time Hydrographs

#### At the dam

9. Nonbase-flow tests. The discharge-time hydrographs at the dam were computed in the same manner as for the first series of tests. The stage-time data (tables 1-8) were used to plot reservoir station-stage profiles at selected times for each test condition. Plate 1 illustrates these profiles for test condition 1.2. The area between the stage profile at time  $t$  and the profile at  $t = 0$  (before breach) when multiplied by the flume width determines the total outflow volume up until time  $t$ . Plate 2 is a plot of the total volume of outflow as a function of time for test condition 1.2. The discharge-time hydrographs were determined by numerically differentiating the volume-time curves.

10. Base-flow tests. As in the nonbase-flow tests, the stage-time data (tables 9-13) were used to plot station-stage profiles for selected times (plate 3) and then were converted to volume of outflow versus time curves as described in paragraph 9. Differentiating the volume of outflow versus time curves gave discharge versus time data. In these tests, the total volume of water flowing past the dam at any time was the sum of the base-flow volume and the reservoir-outflow volume. Plate 4 shows the corresponding reservoir-outflow volume, the base-flow volume, and the sum of these two, which is the total outflow past the dam for test condition 1.2(32).

#### Downstream from the dam

11. Discharge hydrographs for stations downstream from the dam were determined from the relation,

$$Q_d = vA$$

The cross-sectional area  $A$  was computed by multiplying the stage by the flume width. The average velocity  $v$  was obtained from the surface velocity measurements which were made at sta 225, 280, and 350 for all test conditions. They were obtained by photographing and measuring the traces made by confetti sprinkled over the water surface. The camera, grid reference, and time arrangement used to obtain



Fig. 5. Camera setup for determining the stage and discharge hydrographs at stations downstream from the dam

simultaneously all pertinent measurements necessary for determining the discharge-time hydrographs are shown in fig. 5.

12. In the first series of tests, the flume roughness was relatively low and remained essentially constant with variations in the depth of flow. Consequently, the ratio of average velocity to the surface velocity also remained constant with variations in depth of flow. The flume roughness in the second series of tests was highly sensitive to depth of flow. Hence, the relation of average velocity to surface velocity was determined under conditions of uniform flow for several depths of flow. The average

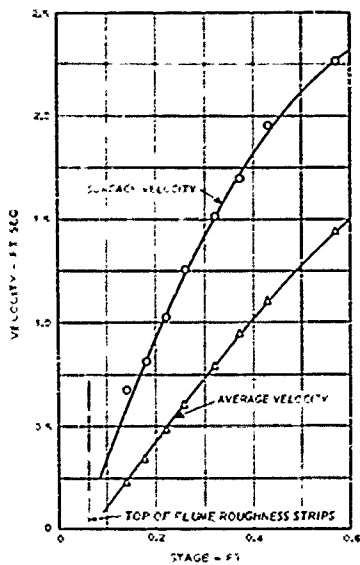


Fig. 6. Surface and average velocities as a function of stage (uniform flow conditions)

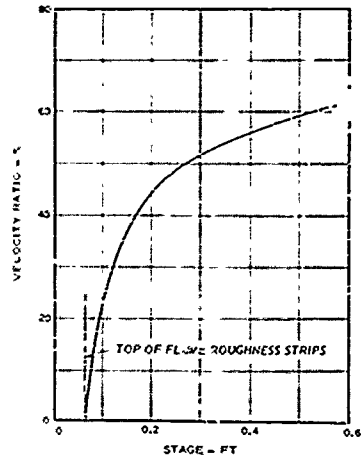


Fig. 7. Velocity correction factor as a function of stage (uniform flow conditions)

velocities were calculated from the weir discharges and flow cross sections using the relation  $v = Q/A$ . These velocities were then compared with the surface velocities for corresponding stage and discharge settings. Fig. 6 shows the two velocity-stage curves so determined, and from these two curves, a velocity ratio (average velocity/surface velocity) was determined as a function of stage.

13. Fig. 7 is a plot of the velocity ratio versus stage. To apply the correction factor, both the stage and surface velocity were determined for a given time,  $t$ . The average velocity used in computing the discharge was then determined from:

$$\text{Average velocity} = \text{surface velocity} \times \text{velocity ratio}$$

Inasmuch as the velocity ratio was established under conditions of steady flow, its use for computing discharge for actual tests (unsteady flow conditions) may involve some error. However, it is believed that the method provides a means of assessing the discharge at downstream stations to a satisfactory degree of accuracy.

Test Results and DiscussionStage-time hydrographs,  
nonbase-flow tests

14. The stage-time data for all recording stations involved in the nonbase-flow test conditions are presented in tables 1-8. Similar data for the base-flow tests are presented in tables 9-13. The stage-time hydrographs for these same tests are shown in plates 5-56. Examination of the stage-time data indicates that the minimum stage recorded for any test was 0.06 ft. This is true because this stage corresponds to the top elevation of the outstanding leg of the roughness strips; hence, for all practical purposes, flow ceased for the nonbase-flow tests at a stage of 0.06 ft. Since after each test water was impounded by the roughness strips to a depth equal to 0.06 ft, all nonbase-flow tests were performed under these wet-flume conditions in order to be consistent.

15. At the dam. The variation in the depth of flow with time at the dam (sta 200) for each breach condition tested is shown in plates 8, 12, 16, 20, 24, 28, 32, and 36. As was true in the first test series, the stage at the dam dropped immediately to approximately 0.5 ft when the entire dam was removed (plate 8). Then as time increased, the stage (at sta 200) gradually decreased. These results verify the work of St. Venant<sup>1</sup> and Schoklitsch<sup>12</sup> who concluded that the depth of flow immediately after removal of the entire dam will equal  $4/9$  to  $1/2$  of its depth before removal. From the stage-time hydrographs of the stations just upstream from the dam, a small dip and recovery of stage immediately after the breach are apparent. A satisfactory explanation for this behavior was not developed. It may be the result of vertical velocity components immediately upstream of the dam seeking and reaching equilibrium after a momentary overshoot.

16. Plates 57 and 58 illustrate the effect of the breach size on the stage at the dam for various times after dam breach. Plate 57 illustrates this effect for test conditions 1.2 through 4.2 which are partial width-full depth breaches ( $D_b/Y_o = 1.0$ ;  $W_b/W_d \leq 1.0$ ), while plate 58 shows the same effect for test conditions 1.2, 7.2, and 8.2 which are partial depth-full width breaches ( $D_b/Y_o \leq 1.0$ ;  $W_b/W_d = 1.0$ ). Both of these plates compare the results of this test series with those obtained in the first test

series and indicate that the larger the breach size, the more effective is the roughness in slowing the rate of decrease of depth at the dam as it becomes increasingly large. For small values of  $t$  (let  $t$  approach zero), there is little or no difference in stage levels at the dam between the first and second test series. This implies convincingly that for similar breach conditions the maximum stage immediately after breach is uninfluenced by roughness effects so long as free flow exists, i.e. no tailwater effect. Plates 57 and 58 may be used to estimate the stage at the dam as a function of time after breach for any size of partial width-full depth or partial depth-full width breach.

17. Downstream from the dam. For the nonbase-flow tests, the downstream hydrograph commenced with the arrival of the positive wave (flood wave) at the particular station being monitored. In general, the flood wave was steep-fronted in shape and progressively decreased in depth with time (no appreciable oscillations were noted in the flood-wave shape). For every test condition, the maximum observed depth of the flood wave decreased as it moved downstream. Also, the time interval between the flood wave's arrival and its peak stage continually increased with distance downstream from the dam. Fig. 8 is a dimensionless plot of the peak stages recorded at sta 350 as a function of breach size for both the first and second series of tests. The data fall on three distinct curves which represent the three breach regimes, viz. partial depth-full width, partial width-full depth, and partial depth-partial width.

18. Although the data for either test series are not altogether conclusive, there exists a rather definite trend for the flood wave to reach a degree of stability by the time it has

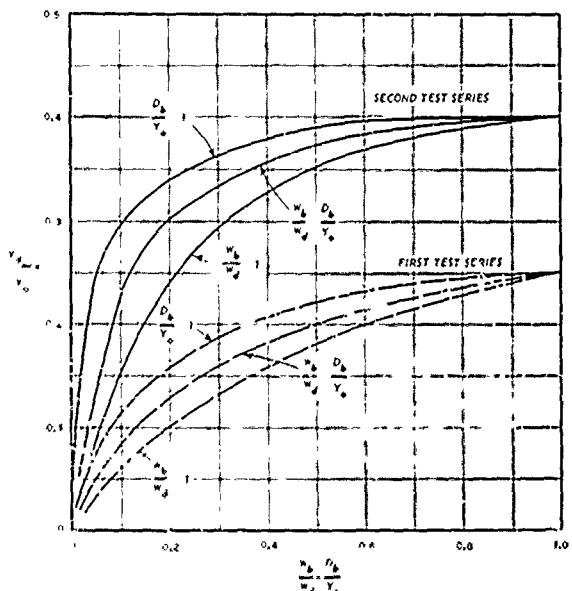


Fig. 8. Dimensionless plot of maximum downstream stage (sta 350) as a function of breach size (nonbase-flow tests) and shape

traveled a distance downstream equivalent to approximately  $100 Y_0$ . The information shown in fig. 8 can therefore be used to estimate the height of the maximum flood wave that might be expected at stations farther downstream ( $X_d \geq 350$ ). The figure also establishes approximate limits for the maximum depth of the flood wave for riverbeds whose slopes approximate 0.005. When roughness is very low (channel is smooth and straight), the maximum depth of the flood wave at considerable distances downstream will approximate  $0.25 Y_0$ ; when the channel exhibits considerable roughness, the maximum stage will approximate  $0.4 Y_0$ . These observations apply when the entire dam is removed instantaneously. Should the downstream channel diverge yet remain essentially straight, the flood wave would likely be characterized by a more gradual rise and would have a lesser maximum depth than predicted. Conversely, should the channel converge and/or meander, the flood wave would likely have a steeper front and a greater maximum depth than might be predicted from the above results.

19 Comparison of the nonbase-flow stage-time hydrographs obtained in these tests for stations downstream of the dam with those obtained in the first series shows that: (a) the flood wave traveled downstream under conditions of supercritical flow in the first series and at subcritical flow in the second, (b) for the same breach size and at the same downstream station, the peak stages were always greater in the second series than in the first, and (c) for the same breach size and at the same downstream station, the length of time between the flood-wave arrival and the peak stage was greater in the second test series than in the first.

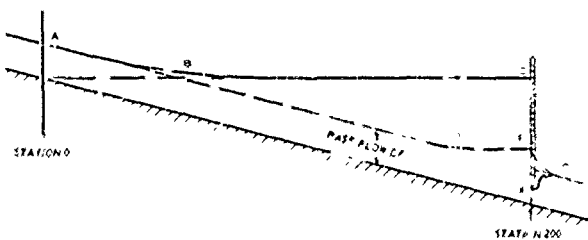


Fig. 9. Schematic diagram of water-surface profiles, before and after breach, for base-flow test conditions

#### Stage-time hydrographs, base-flow tests

20. The delineation of various base-flow terminal stages is illustrated in fig. 9. The water-surface profile for all test conditions prior to actual breaching is defined by ABCFG. Likewise, the final water-surface profile for full breaches is defined by

AG and for partial breaches by ADEFG. The discharges used in the formation of the base flows were the same for both test series. The tabulation below presents the discharges used and the respective base flow depths for each test series:

Base Flow Discharge, cu ft/sec	Base Flow Depth, ft	
	First Series	Second Series
1.00	0.1	0.32
3.07	0.2	0.56

21. At the dam. The influence of the base flows on the stage-time histories at the dam was not appreciable, as shown in plates 39, 43, 47, 51, and 55. Generally the stage immediately after the breach was about the same as in the nonbase-flow tests. At later times, however, the stage at the dam was, as might be expected, greater than in the nonbase-flow tests.

22. Downstream from the dam. Stage-time hydrographs for the base flows downstream of the dam are shown in plates 40, 44, 48, 52, and 56. The shape of the flood-wave front was similar to the shapes noted during the nonbase-flow tests, i.e. a rather abrupt rise to the peak stage followed by a gradual decrease in the depth of flow. With increase in downstream distance from the dam, stages decreased and the time interval between the flood-wave arrival and the peak stage increased for every test condition. Also, in every case, the flood-wave duration was longer in the second test series than in the first.

Fig. 10 shows, by dimensionless plot, the maximum downstream stages observed at sta 350 for the base-flow test conditions, and compares the maximum stages observed at sta 350 for both test series.

#### Discharge-time hydrographs at the dam

23. Nonbase-flow tests.  
The discharge-time hydrographs

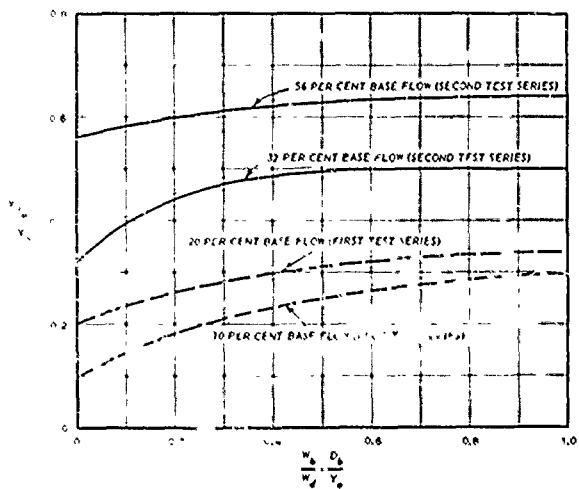


Fig. 10. Dimensionless plot of maximum downstream stage (sta 350) as a function of breach size (base-flow tests)

at the dam for the nonbase-flow test conditions are shown in plates 59 and 60. The maximum discharges in all tests occurred at the instant of dam release. Comparison of these maximum discharges shows the effect of breach size on the maximum discharge. The following tabulation presents a comparison of the experimentally obtained peak discharges for both the first and second test series with the values obtained using Schoklitsch's equation,<sup>12</sup>

$$Q_{\max} = \frac{8}{27} W_d \sqrt{g} Y_o^{3/2}$$

The development of this equation into a form applicable for the type breaches studied herein is given in Report 1.

#### Comparison of Maximum Discharges at the Dam

(Nonbase-Flow Tests)

Test Condition	Maximum Discharge, cu ft/sec		
	First Test Series	Second Test Series	Schoklitsch
1	6.50	6.41	6.72
2	4.54	4.11	4.57
3	2.67	2.47	2.72
4	1.70	1.54	1.62
7	3.57	3.42	3.70
8	1.42	1.43	1.66
11	2.52	2.53	2.52
12	0.56	0.63	0.67

The average deviation of the first test series data from the data computed using the Schoklitsch equation is about 4.7 per cent; the deviation of the data of the second series from the Schoklitsch data is about 5.5 per cent. These variances are small and indicate that roughness has little or no effect on the magnitude of the peak discharge which seems to be almost entirely a function of breach size and shape.

24. Fig. 11 is a plot of the maximum discharge at the dam as a function of breach size for the three breach regimes investigated. From the curves presented, the approximate maximum discharge can be determined for a variety of breach patterns other than for the specific patterns tested. Since the values of  $Q_{\max}$  for comparable test conditions are essentially equal for the two test series, there is very little difference between this curve and its equivalent in the first report.<sup>15</sup>

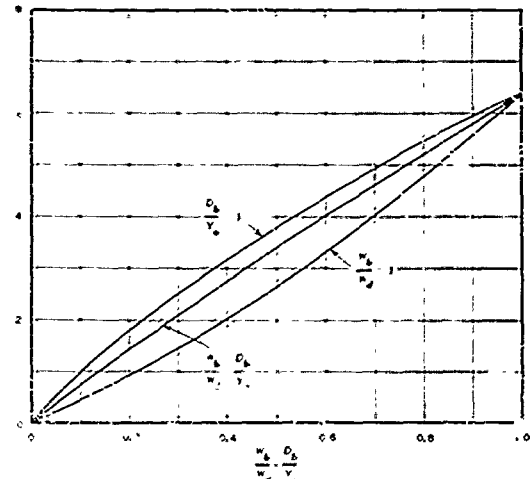


Fig. 11. Maximum discharge at the dam as a function of breach size and shape (nonbase-flow tests)

25. A more generally applicable plot, which relates in dimensionless form the maximum discharge at the dam to the breach size, is presented in fig. 12. The tabulation in paragraph 23 presents the data from which the plot was made. The curve shown agrees with the data presented in the first report and therefore has the same empirical equation, namely:

$$Q_{\max} = 0.29 \sqrt{g} W_b D_b^{3/2} \left( \frac{W_d}{W_b} \cdot \frac{Y_o}{D_b} \right)^{0.28}$$

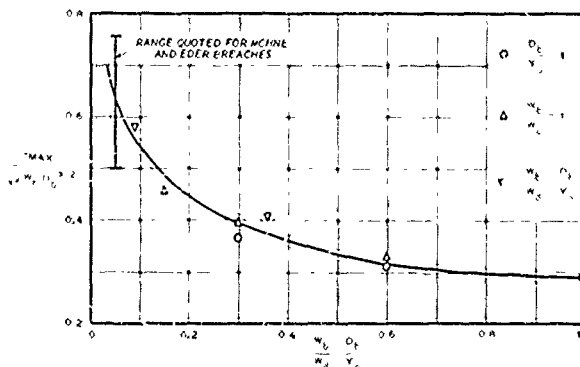


Fig. 12. Dimensionless plot of the maximum discharge at the dam as a function of breach size (nonbase-flow tests)

From this relation, the value of the maximum discharge issuing through a given breach can be computed provided

$$1.0 \leq \left( \frac{W_d}{W_b} \cdot \frac{Y_o}{D_b} \right) \leq 20$$

The accuracy of the prediction will improve as the term

$$\left( \frac{W_d}{W_b} \cdot \frac{Y_o}{D_b} \right)$$
 approaches 1.0,

since less experimental scatter was observed near this value.

26. Plates 61 and 62 show in dimensionless form the relation of the discharge-time hydrographs noted at the dam for each test series and the various test conditions. The plots reveal that the discharge at any given time after breach is highly dependent on the elapsed time after breach and the total volume in storage that lies above the breach level ( $V_{+b} = 35 \pm .56$  cu ft). In every case the curves of the second series initially lie below those of the first series. Eventually, the curves cross and the second series curves lie above the first series results. Since the total volume of outflow is roughly equivalent in each test series for comparable test conditions, when allowances are made for the storage volume lost due to water being impounded by the roughness strips, the areas beneath the curves for comparable test conditions are approximately equal. Integration of these curves serves as a check on the validity of the plotted discharge-time hydrographs.

27. Base-flow tests. The discharge-time hydrographs at the dam for each test condition are given in plate 63. The following tabulation compares the maximum discharges at the dam for the various base-flow test conditions.

#### Comparison of Maximum Discharges at the Dam

(Base-Flow Tests)

<u>First Test Series</u>		<u>Second Test Series</u>	
<u>Test Condition</u>	<u>Maximum Discharge*</u> <u>cu ft/sec</u>	<u>Test Condition</u>	<u>Maximum Discharge</u> <u>cu ft/sec</u>
1.1(10)	6.7	1.2(32)	5.54
1.1(20)	7.8	1.2(56)	6.77
2.1(10)	5.0	2.2(32)	4.64
2.1(20)	6.5	2.2(56)	5.85
3.1(10)	3.4	3.2(32)	3.27

\* Obtained from plate 89, Report 1.

Fig. 13 presents a plot of the maximum discharge at the dam as a function of the breach size and compares these results with those of the first test series. The curves may be used to estimate the maximum discharge that would result from a variety of breaches having the base flows indicated. Also, comparison of the curves demonstrates that greater maximum discharges occurred in the first test series.

28. In spite of the added roughness to the flume bottom and sides, the time interval during which the discharge decreased from the observed maximum to the base-flow discharge is not greatly different from the time histories observed in the first test series. The dimensionless plots in plate 64 show a greater apparent difference; however, this difference is accentuated by the fact that the  $V_{pb}$  term is decreased from a storage volume of 400 cu ft in the first test series to approximately 350 cu ft in the second series. Insufficient data exist upon which to base a more elaborate interpretation of the base-flow results.

#### Discharge-time hydrographs, downstream from dam

29. Nonbase-flow tests. Plates 65-68 present both the velocity-time and the discharge-time hydrographs at the three downstream stations where observations were obtained during the nonbase-flow tests. Table 14 gives the velocity-time data for these tests.

30. The maximum discharge attained by the flood wave decreased from its peak at sta 200 to a lesser value at sta 350 in each of the various tests. The amount of this decrease was dependent upon the breach size; between the breach section (sta 200) and sta 350, the maximum discharge of the full-breach test decreased about 75 per cent. For the smallest breach

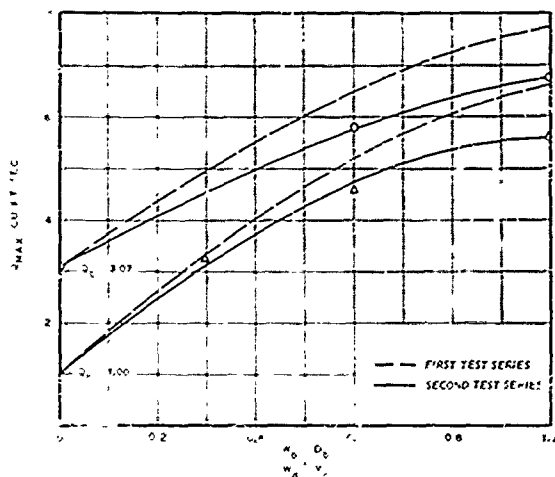


Fig. 13. Maximum discharge at the dam as a function of breach size (base-flow tests)

(test condition 12.2), the decrease in maximum discharge over the same range was approximately 30 per cent. By graphically integrating the discharge-time hydrographs over the time range common to each test condition, the volume of flow past each of the observed downstream stations was obtained. Allowing for the additional amount of water between the dam and the observed station, these volumes were compared with the total outflow through the given breach. Using this technique for computing total flow, the average deviation of the downstream volumes when compared to the breach outflow was 5.7 per cent (the maximum was 12.8 per cent). Considering the scope of the test conditions, it is felt that the relatively small errors that accrue justify the use of the procedures described in paragraphs 11-13.

31. Base-flow tests. Plates 69-71 present both the velocity-time and discharge-time hydrographs at the three downstream stations observed for the various base-flow tests. Table 15 gives the velocity-time data for these tests.

32. The velocity-time hydrographs for the downstream stations under base-flow conditions are characterized by an increase in the velocity above those common to the nonbase-flow tests. However, the increase was of short duration, particularly for the 56 per cent (0.56-ft) base flows.

Upstream negative wave

33. Nonbase-flow tests. The average arrival time of the negative wave at various stations upstream from the dam for all the nonbase-flow test conditions is shown in plate 72. The arrival times associated with the first test series as well as the theoretical arrival time as given by the equation  $t_a = -7.6 [(1 - 0.005 X_u)^{1/2} - 1]$  are included also for comparison. The development of this theoretical arrival-time equation is given in paragraph 54 of the first report.<sup>15</sup> The average of the arrival times from the second test series does not agree with the theoretical values as closely as did those of the first test series. Some variance is to be expected as the wave travels into the shallower depths where it begins to be affected by the roughness along the bottom; however, the agreement is close enough to conclude that the flume roughness has little effect on the arrival time of the negative wave other than at

the very upper end (shallow reaches) of the reservoir.

34. Base-flow tests. The negative-wave arrival times at various upstream stations from the dam for the base-flow test conditions are shown in plate 73. As might be expected intuitively, this plate shows that the irregular water surface caused by the base flow through the reservoir, with its attendant downstream velocities, has a pronounced effect on the propagation rate of the negative wave. The plate also shows that the variations in breach size have little effect on the propagation of the negative wave when the flume roughness and the base-flow discharge remain constant.

#### Downstream positive wave (flood wave)

35. Nonbase-flow tests. Plates 74-76 show plots of the flood-wave arrival times from time of breach at three downstream stations. Plate 74 presents the data obtained from all the full depth-partial width breach tests, plate 75 the full width-partial depth test results, and plate 76 the partial width-partial depth test results. The positive-wave arrival times for comparable test conditions from the first test series are also shown in each of these plates. Considering all the nonbase-flow tests in both test series, the speed of propagation of the positive wave varies directly with the initial discharge through the breach section and inversely with the roughness of the flume. In every test condition, the velocity of the positive wave gradually decreased as it moved downstream.

36. Base-flow tests. Plate 77 is a plot of the arrival time of the positive wave at three downstream stations from the dam for the base-flow test conditions. The downstream propagation speed was affected directly by the initial breach discharges and the velocity of the base flow (which was itself affected inversely by the flume roughness). Similar to the nonbase-flow test conditions, the positive-wave velocities of the base-flow tests gradually decreased as the wave progressed downstream.

#### Conclusions

##### Improvements in test procedure

37. Five major changes, listed in paragraph 8, were incorporated in the methods of obtaining test data in the second series of tests. All of

these changes were helpful in improving the efficiency of carrying out the model tests.

#### Stage-time measurements

38. At the dam. As in the first series of tests, the stage at the dam for the full-breach test dropped immediately to essentially one-half the prebreach depth, which agrees with the findings of St. Venant<sup>1</sup> and Schoklitsch.<sup>12</sup> Plates 57 and 58 compare the effects of breach width and depth on the outflow depth for the two test series. Both of these plates show that the larger the breach size, the greater is the effect of flume roughness on the maximum stage observed at the dam.

39. The influence of the base flows on the stage-time histories at the dam was not significant, since the stage immediately after the breach was about the same as in the nonbase-flow tests. At later times, however, the stages at the dam were, as might be expected, greater than those in the nonbase-flow tests.

40. Downstream from the dam. The maximum observed depth at the recording station farthest downstream from the dam was considerably greater in the second test series than in the first for comparable test conditions. This increase in depth varied from 60 per cent when the entire dam was removed to as much as 150 per cent for the smaller breach conditions.

41. From these results one may conclude that when an entire dam is removed instantaneously, the maximum depth likely to be encountered at large distances downstream from the dam ( $X_d > 350$ ) will be about  $Y_o/2$  for rough channels and about  $Y_o/4$  for smooth channels. These observations apply only to those cases wherein the channel slope approximates 0.005 and where the channel is relatively straight and of uniform width.

42. The base-flow tests revealed a substantial increase in the maximum stage as compared to those in the first test series. At station 50, maximum stages two to three times as great were observed (see Fig. 10). At later times in the hydrograph, this same trend is apparent. The greater depths of flow are attributed to the substantial increase in roughness, the effect of which becomes increasingly pronounced as the stage decreases.

#### Discharge-time measurements

43. At the dam. Results of the second test series show that

roughness had little or no effect on the maximum discharge at the dam, which seems to be entirely a function of the breach size and shape. Hence, the empirical equation

$$Q_{\max} = 0.29 \sqrt{g} w_b D_b^{3/2} \left( \frac{w_d}{w_b} \cdot \frac{Y_o}{D_b} \right)^{0.28}$$

developed in the first test series is equally applicable to the second series. The decay of discharge with time for nonbase-flow conditions is obtainable from plates 61 and 62. Similarly, the variation of discharge with time for the base-flow tests may be obtained from plate 64.

44. Downstream from the dam. In all of the nonbase-flow tests of the second test series, the maximum discharge decreased in magnitude with increasing distance downstream from the dam. This trend, though not conclusive, was implied in the base-flow tests also. In each case, the amount of the decrease was dependent on the breach size.

#### Propagation of the negative wave

45. A comparison of the negative-wave arrival times for all of the nonbase-flow test conditions of the first and second test series indicates that the negative-wave propagation speed is independent of breach size or reservoir roughness except near the upper end of the reservoir. A similar comparison of the base-flow test results indicates that the negative-wave propagation speed is definitely reduced by the base-flow velocity through the reservoir.

#### Propagation of the downstream flood wave

46. Considering all the test conditions of both series of tests, no average propagation speed could be deduced for the positive wave because the wave velocity varied directly with the initial discharge through the breach section and inversely with the flume roughness. For every test condition the front velocity of the flood wave gradually decreased as the wave progressed downstream.

#### Applications to Prototype Situations

47. Extrapolation of these results to prototype situations is limited to those cases that are geometrically similar to the conditions

tested in the model. Significant departure from this limitation may yield completely erroneous results. It is believed, however, that these results may be applied to prototype situations where the scale ratio (prototype to model) is less than or equal to 100. Qualitative estimates of flood parameters can be computed for scale ratios as high as perhaps 200. Procedures for extrapolating these results (as well as those contained in the first test series) will be the subject of a final report. In the final report, studies will be made to assess the possibility of interpreting these data using distorted scaling procedures. With this tool, it will then be possible to evaluate floodflows from reservoirs of different shapes and outflow channels of different slopes.

#### Recommendation

48. During the course of this study, "Floods Resulting from Suddenly Breached Dams," several conferences were held between Waterways Experiment Station personnel and outside consultants to evaluate the progress being made and to formulate plans for a logical course of action in the future. At this point it is not known conclusively whether additional tests are necessary to the analysis of the empirical data along the lines suggested by analytical and theoretical studies that have been conducted or contracted for by the Army Map Service, the agency assigned the responsibility of developing means of evaluating quantitatively floods that are released by the sudden breaching of any given dam. It is recommended that the results obtained during the first two test series be rigorously analyzed and compared with theoretical solutions of the dam-breach problem, and that recommendations for additional tests, if needed, come from the study being made by Army Map Service.

List of References

1. Barré de Saint Venant, A., "Théorie du mouvement non permanent des eaux." Comptes Rendus des Séances de l'Académie des Sciences, vol 73 (1871), pp 147-154, 237-240.
2. Dressler, Robert F., "Hydraulic resistance effect upon the dam-break functions." Journal of Research of the National Bureau of Standards, vol 49 (July-December 1952), pp 217-225.
3. , Comparison of Theories and Experiments for the Hydraulic Dam-Break Wave. Publication No. 38, de l'Association Internationale d'Hydrologic (Assemblée générale de Rome, tome II).
4. Frank, Joseph, "Betrachtungen über den Ausfluss beim Bruch von Stauwänden (Consideration on Discharge at Breaks of Dams)." Schweizerische Bauzeitung, vol 69, No. 29 (21 July 1951), pp 401-406.
5. King, Horace Williams, Handbook of Hydraulics. Revised edition, McGraw-Hill Book Company, Inc., New York, N. Y., 1954.
6. Kirschmer, Otto, "Zerstörung und Schutz von Talsperren und Dämmen (Destruction and Protection of Dams and Levees)." Schweizerische Bauzeitung, vol 67, No. 20 (14 May 1949), pp 277-281.
7. Levin, L., "Evolution of waves created by the bursting of large dams." Transaction of the Second Meeting of the Yugoslav National Committee on Large Dams (September 1952).
8. Lewin, Joseph D., Report on Study Trip in Europe. November 1948.
9. Quast, Hermann, Zerstörung und Wiederaufbau der Möhne - und Eder - Talsperre. Wasser und Energie Wirtschaft - v.41.
10. Ritter, A., Die Fortpflanzung der Wasser-Wellen. z. Ver deut. Ing. 36, 1892.
11. Rouse, Hunter, Engineering Hydraulics. John Wiley and Sons, Inc., New York, N. Y., 1950.
12. Schoklitsch, Armin, Über Dammbuchwellen. Sitzber. Akad. Wiss. Wien. 126, 1917.
13. U. S. Army Engineer District, Washington, Flow Through a Breached Dam (U) Military Hydrology Manual No. H-2(X) Supplement, June 1955. CONFIDENTIAL report.
14. , Flow Through a Breached Dam. Military Hydrology Pulletin 9, June 1957.

15. U. S. Army Engineer Waterways Experiment Station, CE, Floods Resulting from Suddenly Breached Dams; Conditions of Minimum Resistance. Miscellaneous Paper No. 2-374, Rept 1, Vicksburg, Mississippi, February 1960.























Table 12  
Results of Stage-Time Measurements, Test Condition 2.2(56)  
Time, seconds      Stage, feet\*

Time	Upstream Stations												Dkm	Downstream Stations					
	70	100	120	140	150	160	170	180	190	194	198	204		220	240	350			
0	0.59	0.64	0.68	0.72	0.73	0.84	0.85	0.91	0.94	0.93	0.97	0.97	0.99	0.99	1.01	0.56	0.56	0.56	
0.5										0.97	0.97	0.97	0.91	0.83	0.67				
1.0										0.94	0.90	0.82	0.75	0.69					
1.5										0.92	0.84	0.83	0.76	0.72	0.75				
2.0										0.93	0.86	0.77	0.77	0.79	0.77				
2.5										0.86	0.81	0.73	0.73	0.78	0.73				
3										0.91	0.86	0.79	0.71	0.78	0.76	0.76			
4										0.86	0.81	0.73	0.73	0.78	0.74	0.66			
5										0.83	0.82	0.79	0.77	0.77	0.77	0.74			
6										0.82	0.82	0.79	0.77	0.77	0.78	0.74			
7										0.82	0.82	0.79	0.77	0.77	0.78	0.74			
8										0.81	0.80	0.76	0.77	0.76	0.76	0.74			
9										0.82	0.78	0.76	0.76	0.76	0.76	0.74			
10										0.73	0.80	0.75	0.75	0.76	0.77	0.73	0.67		
11										0.77	-----	-----	-----	-----	-----	-----			
12										0.76	0.73	0.73	0.73	0.73	0.73	0.73			
13										0.75	-----	-----	-----	-----	-----	-----			
14										0.73	-----	-----	-----	-----	-----	0.56			
15										0.75	0.73	0.71	0.74	0.75	0.75	0.72	0.71	0.61	
16										0.73	0.71	0.71	0.71	0.71	0.71	0.71	0.71	0.61	
17										0.72	0.71	0.71	0.71	0.71	0.71	0.71	0.71	0.61	
18										0.70	-----	-----	-----	-----	-----	-----	-----		
20										0.69	0.69	0.70	0.71	0.72	0.73	0.74	0.72	0.65	
22										0.68	-----	-----	-----	-----	-----	-----	0.70	0.65	0.57
25										0.66	0.66	0.66	0.69	-----	-----	-----	0.70	0.65	0.59
27										0.64	-----	-----	-----	-----	-----	-----	-----	0.66	0.59
28										0.64	-----	-----	-----	-----	-----	-----	-----	0.66	0.59
30										0.64	0.65	0.65	0.67	0.68	0.71	0.71	0.69	0.65	0.59
35										0.62	0.63	-----	-----	-----	-----	-----	-----	0.60	0.59
40										0.61	0.62	0.63	0.63	0.65	0.67	0.69	0.70	0.67	0.61
50										0.59	0.60	0.60	0.61	0.64	0.65	0.67	0.63	0.67	0.62
60										0.59	0.60	0.61	0.61	0.63	0.64	0.65	0.66	0.65	0.64
70										0.57	0.59	0.60	0.60	0.62	0.63	0.65	0.61	0.64	0.63
75										0.53	-----	-----	-----	0.63	-----	-----	-----	-----	-----
90										0.58	0.59	0.59	0.61	0.60	0.63	0.64	0.63	0.62	0.64
90										0.56	0.58	0.59	0.59	0.60	0.61	0.63	0.62	0.62	0.63
105										0.57	-----	0.61	-----	-----	0.62	-----	0.60	-----	0.63
120										0.57	0.57	0.58	0.59	0.61	0.61	0.61	0.60	0.60	0.61
150										0.56	0.56	0.57	0.58	0.58	0.60	0.61	0.60	0.60	0.59
180										0.56	0.57	0.57	0.58	0.59	0.60	0.59	0.60	0.59	0.57
210										0.57	0.56	0.57	0.59	0.59	0.60	0.59	0.57	0.57	0.57
240										0.56	0.59	0.59	0.59	0.59	0.60	0.59	0.56	0.56	0.56

**Table 13**  
**Results of Stage-Time Measurements, Test Condition 3.2(32)**

Time	Upstream Stations										Downstream Stations					
	70	100	120	140	150	16	172	180	190	194	198	202	Dam	224	240	350
0	0.40	0.52	0.61	0.71	0.76	0.81	0.86	0	0.93	0.95	0.97	0.98	0.99	1.00	1.00	0.32
0.5									0.93	0.95	0.97	---	0.94	0.95	0.94	
1.0									0.93	0.95	0.96	0.90	0.91	0.94	0.95	
1.5									0.93	0.95	0.90	0.84	0.85	0.85	0.85	
2.0									0.93	0.92	0.84	0.84	0.85	0.85	0.85	
2.5									---	0.87	0.82	0.85	0.85	---	---	
3.0									0.90	0.89	0.84	0.84	0.85	0.84	0.85	
3.5									---	0.85	0.82	---	---	---	---	
4									0.86	0.88	0.82	0.82	0.83	0.84	0.85	
5									0.85	0.84	0.80	0.81	0.81	0.84	0.83	0.32
6									0.79	---	0.81	---	0.84	0.84	0.83	
7							0.31	0.79	0.77	0.80	---	0.81	---	---	0.43	
8							0.20	---	---	---	---	---	---	---	---	
9							0.76	---	0.73	---	---	---	---	---	---	
10							0.75	0.75	---	0.77	0.79	0.80	0.81	0.82	0.83	0.47
11							---	0.72	---	---	---	---	---	---	---	
12						0.71	0.71	0.70	---	---	---	---	---	---	---	
14						0.67	0.69	---	---	---	---	---	---	---	---	
15						0.66	---	0.71	0.75	0.77	---	0.80	0.81	0.82	0.81	0.49
16						0.61	---	0.65	---	---	---	0.76	0.77	0.77	0.77	
18						0.58	0.60	0.63	---	0.70	0.73	0.76	0.73	0.79	0.80	0.80
20						0.52	0.52	0.59	0.61	0.65	---	---	---	---	0.51	0.35
22						0.50	0.52	0.59	0.61	0.65	---	---	---	---	0.52	0.39
25						0.40	0.47	0.50	0.57	0.60	0.64	0.67	0.72	0.73	0.75	0.76
30						0.37	0.43	0.48	0.55	0.57	0.60	0.64	0.63	0.70	0.71	0.73
37						0.37	0.43	0.48	0.55	0.57	0.60	0.64	0.63	0.70	0.71	0.73
40						0.34	0.40	0.43	0.49	0.52	0.55	0.58	0.61	0.63	0.65	0.67
45						0.35	0.41	0.46	0.52	0.55	0.57	0.60	0.65	0.68	0.69	0.72
50						0.34	0.40	0.43	0.49	0.52	0.55	0.58	0.61	0.63	0.65	0.68
60						0.34	0.38	0.39	0.42	0.44	0.48	0.50	0.50	0.51	0.52	0.51
70						0.34	0.38	0.39	0.42	0.44	0.48	0.50	0.50	0.51	0.52	0.41
75						0.33	0.35	0.36	0.39	0.40	0.43	0.45	0.46	0.46	0.48	0.45
80						0.33	0.35	0.36	0.39	0.40	0.43	0.42	0.43	0.44	0.44	0.42
90						0.33	0.35	0.36	0.38	0.40	0.40	0.42	0.43	0.44	0.44	0.42
105						0.33	0.35	0.36	0.38	0.39	0.42	0.40	0.41	0.42	0.42	0.40
120						0.32	0.34	0.35	0.38	0.40	0.43	0.45	0.46	0.47	0.47	0.47
150						0.33	0.35	0.36	0.39	0.40	0.43	0.45	0.46	0.47	0.48	0.45
180						0.33	0.35	0.36	0.38	0.38	0.40	0.42	0.43	0.44	0.44	0.42
210						0.32	0.33	0.34	0.35	0.35	0.37	0.38	0.40	0.41	0.42	0.40
240						0.33	0.33	0.34	0.35	0.37	0.38	0.40	0.39	0.40	0.40	0.37
270						0.34	0.33	0.33	0.34	0.35	0.37	0.39	0.39	0.39	0.38	0.36
300						0.33	0.33	0.33	0.34	0.36	0.37	0.39	0.39	0.39	0.38	0.34
360						0.32	0.33	0.34	0.36	0.37	0.38	0.39	0.39	0.37	0.34	0.34
360						0.32	0.33	0.34	0.36	0.37	0.38	0.39	0.39	0.37	0.33	0.33



Table 15  
Downstream Average Velocity\* Data  
 Buoy Flow Test Conditions

Time sec	Test Condi- tion 1.2(32)			Test Condi- tion 1.2(56)			Test Condi- tion 2.2(32)			Test Condi- tion 2.2(56)			Test Condi- tion 3.2(32)		
	Station			Station			Station			Station			Station		
	225	280	350	225	280	350	225	280	350	225	280	350	225	280	350
0	0.78	0.78	0.78	1.37	1.37	1.37	0.78	0.78	0.78	1.37	1.37	1.37	0.78	0.78	0.78
5	1.80	0.78		1.90			0.96			1.45			0.78		
7	1.90	0.78		1.90			1.30			1.45			1.30		
10	1.95	0.78		1.90			1.50			1.50			1.40		
12	1.85	0.78		1.80	1.37		1.55			1.50	1.37		1.45		
15	1.70	0.81		1.75	1.65		1.60	0.78		1.50	1.45		1.40		
17	1.65	1.15		---	1.70		1.60	0.82		---	1.45		1.40	0.78	
20	1.60	1.40		1.70	1.70		1.60	1.10		1.50	1.50		1.35	0.92	
22	---	1.45		---	---		---	1.25		---	---		---	1.05	
25	1.45	1.50		1.60	1.70	1.37	1.50	1.30		1.50	1.50	1.37	1.30	1.20	
27	---	1.50		---	---	1.40	---	1.40		---	---	1.40	---	1.20	
30	1.35	1.50		1.55	1.60	1.50	1.45	1.40		1.50	1.50	1.50	1.25	1.25	
32	---	0.78		---	1.50		---	0.78		---	1.50		---	---	
35	1.30	1.40	0.85	1.50	1.60	1.50	1.35	1.40	0.90	1.50	1.50	1.50	1.20	1.30	
37	---	0.91		---	---		---	0.97		---	---		---	0.78	
40	1.20	1.35	0.98	1.50	1.50	1.50	1.25	1.40	1.05	1.50	1.50	1.55	1.20	1.30	0.81
42	---	1.00		---	---		---	1.10		---	---		---	0.84	
45	1.15	1.35	1.05	1.50	1.50	1.50	1.20	1.30	1.15	1.50	1.50	1.60	1.15	1.30	0.89
47	---	1.05		---	---		---	1.15		---	---		---	---	
50	1.15	1.35	1.10	1.40	1.45	1.50	1.10	1.20	1.20	1.50	1.50	1.60	1.10	1.20	0.96
55	---	1.15		---	---		---	---		---	---		---	---	
60	1.05	1.25	1.15	1.40	1.45	1.50	1.00	1.15	1.25	1.45	1.50	1.55	1.10	1.15	1.05
70	1.00	1.25	1.15	1.40	1.40	1.50	0.94	1.10	1.25	1.45	1.50	1.50	1.05	1.15	1.15
80	1.00	1.15	1.15	1.40	1.40	1.50	0.90	1.10	1.20	1.45	1.50	1.50	1.05	1.10	1.15
90	0.96	1.10	1.15	1.40	1.40	1.50	0.87	1.05	1.20	1.45	1.50	1.50	1.00	1.15	1.15
100	0.93	1.05	1.10	---	1.50	---	---	---	---	---	---	---	---	---	
105	---	---	---	---	---	0.84	0.99	1.10	1.45	1.45	1.50	0.99	1.05	1.10	
110	0.88	1.00	1.10	1.40	1.40	1.45	---	---	---	---	---	---	---	---	
120	0.86	0.97	1.05	1.40	1.40	1.45	0.82	0.96	1.10	1.45	1.45	1.45	0.91	0.99	1.05
130	0.84	0.94	1.00	---	---	---	---	---	---	---	---	---	---	---	
140	0.82	0.90	0.97	---	---	---	---	---	---	---	---	---	---	---	
150	0.81	0.90	0.91	1.37	1.40	1.40	0.81	0.87	0.99	1.40	1.40	1.40	0.82	0.94	0.99
160	0.81	---	0.88	---	---	---	---	---	---	---	---	---	---	---	
170	0.81	0.87	0.84	---	---	---	---	---	---	---	---	---	---	---	
180	0.79	0.87	0.84	1.37	1.37	1.40	0.79	0.82	0.87	1.40	1.37	1.37	0.81	0.87	0.94
210	0.79	0.81	0.81	1.37	1.37	0.78	0.79	0.82	1.37	1.37	1.37	1.37	0.81	0.81	0.90
240	0.78	0.79	0.79	1.37	1.37	0.78	0.78	0.81	1.37	1.37	1.37	1.37	0.79	0.81	0.85
270	0.78	---	0.79	---	---	0.78	0.78	0.79	---	---	0.79	0.79	0.79	0.79	0.82
300	0.78	0.78	0.78	---	1.37	0.78	0.78	0.78	0.78	---	---	0.78	0.78	0.78	0.79
360	0.78	0.78	0.78	---	---	---	---	0.78	0.78	0.78	0.78	0.78	0.78	0.78	0.78
420	0.78	0.78	0.78	---	---	---	---	0.78	0.78	0.78	0.78	0.78	0.78	0.78	0.78

\* Velocity in feet per second.

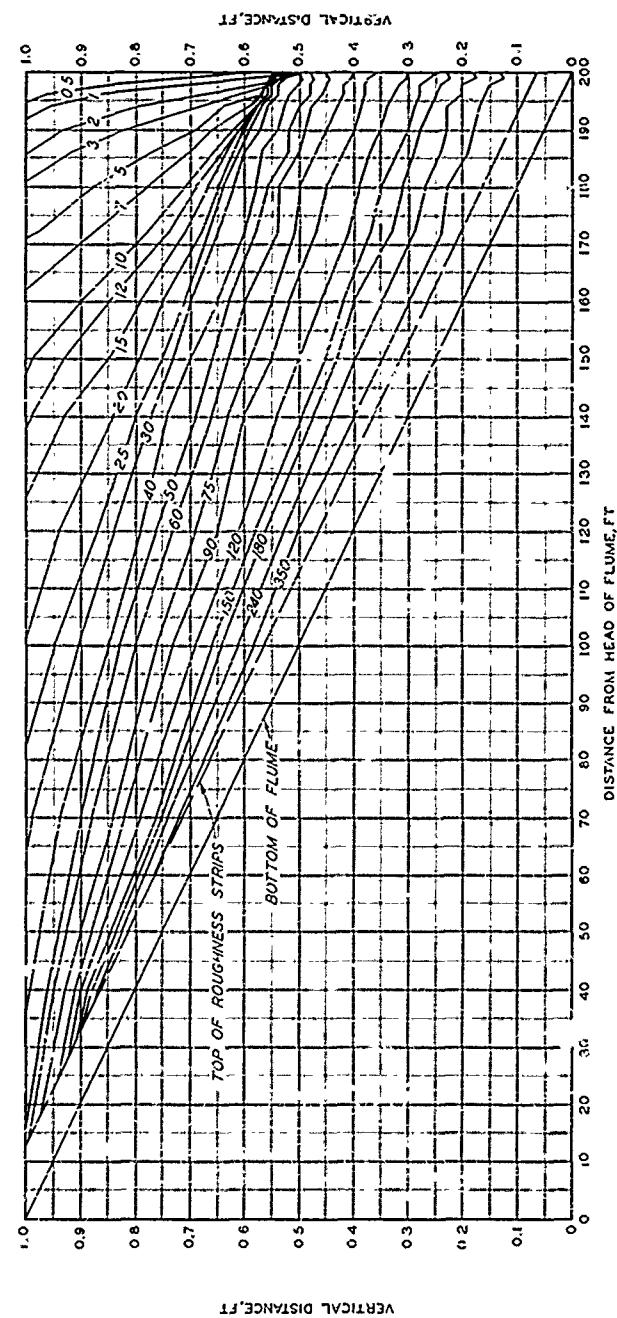
Table 16  
Measurements of the Mohne and Eder Dams and Their Breaches\*

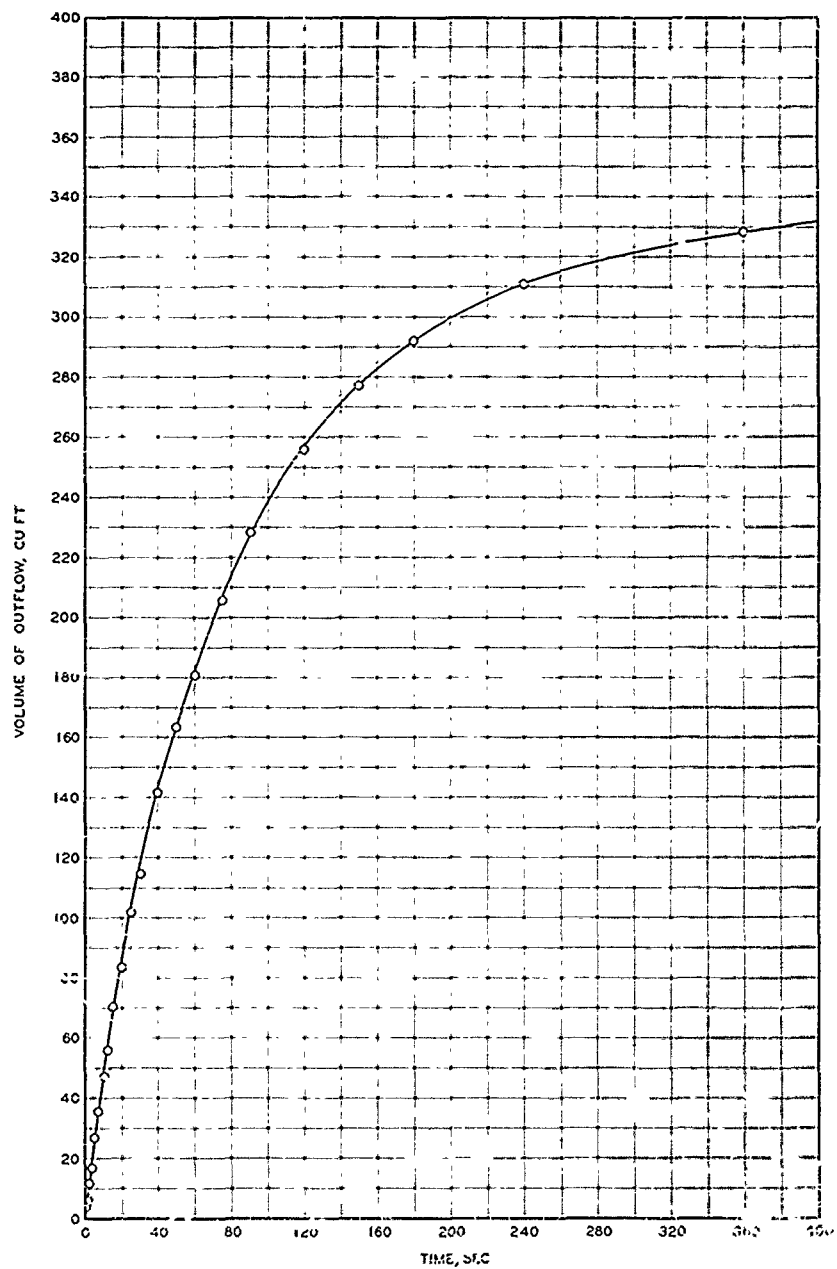
Dam	Dimension	C. H. Miller	H. Quast	Wolfe Dam	J. D. Lovin	L. Lovin	J. Frank
<u>TYPE</u>							
Construction material							
Height, ft.	131						
Cross-section, ft.	2,130						
Base thickness, ft.	112						
Crest thickness, ft.	205						
<u>Reservoir</u>							
Depth at time of breach, ft.	120						
Volume at time of breach, acre-ft.	167,000						
Capacity, acre-ft.	126,000						
Surface area when full, acre	2,130						
Drainage basin area, sq mile	165						
Annual inflow, million cu ft	2,500						
<u>Breach</u>							
Shape	Parabolic						
Depth, ft.	7½						
Below dam crest	7½						
Below original water level	4½						
Width, ft.	720						
At dam crest	112						
At original water level	119						
At bottom of breach	142						
Area below original water level, sq ft	3,000						
<u>Water Flow</u>							
Height, ft	33						
Discharge, cu ft per sec							
Maximum	310,000						
During first hour	317,000						
After 5-3/4 hr	20,600						
After 6-3/4 hr	55,300						
Maximum 116% water discharge on Mohne River, cu ft per sec	14,000						
Velocity, ft per sec							
Wave crest at dam	53						
Wave crest at dam	53						
Wave tip 50 miles downstream	156						
Wave tip 70 miles downstream	447						
Total volume of outflow, cu ft	92,700						
Duration, hours	12						
Flow lost	1,000						
<u>Calculations</u>							
$D_b/k_o$	0.14						
$W_b/k_a$	0.11						
$(D_b/k_o) \cdot (W_b/k_a)$	0.059						
$Q_{max}/\sqrt{g D_b}^{3/2}$	0.728						

\* Data taken from reference 1, 2, 3, 4, 5, 6, 7, 8, and 9.

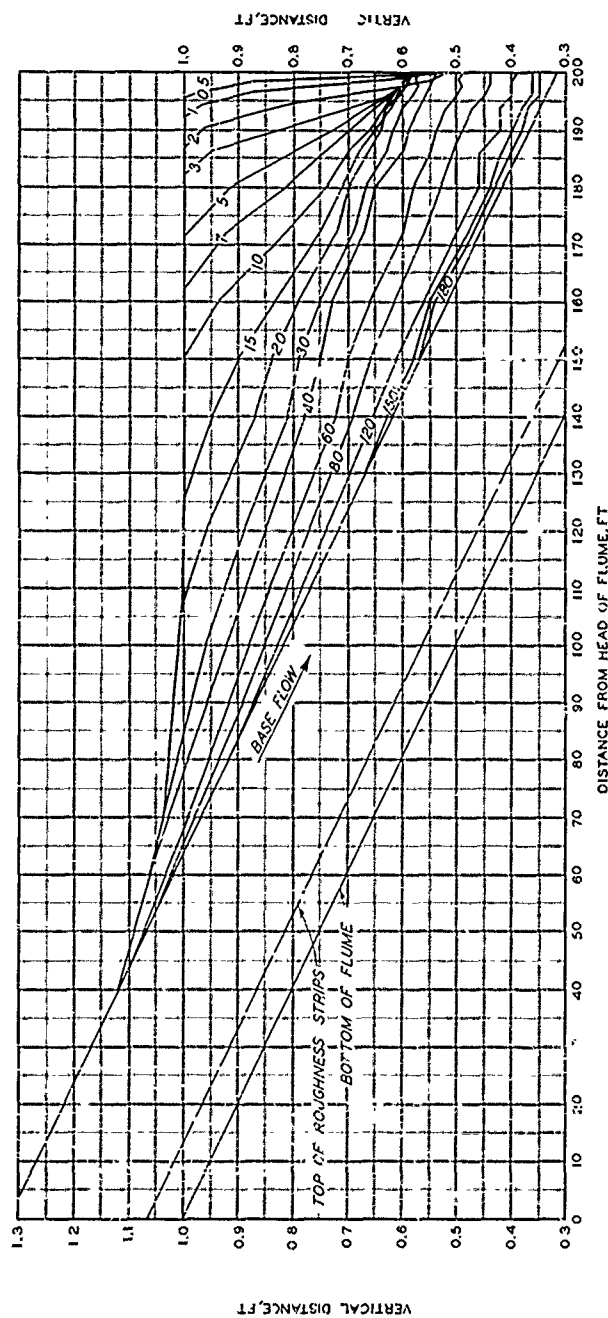
WATER-SURFACE PROFILES  
TEST CONDITION 1.2

NOTE TIME IN SECONDS AS INDICATED





VOLUME OF OUTFLOW  
AS A FUNCTION OF TIME  
TEST CONDITION 1.2

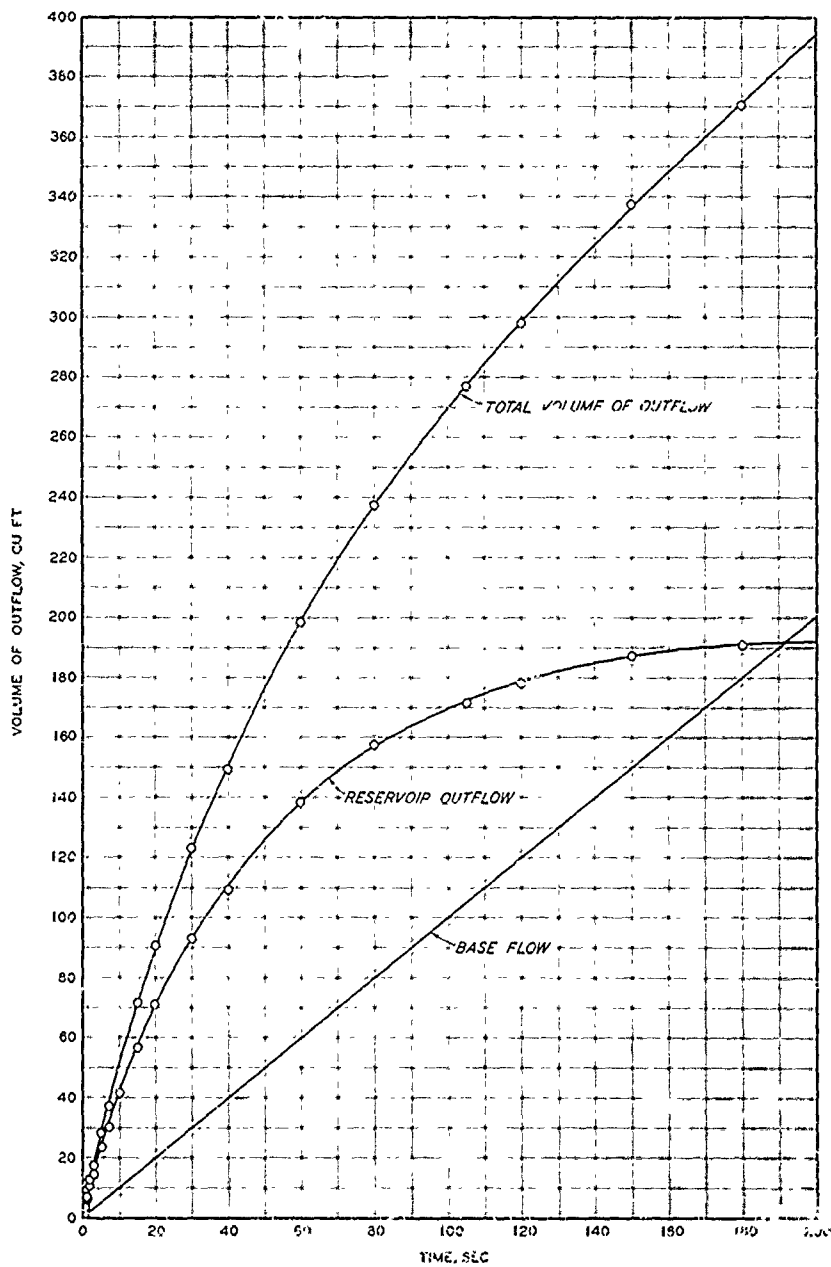


WATER-SURFACE PROFILES

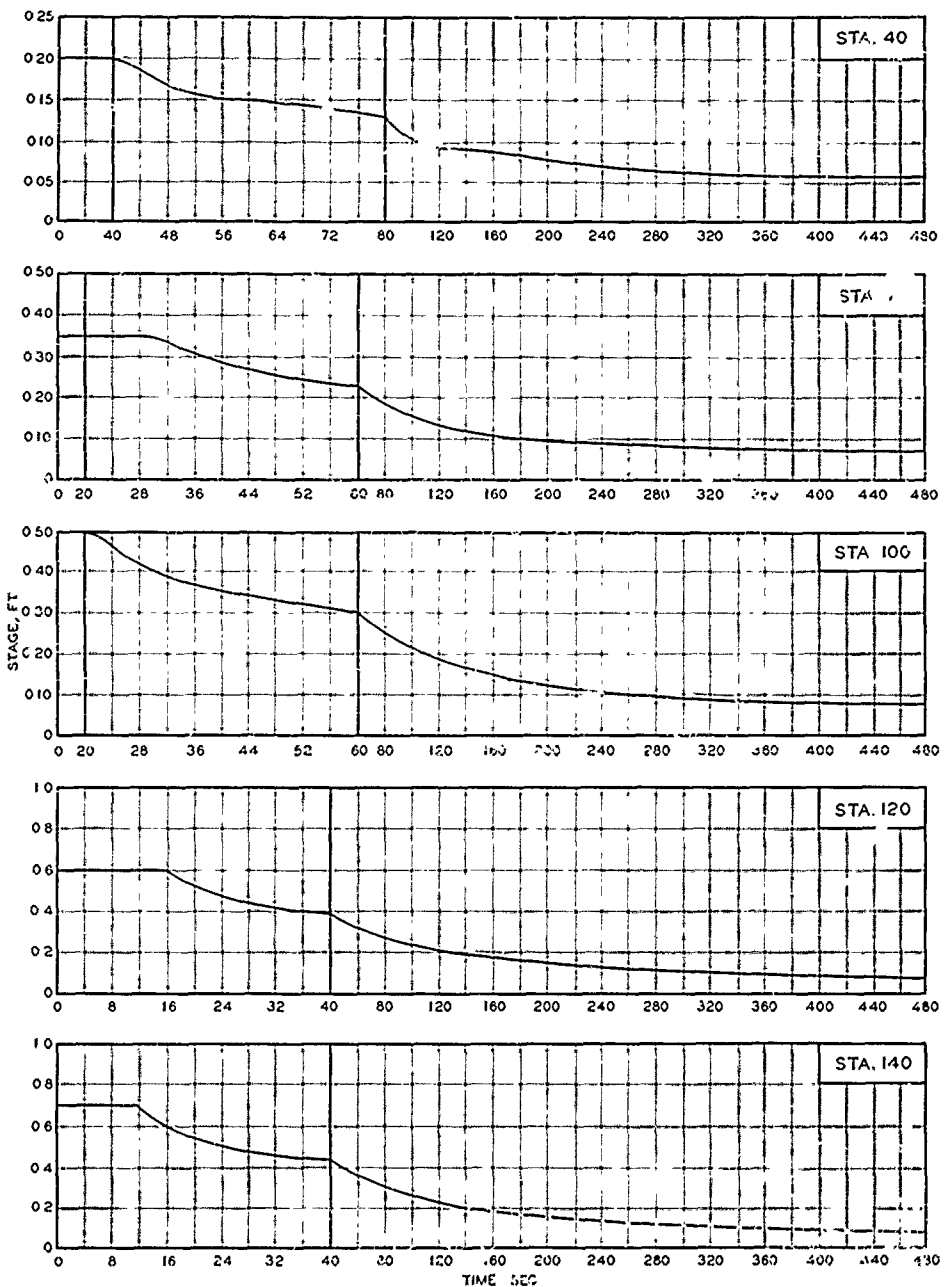
TEST CONDIT. i 1.2 (32)

NOTE: TIME IN SECS. INDICATED

PLATE 3



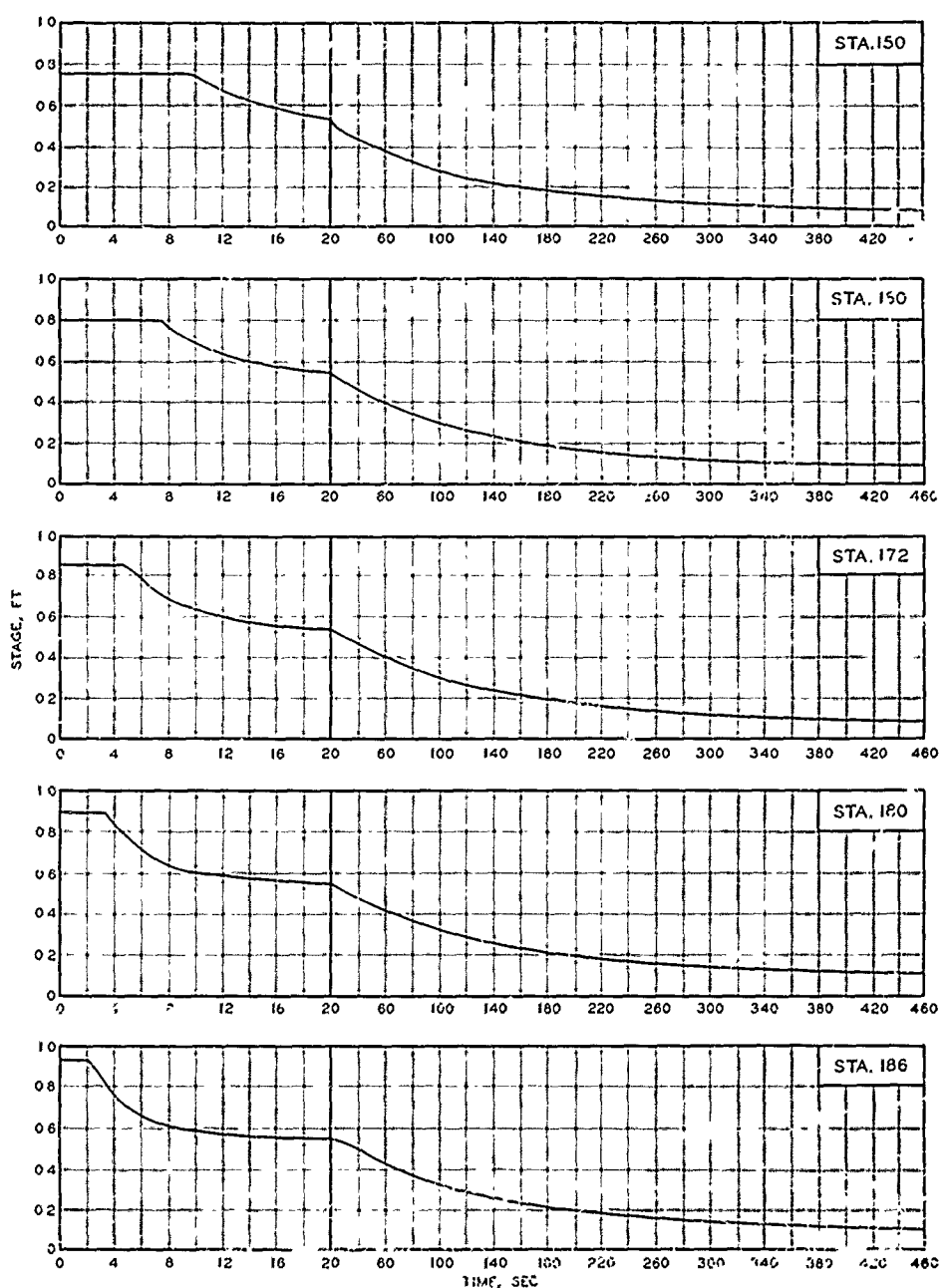
VOLUME OF OUTFLOW  
AS A FUNCTION OF TIME  
TEST CONDITION 1.2 (32)



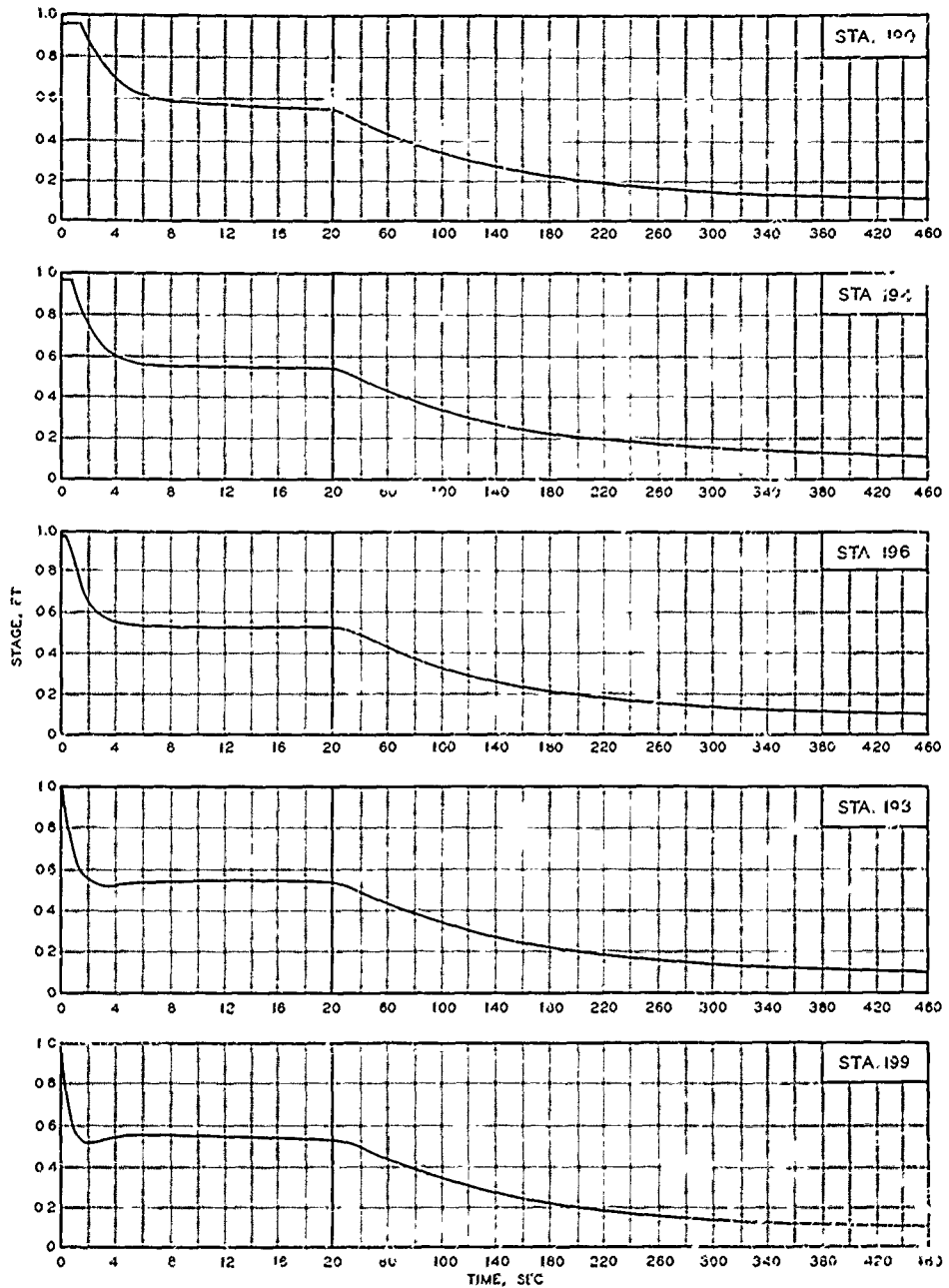
### STAGE-TIME HYDROGRAPHS

STATIONS 40, 70, 100, 120, AND 140

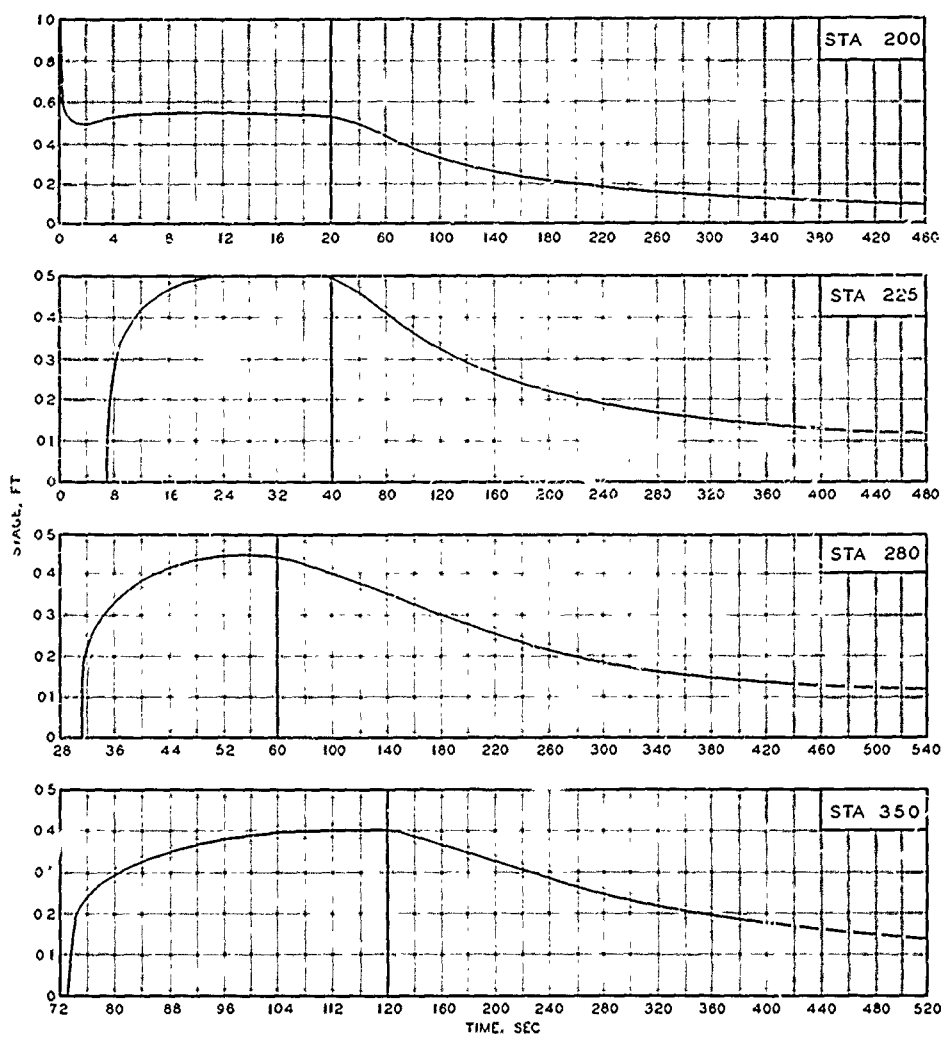
TEST CONDITION 1.2



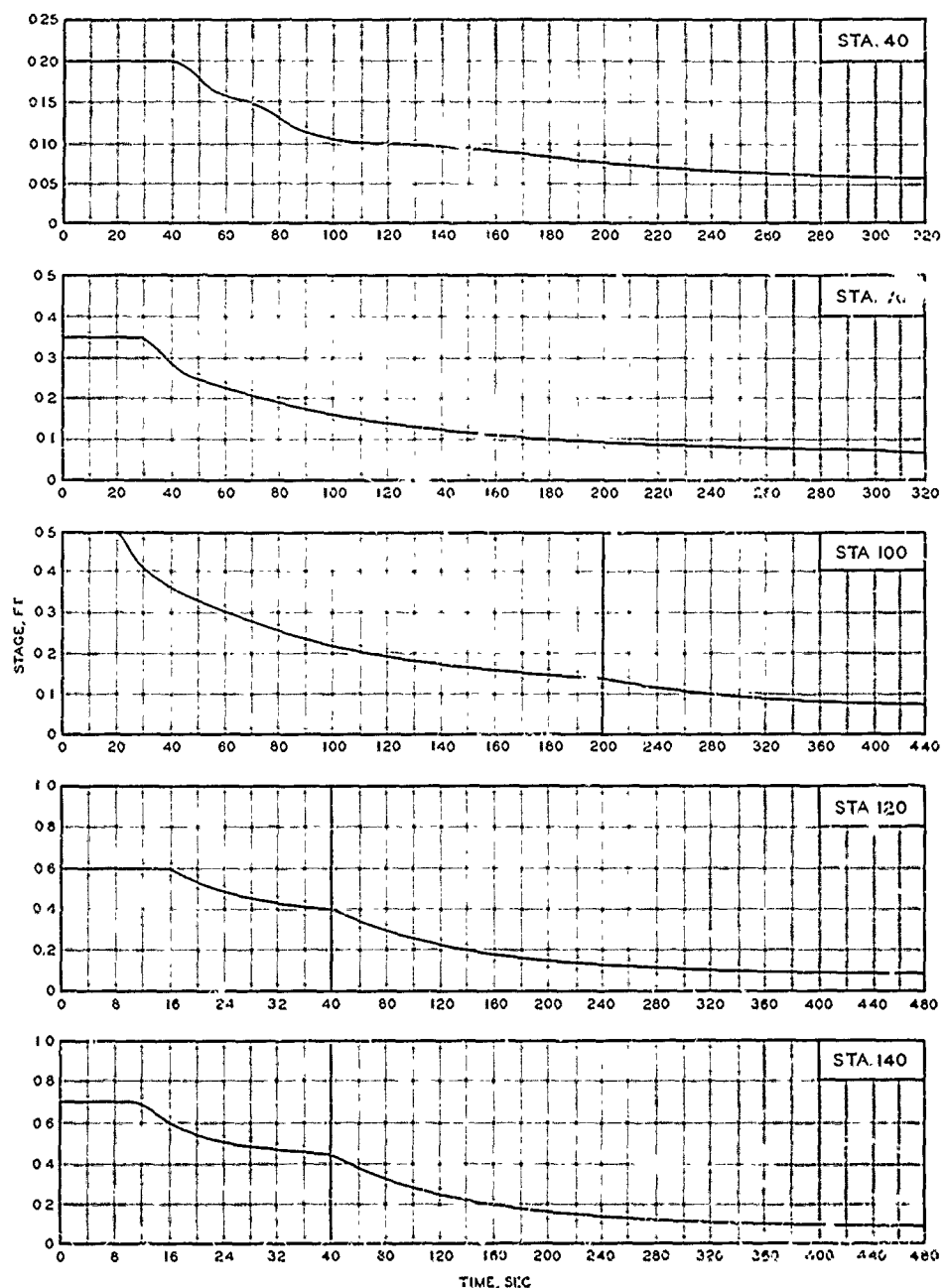
STAGE-TIME HYDROGRAPHS  
STATIONS 150, 160, 172, 180, AND 186  
TEST CONDITION 1.2



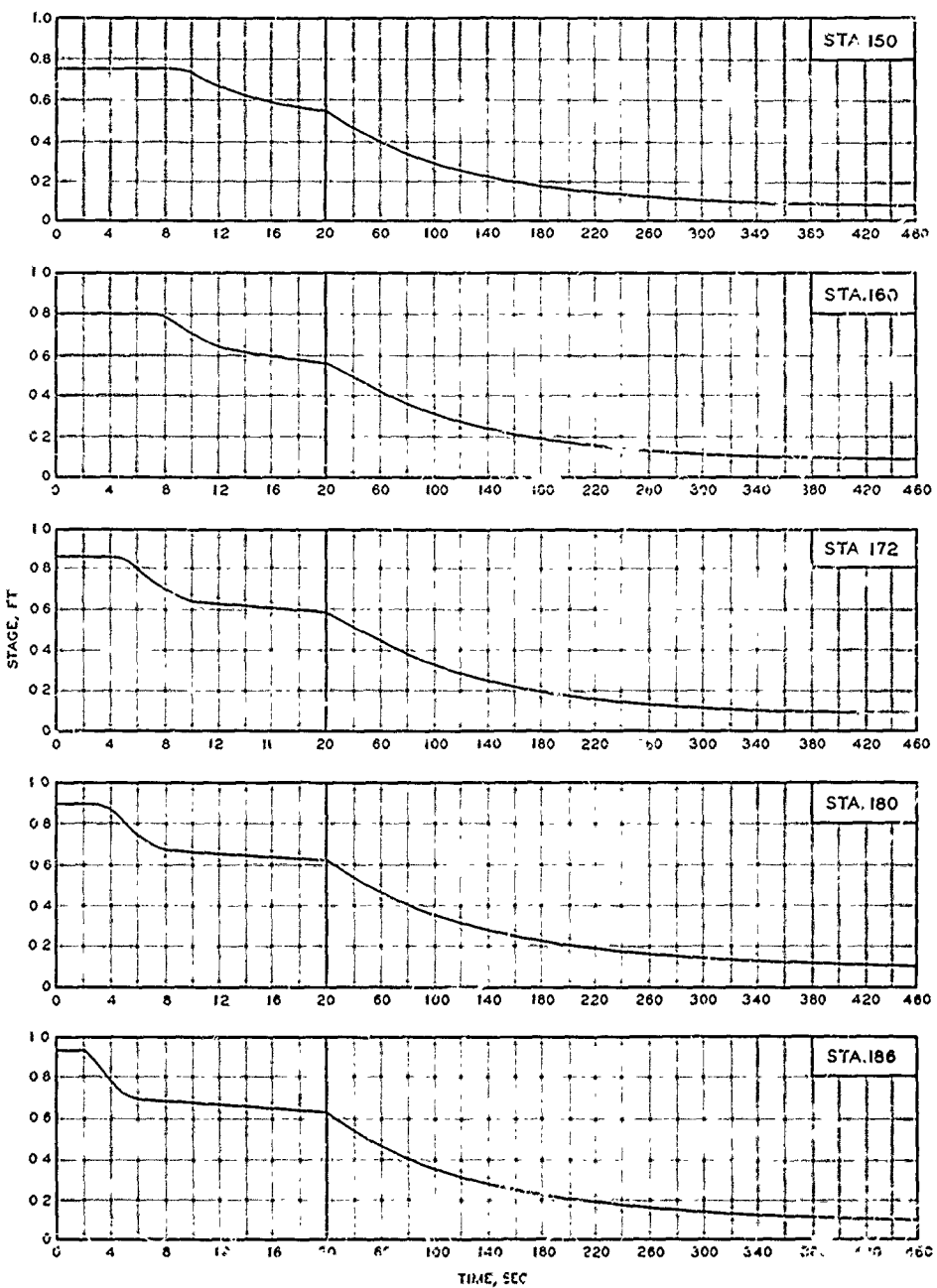
STAGE-TIME HYDROGRAPHS  
STATIONS I90, I94, I96, I98, AND I99  
TEST CONDITION 1.2



STAGE-TIME HYDROGRAPHS  
STATIONS 200, 225, 280, AND 350  
TEST CONDITION 1.2

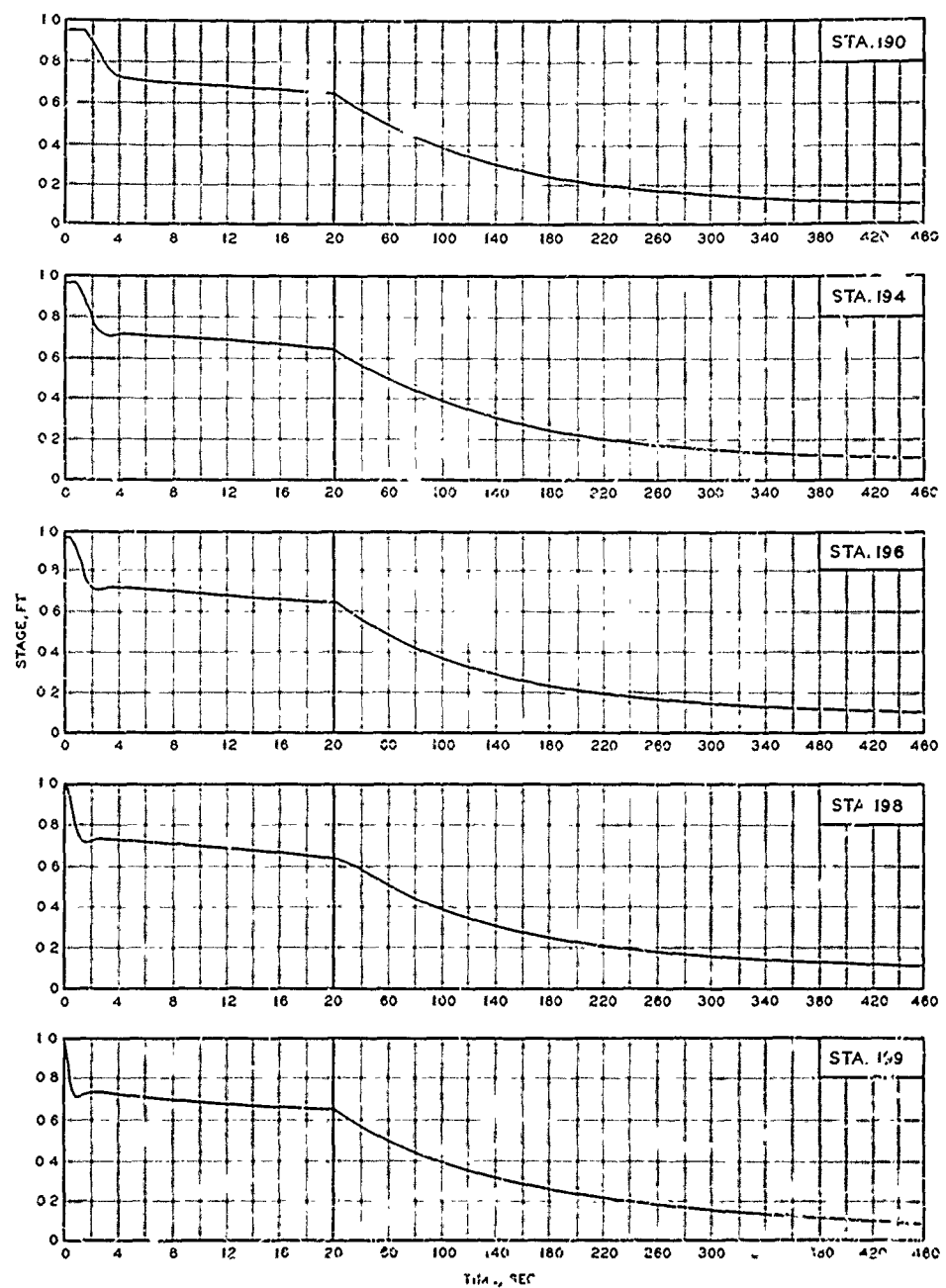


STAGE-TIME HYDROGRAPHS  
STATIONS 40, 70, 100, 120, AND 140  
TEST CONDITION 2.2

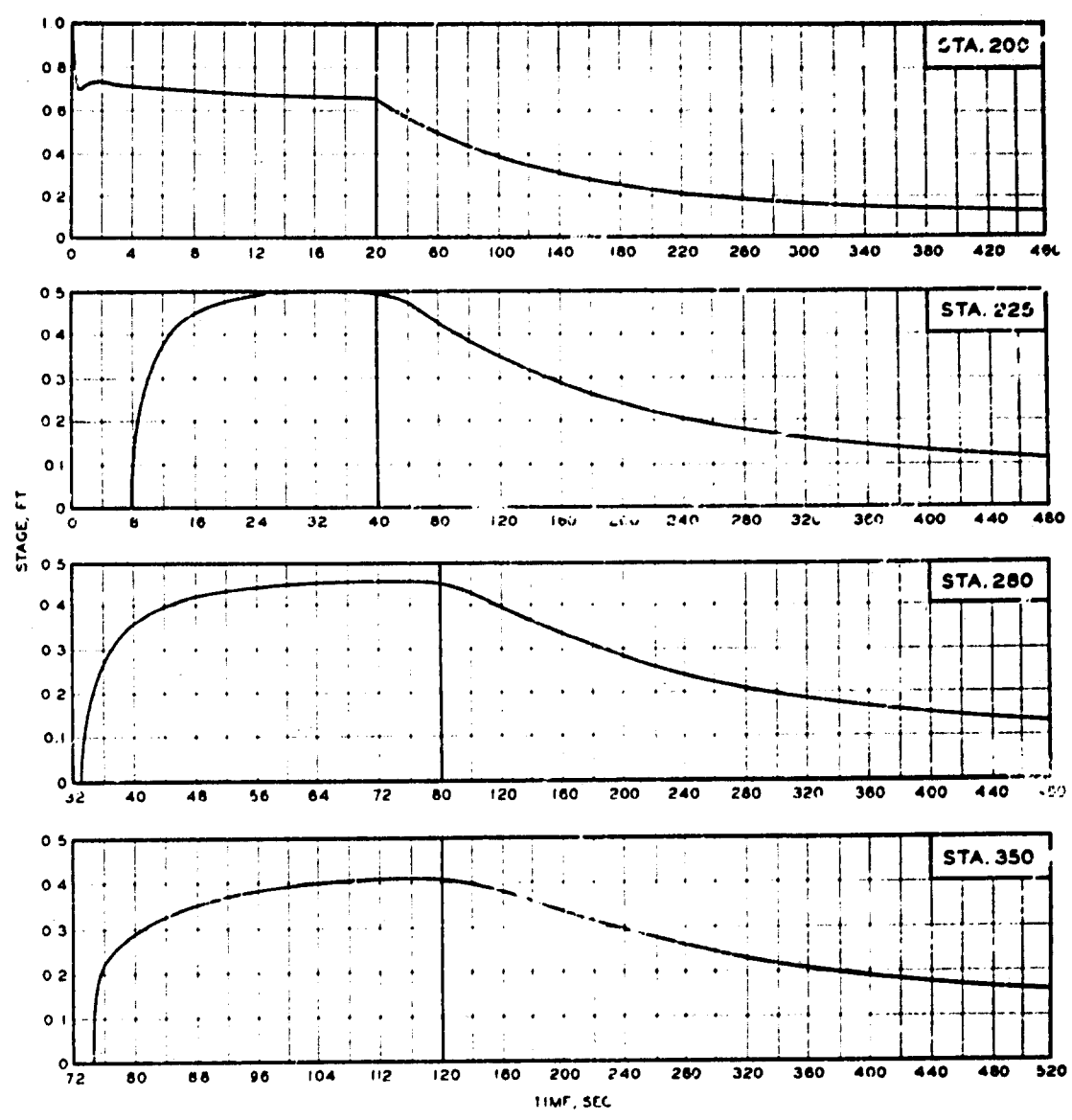


### STAGE-TIME HYDROGRAPHS

STATIONS 150, 160, 172, 180, AND 186  
TEST CONDITION 2.2

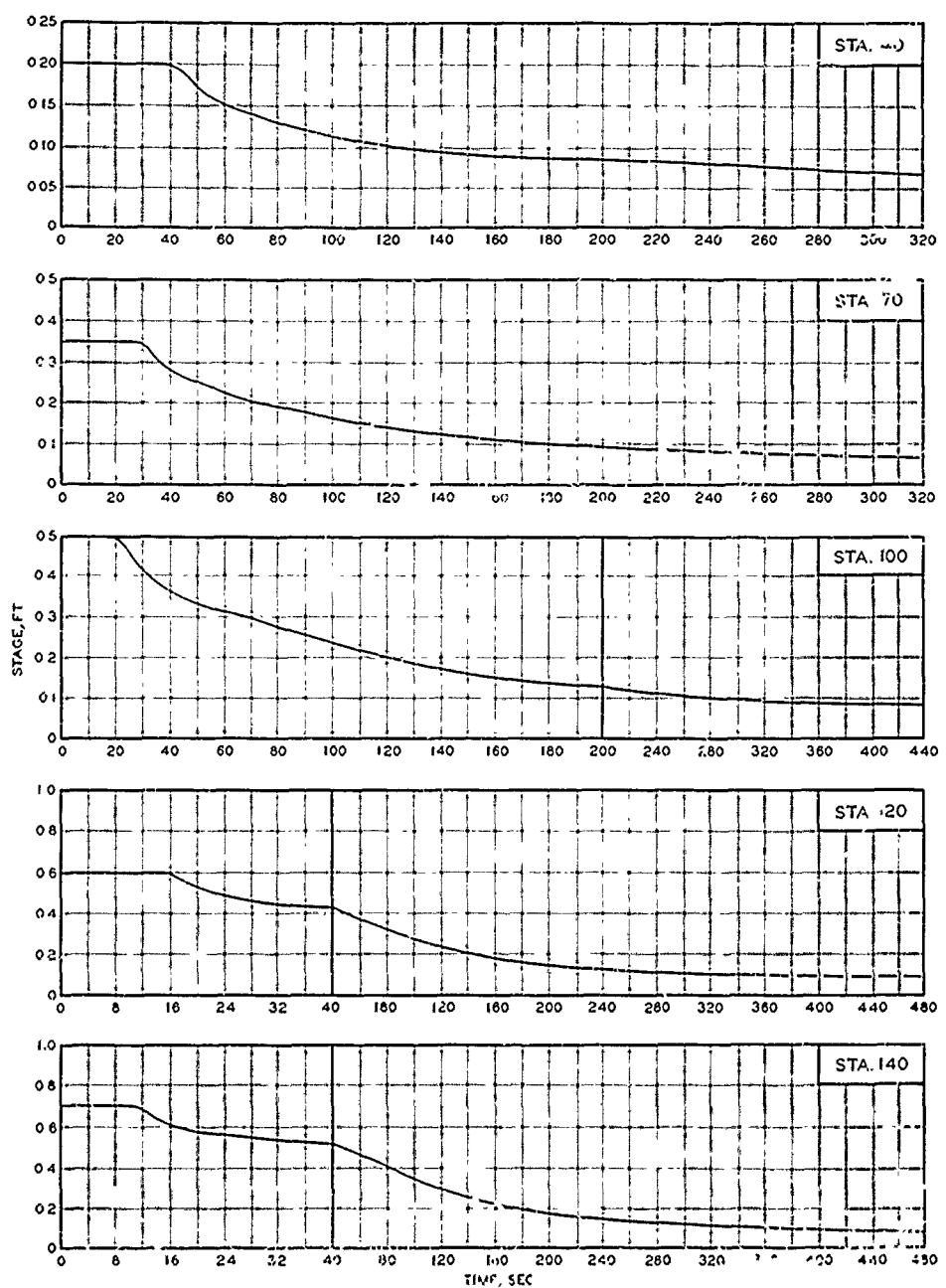


STAGE - TIME HYDROGRAPHS  
STATIONS 190, 194, 196, 198, AND 199  
TEST CONDITION 2.2

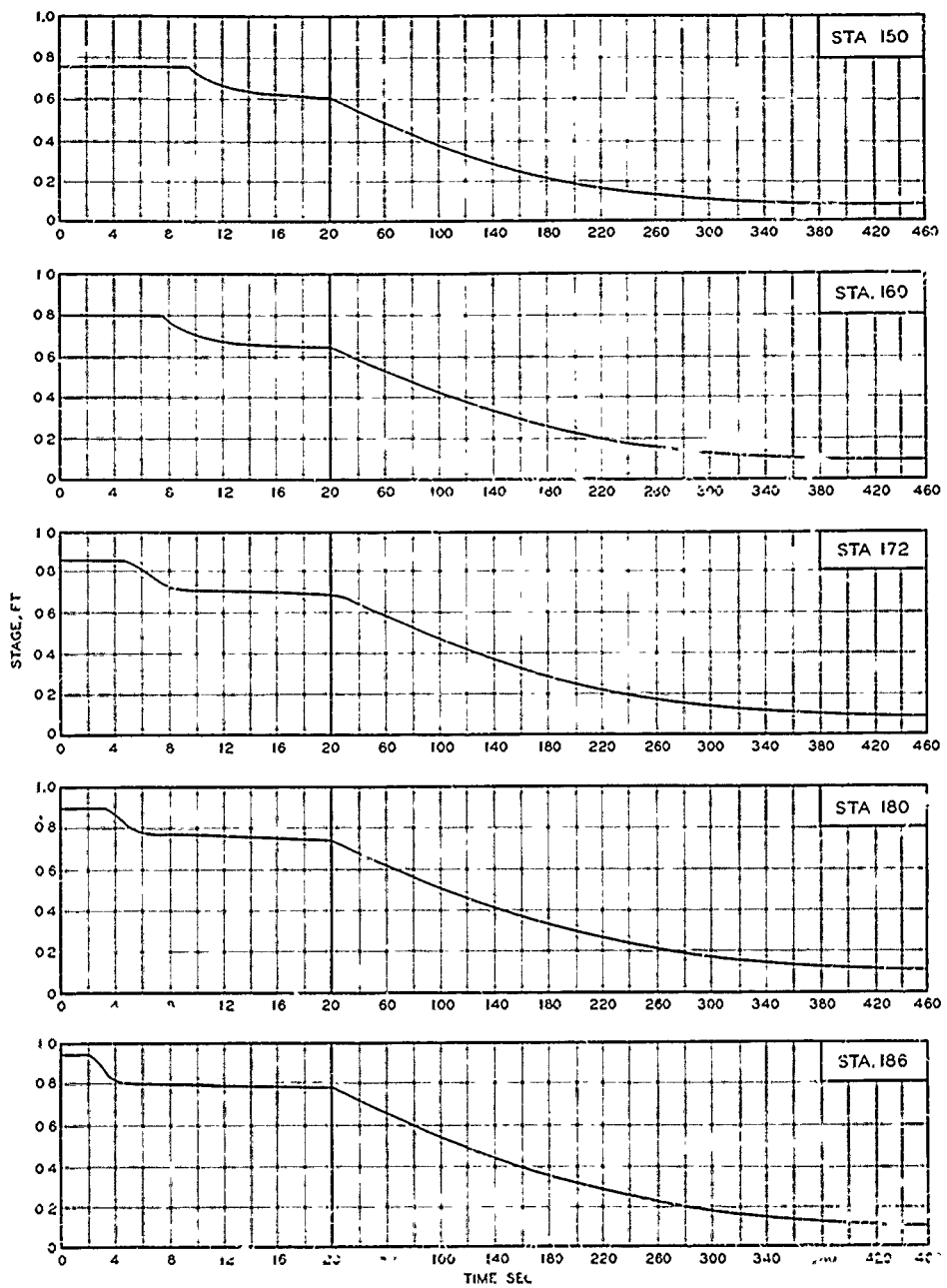


STAGE-TIME HYDROGRAPHS  
STATIONS 200, 225, 280, AND 350  
TEST CONDITION 2.2

PLATE 12



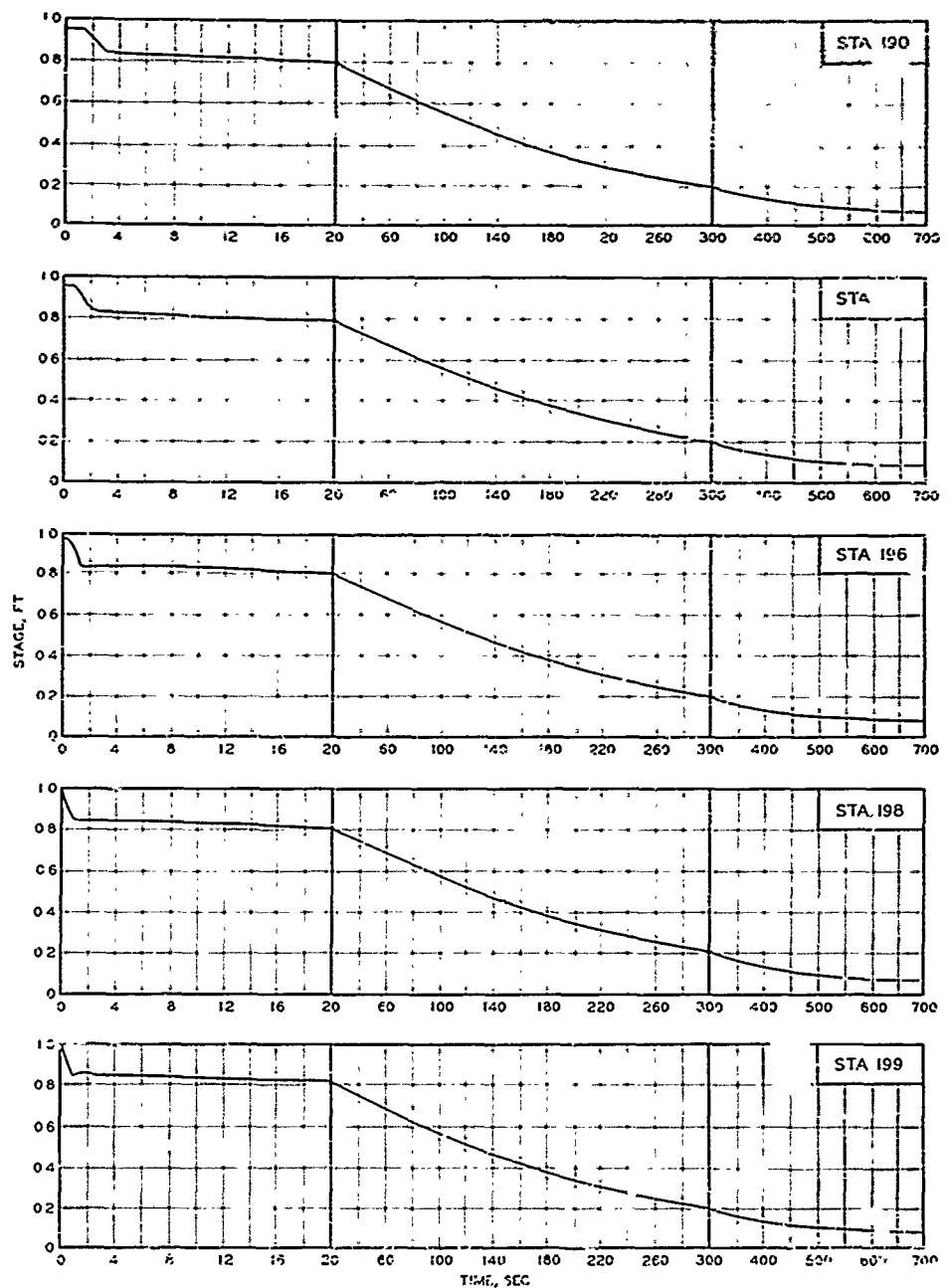
STAGE-TIME HYDROGRAPHS  
STATIONS 40, 70, 100, 120, AND 140  
TEST CONDITION 3.2



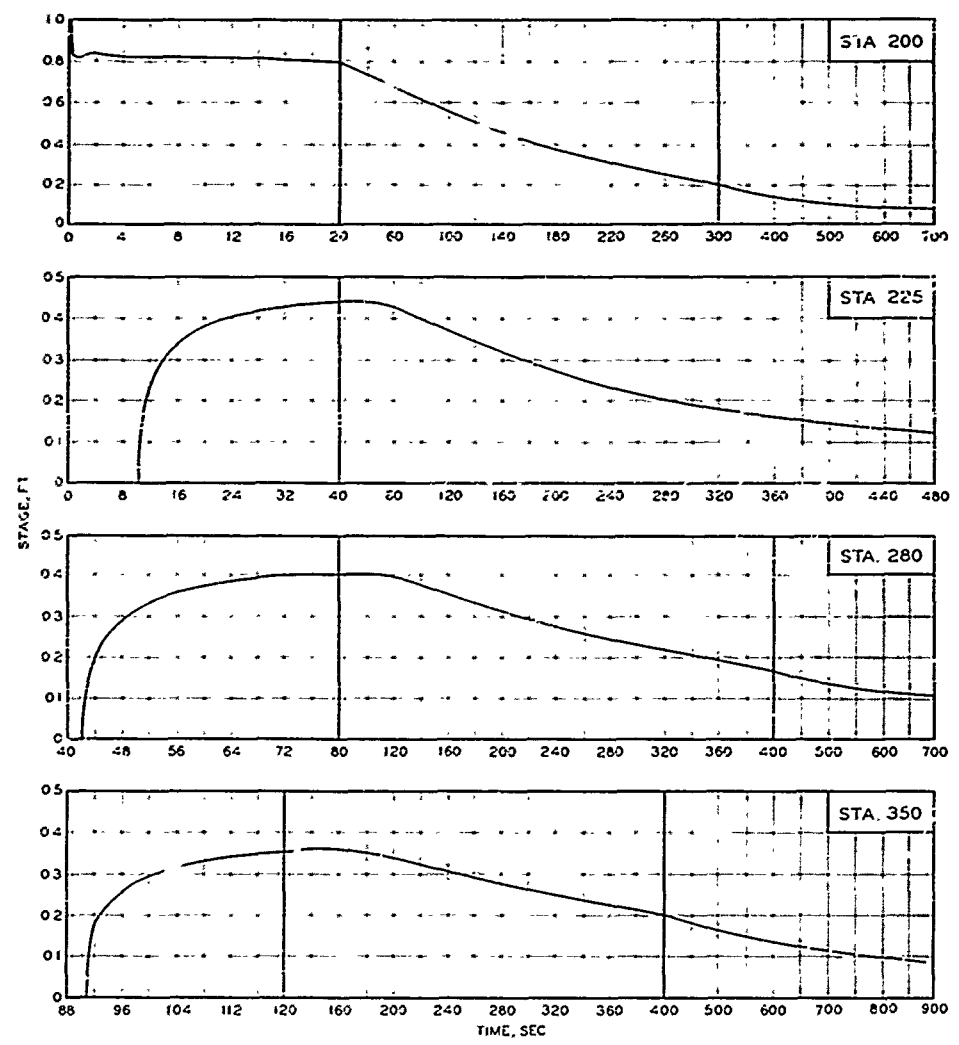
### STAGE-TIME HYDROGRAPHS

STATIONS 150, 160, 172, 180, AND 186

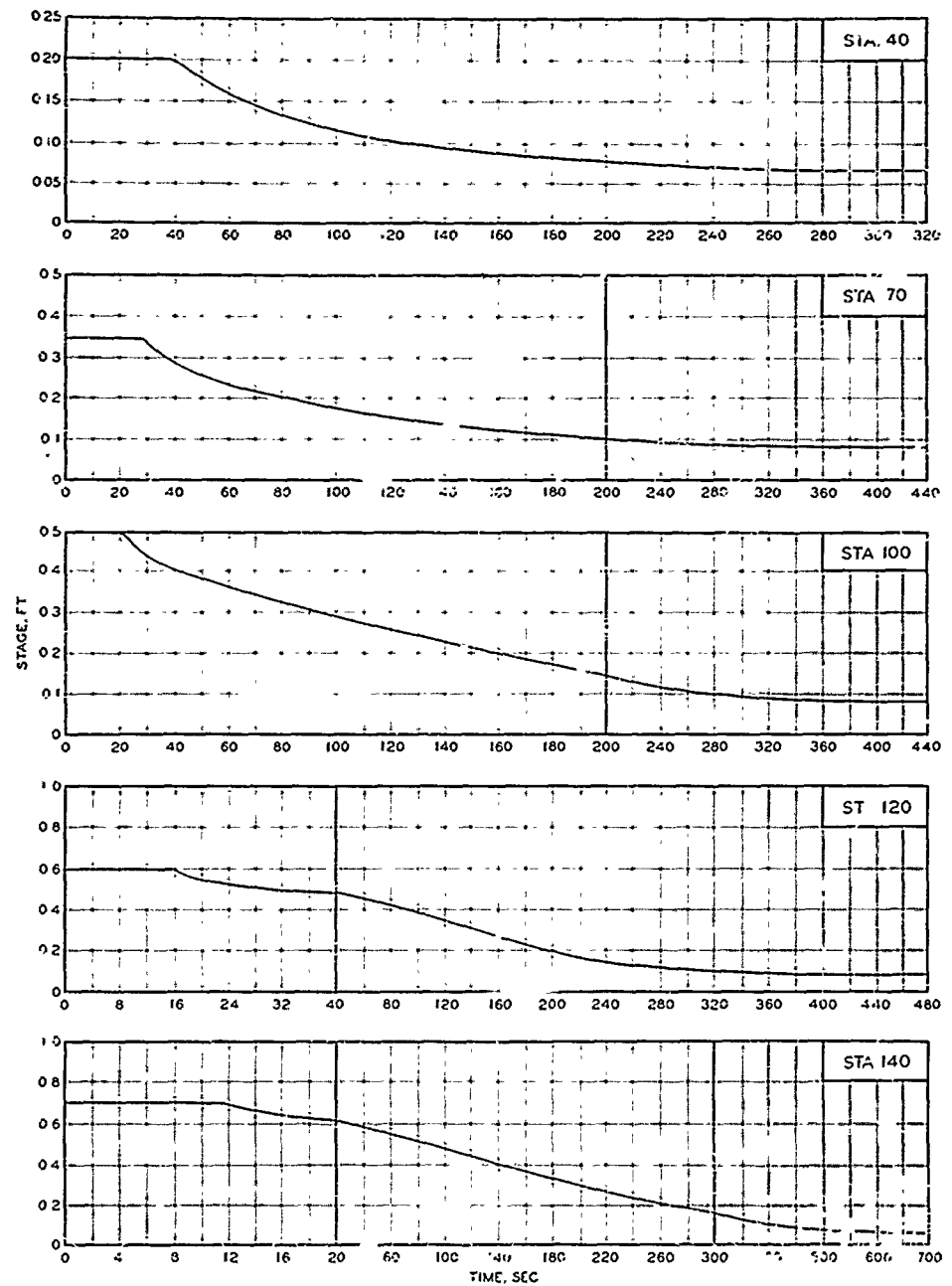
TEST CONDITION 3.2



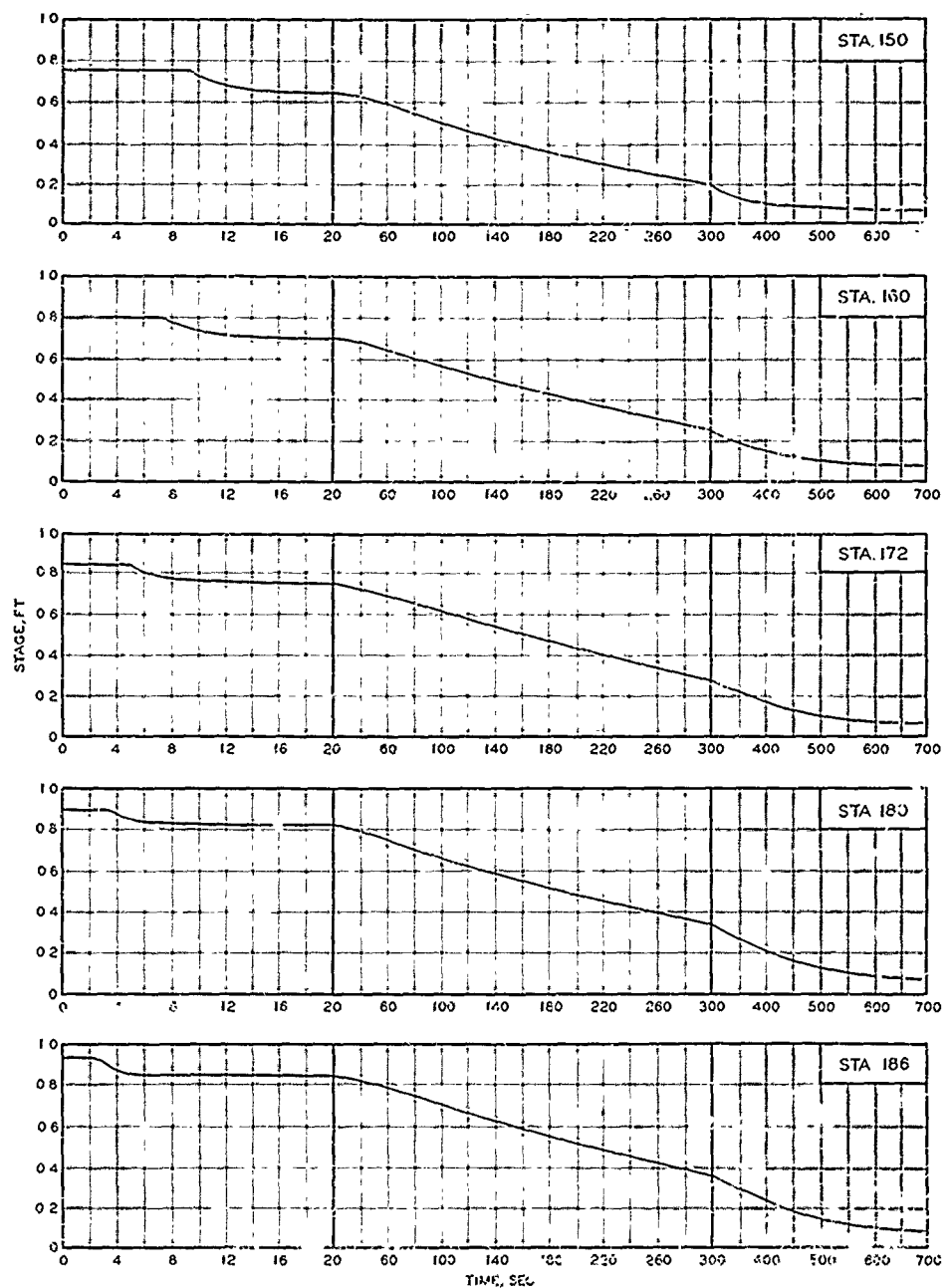
STAGE-TIME HYDROGRAPHS  
STATIONS I90, I94, I96, I98, AND I99  
TEST CONDITION 3.2



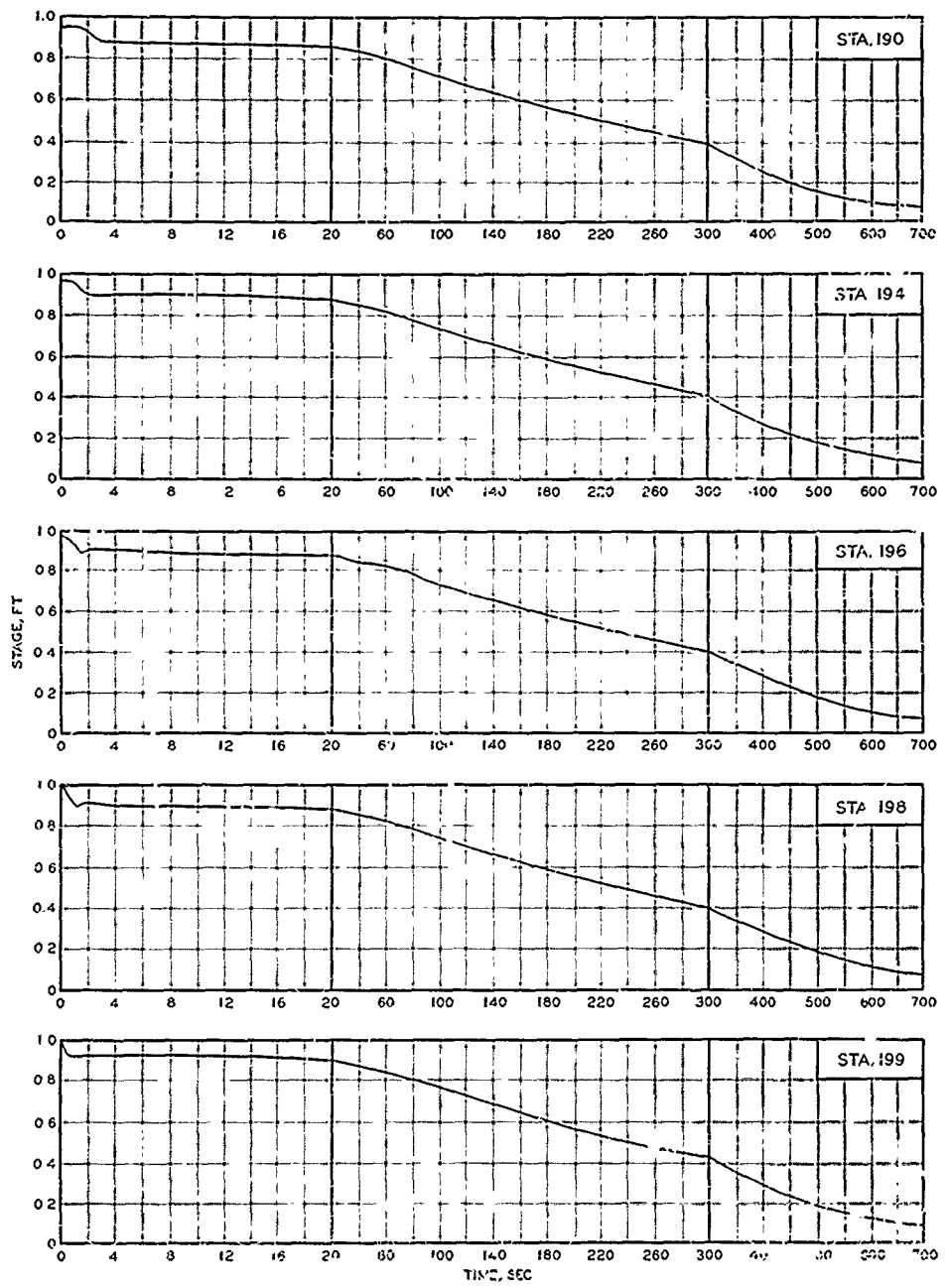
STAGE-TIME HYDROGRAPHS  
STATIONS 200, 225, 280, AND 350  
TEST CONDITION 3.2



STAGE-TIME HYDROGRAPHS  
STATIONS 40, 70, 100, 120, AND 140  
TEST CONDITION 4.2



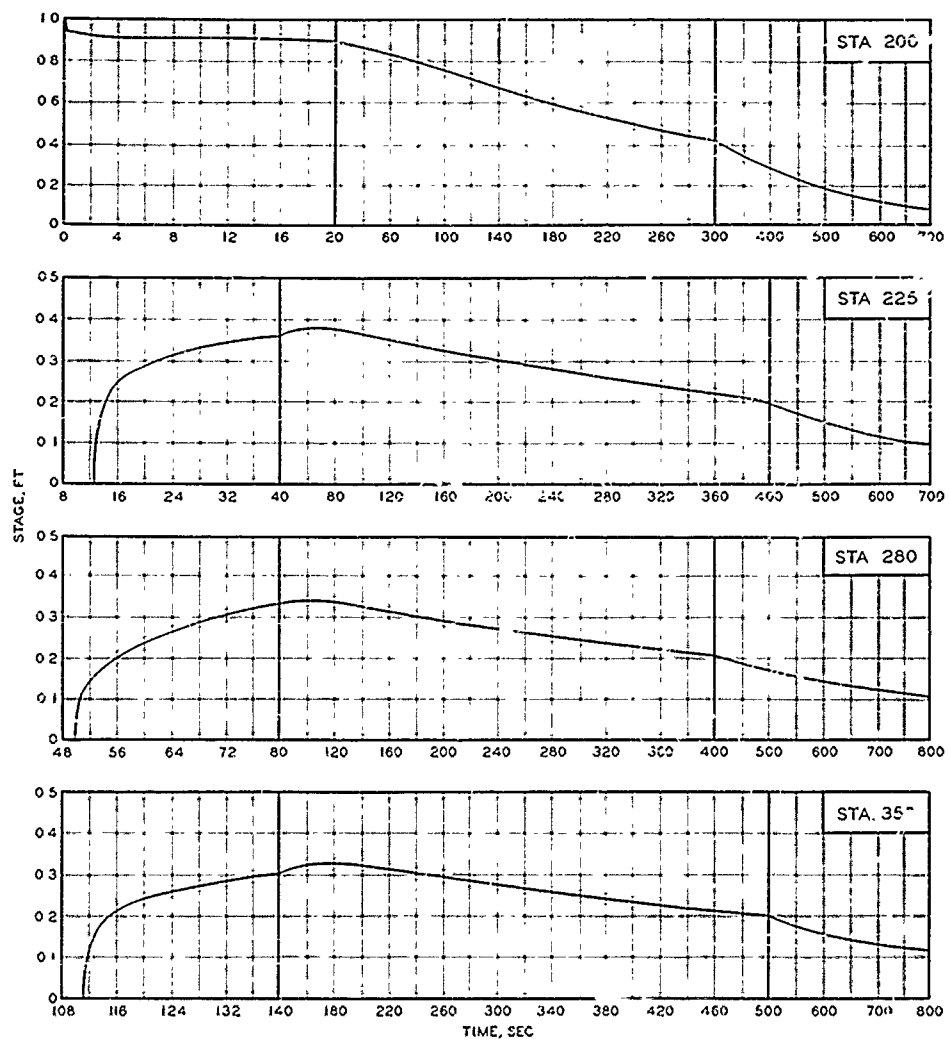
STAGE-TIME HYDROGRAPHS  
STATIONS 150, 160, 172, 180, AND 186  
TEST CONDITION 4.2



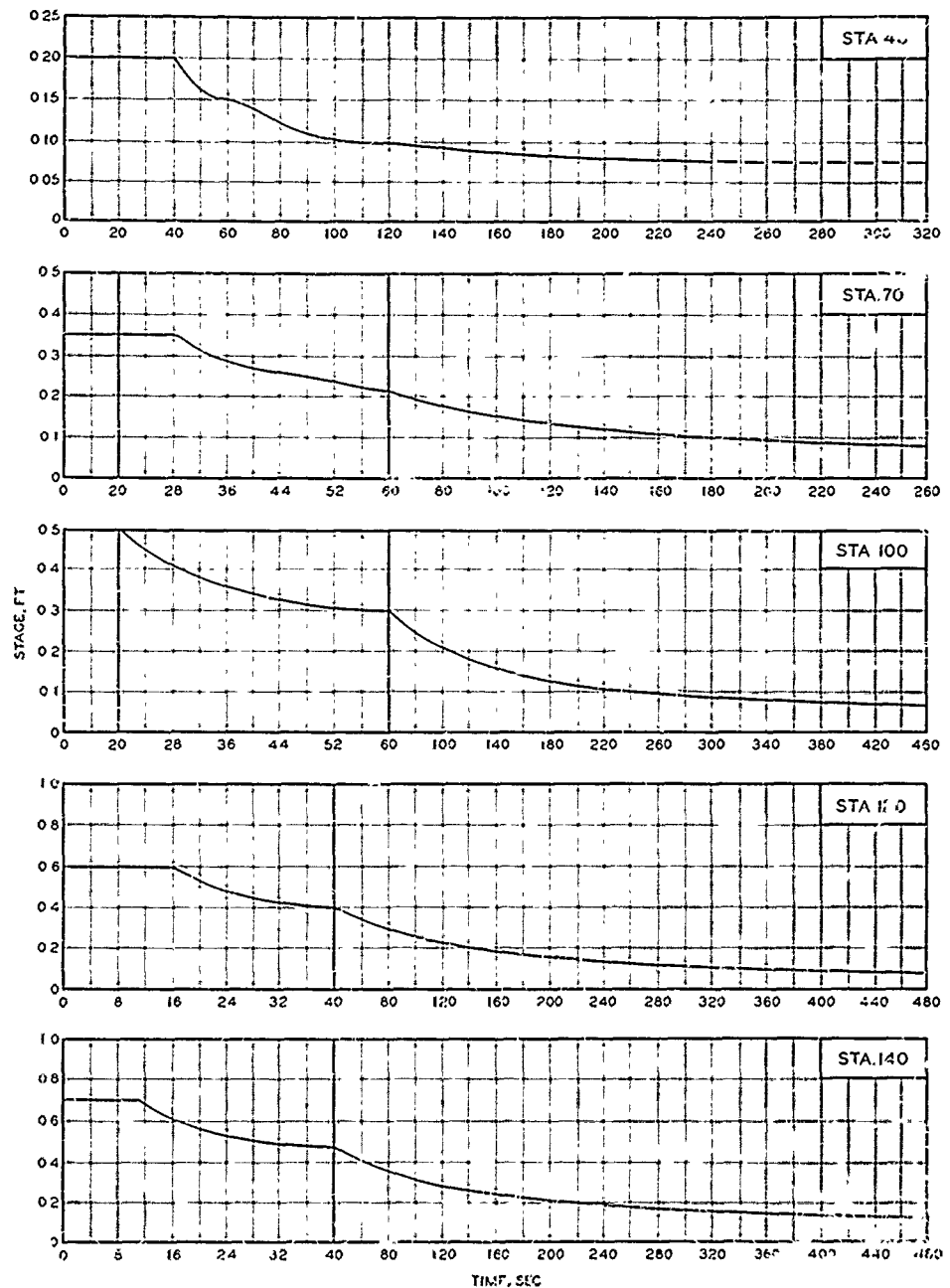
### STAGE-TIME HYDROGRAPHS

STATIONS 190, 194, 196, 198, AND 199

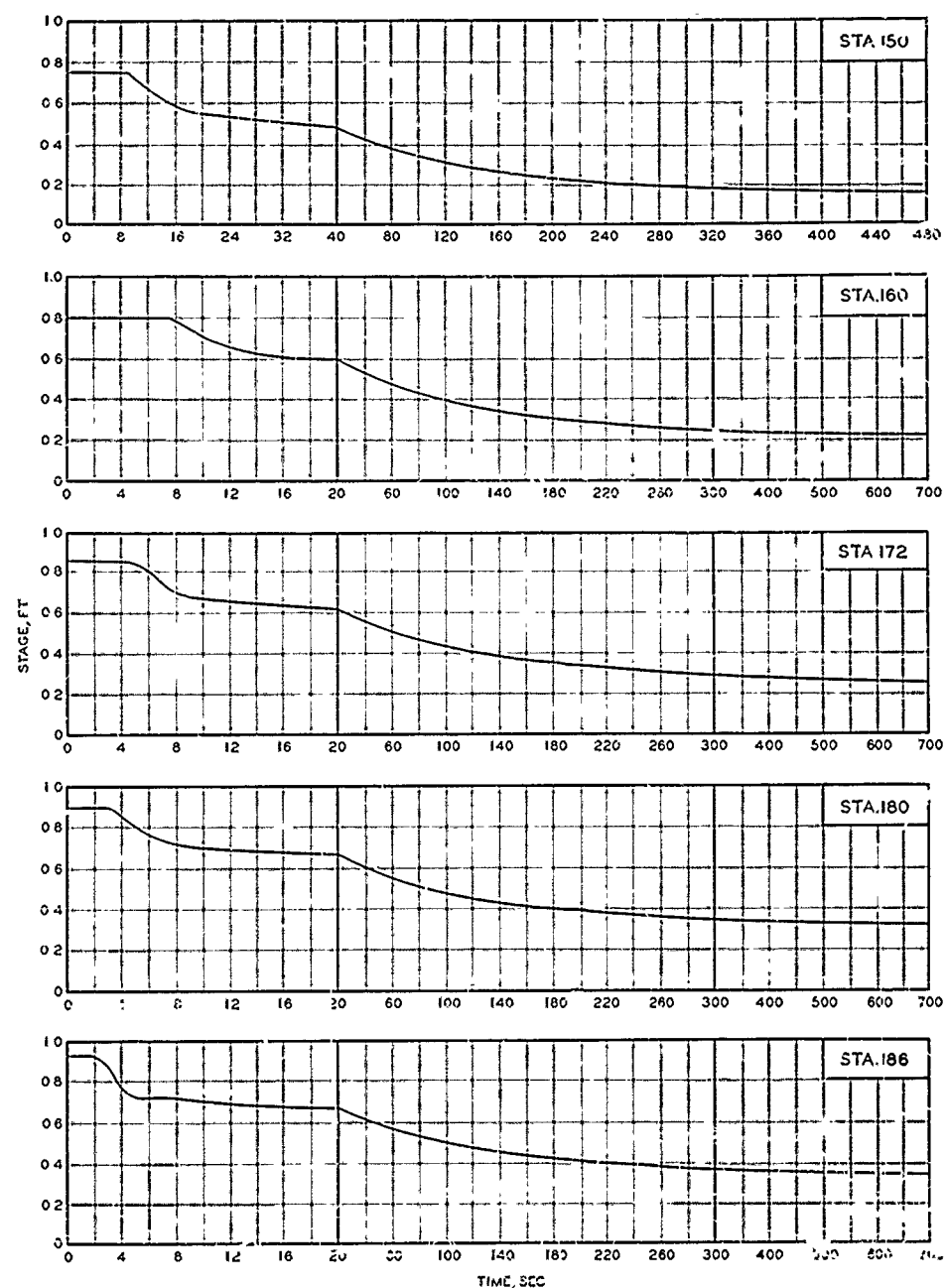
TEST CONDITION 4.2



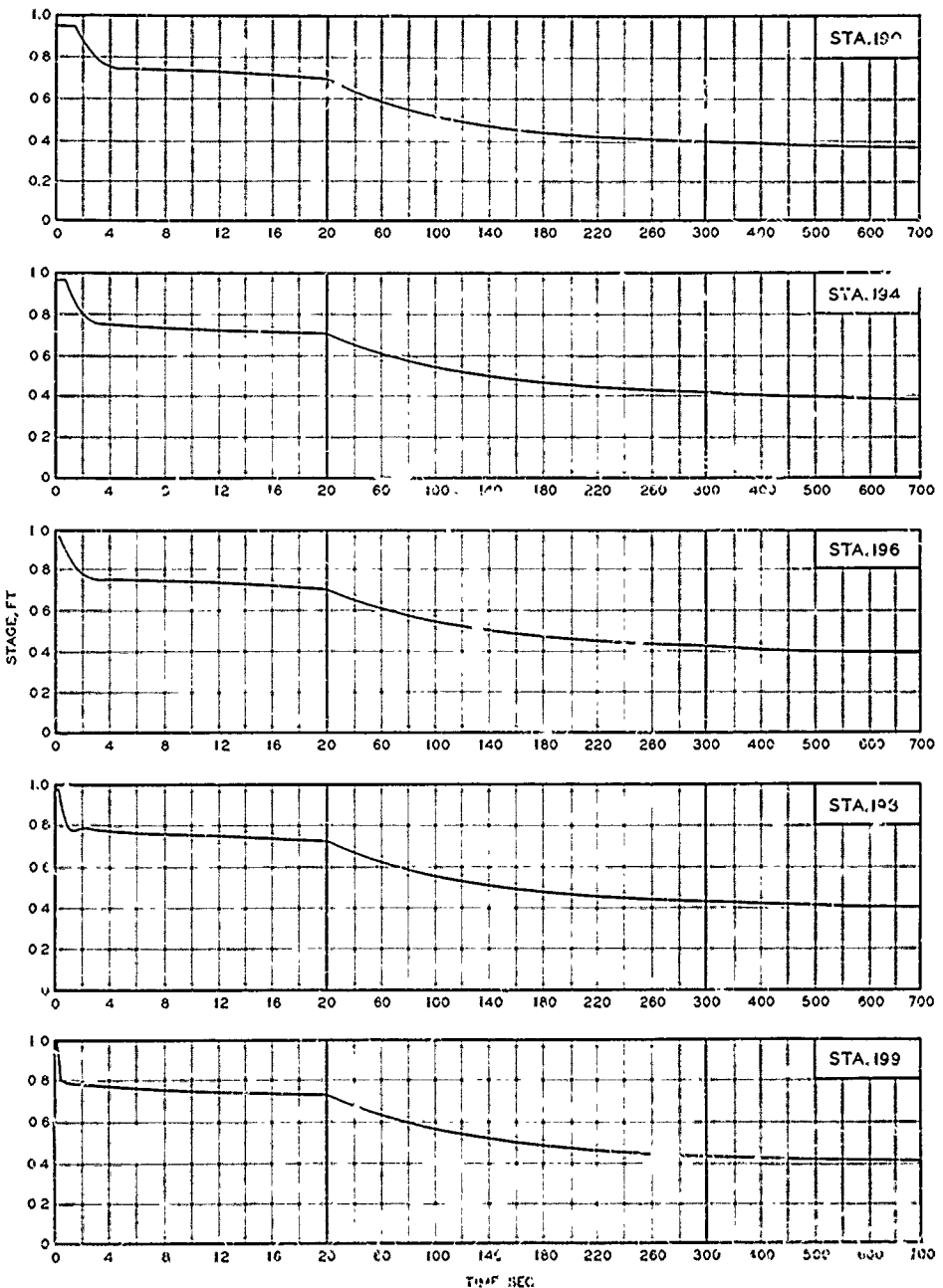
STAGE-TIME HYDROGRAPHS  
STATIONS 200, 225, 280, AND 350  
TEST CONDITION 4.2



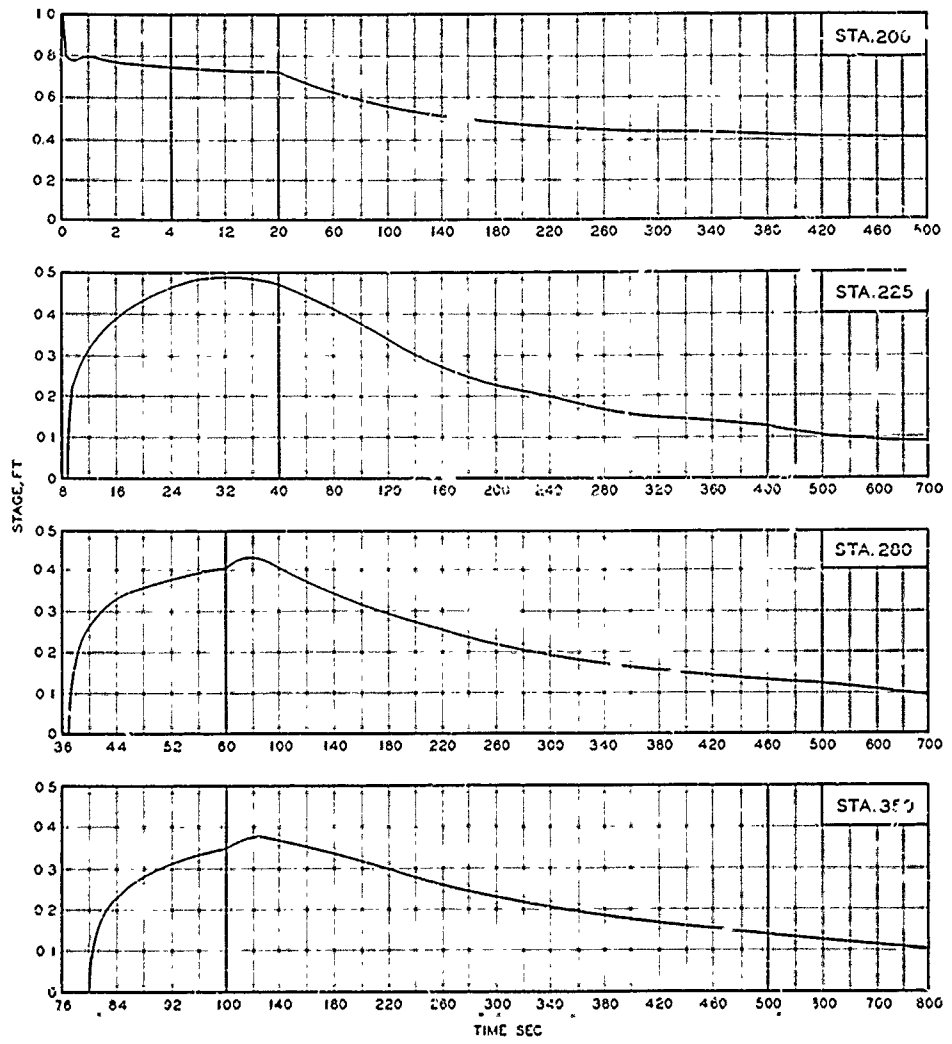
STAGE-TIME HYDROGRAPHS  
STATIONS 40, 70, 100, 120, AND 140  
TEST CONDITION 7.2



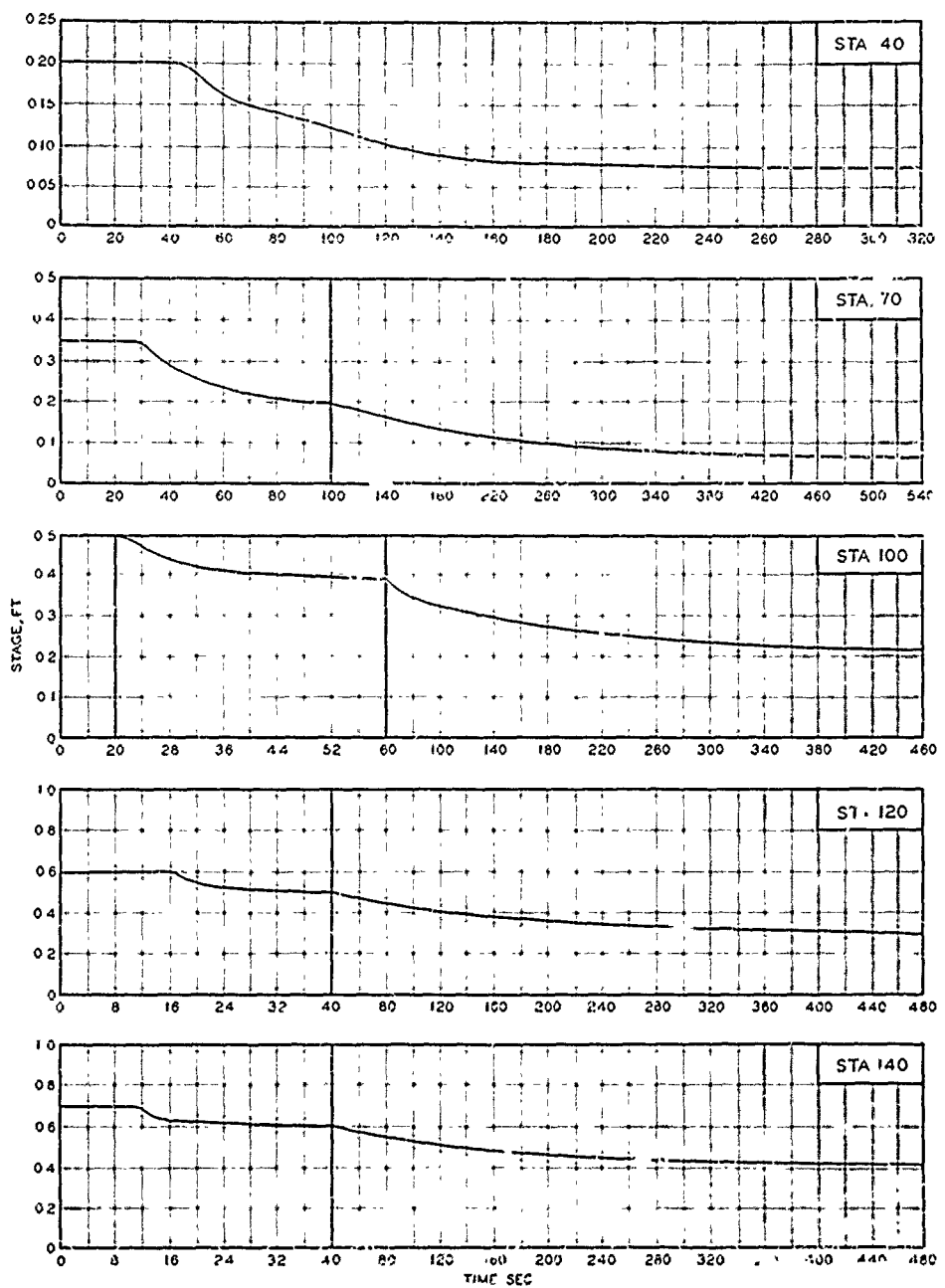
STAGE-TIME HYDROGRAPHS  
STATIONS 150, 160, 172, 180, AND 186  
TEST CONDITION 7.2



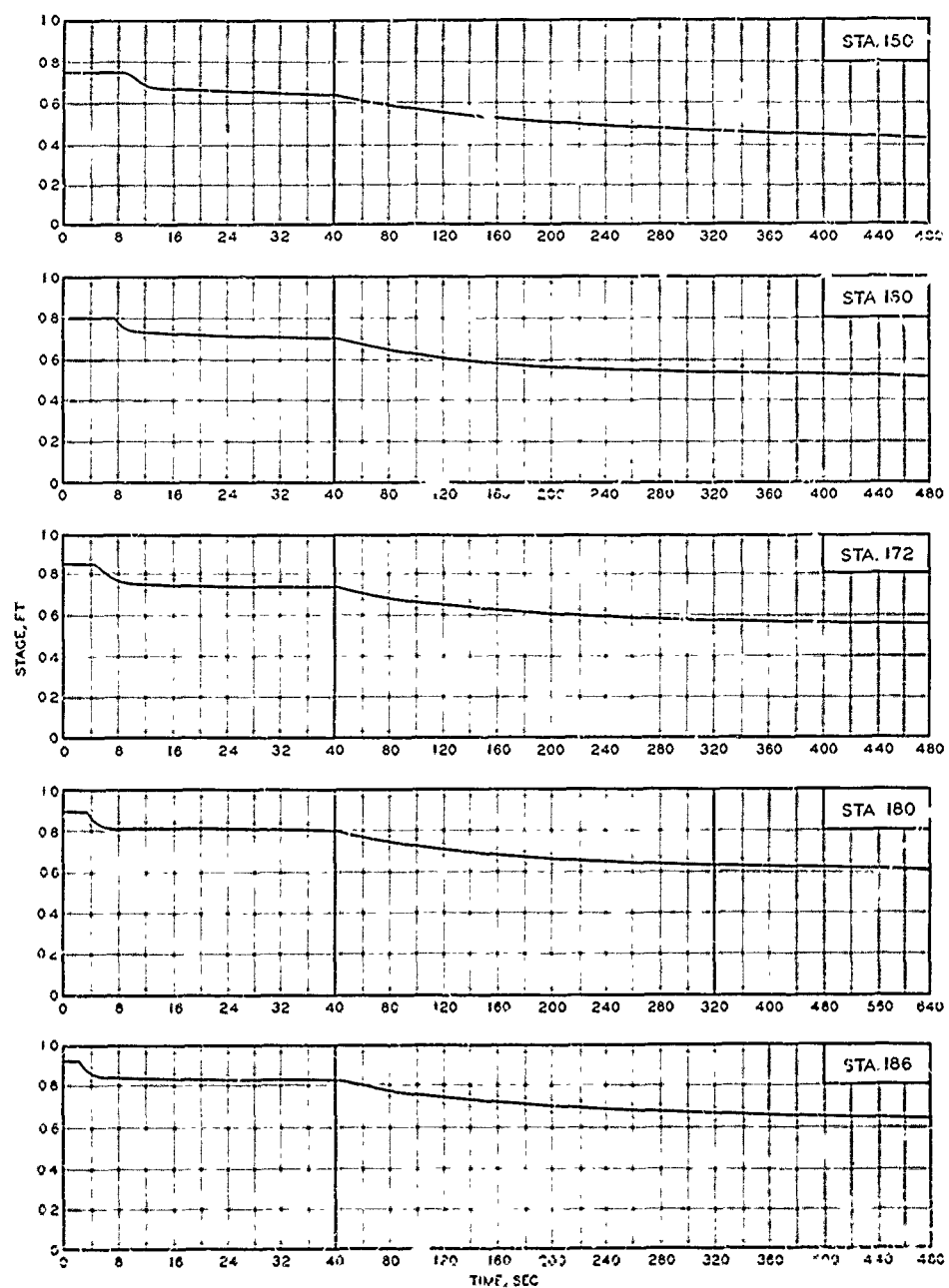
STAGE - TIME HYDROGRAPHS  
STATIONS 190, 194, 196, 198, AND 199  
TEST CONDITION 7.2



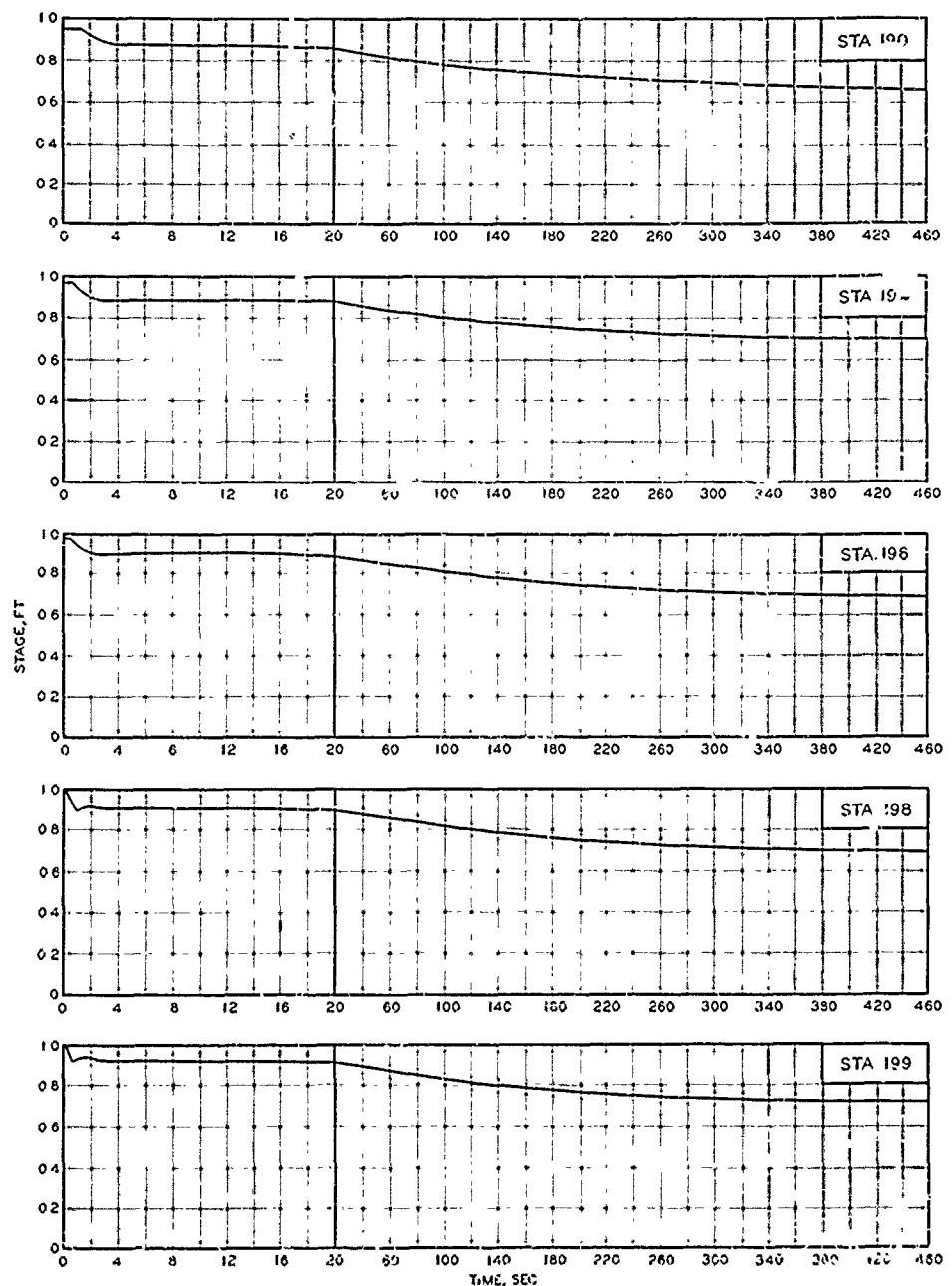
STAGE-TIME HYDROGRAPHS  
STATIONS 200, 225, 280, AND 350  
TEST CONDITION 7.2



STAGE-TIME HYDROGRAPHS  
STATIONS 40, 70, 100, 120, AND 140  
TEST CONDITION 8.2



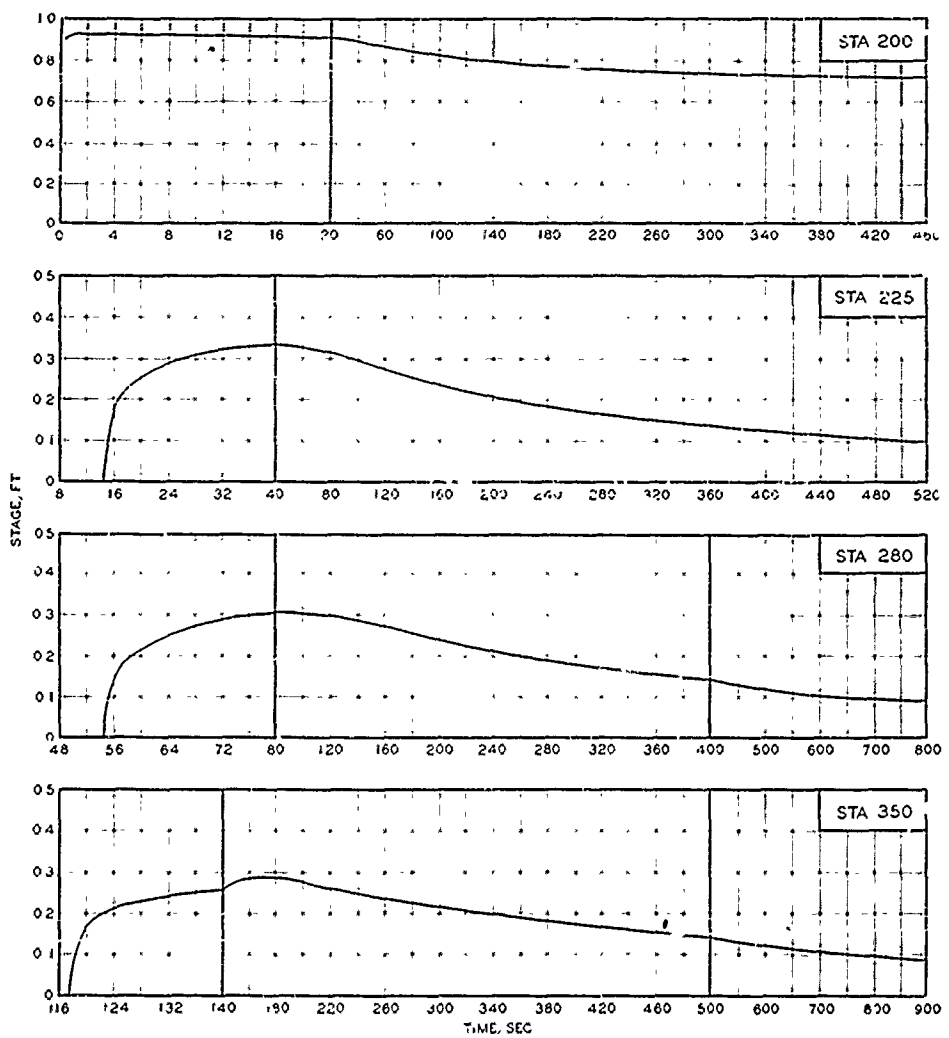
STAGE-TIME HYDROGRAPHS  
STATIONS 150, 160, 172, 180, AND 186  
TEST CONDITION 8.2



### STAGE - TIME HYDROGRAPHS

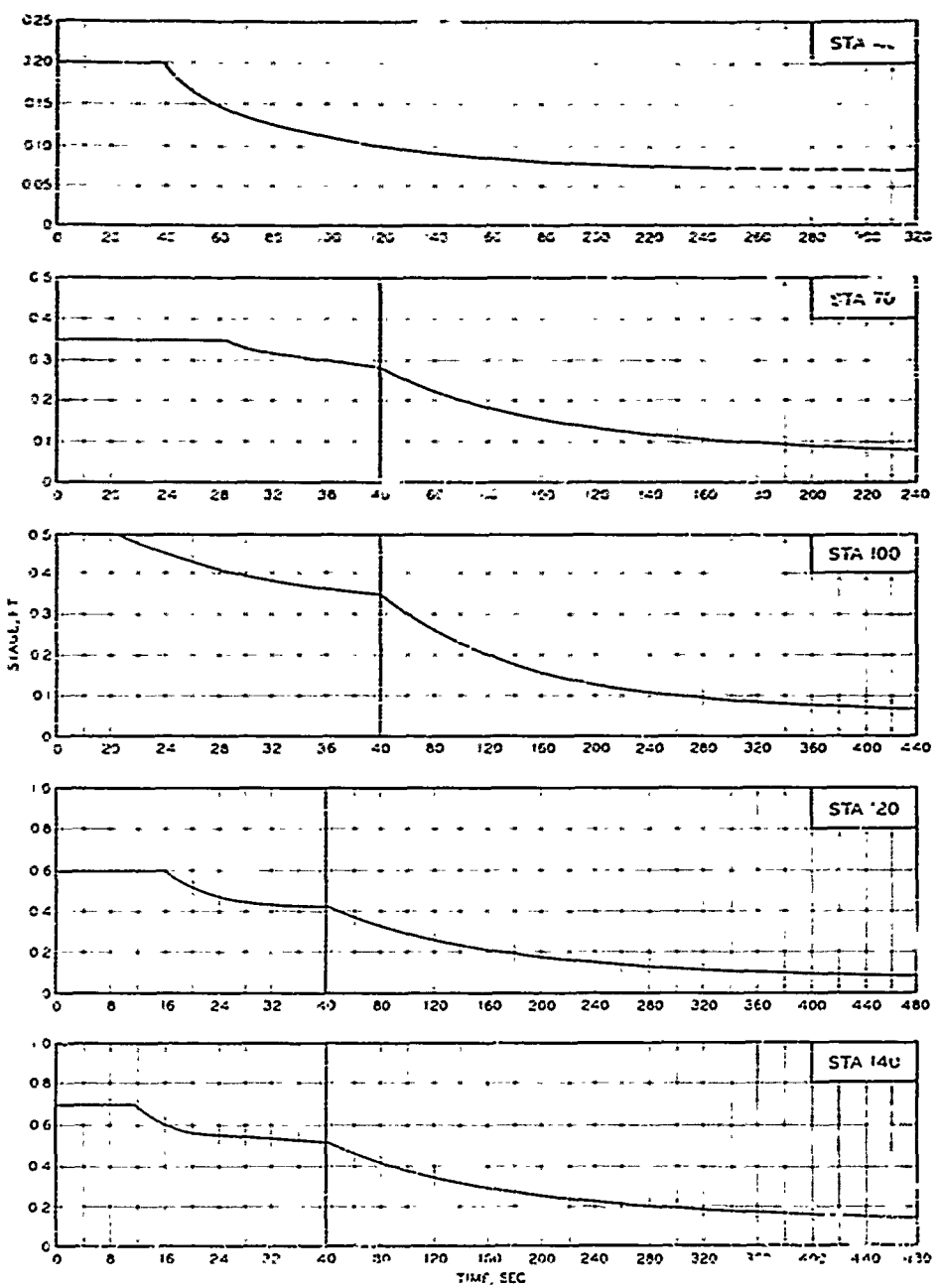
STATIONS 190, 194, 196, 198, AND 199

TEST CONDITION 8.2

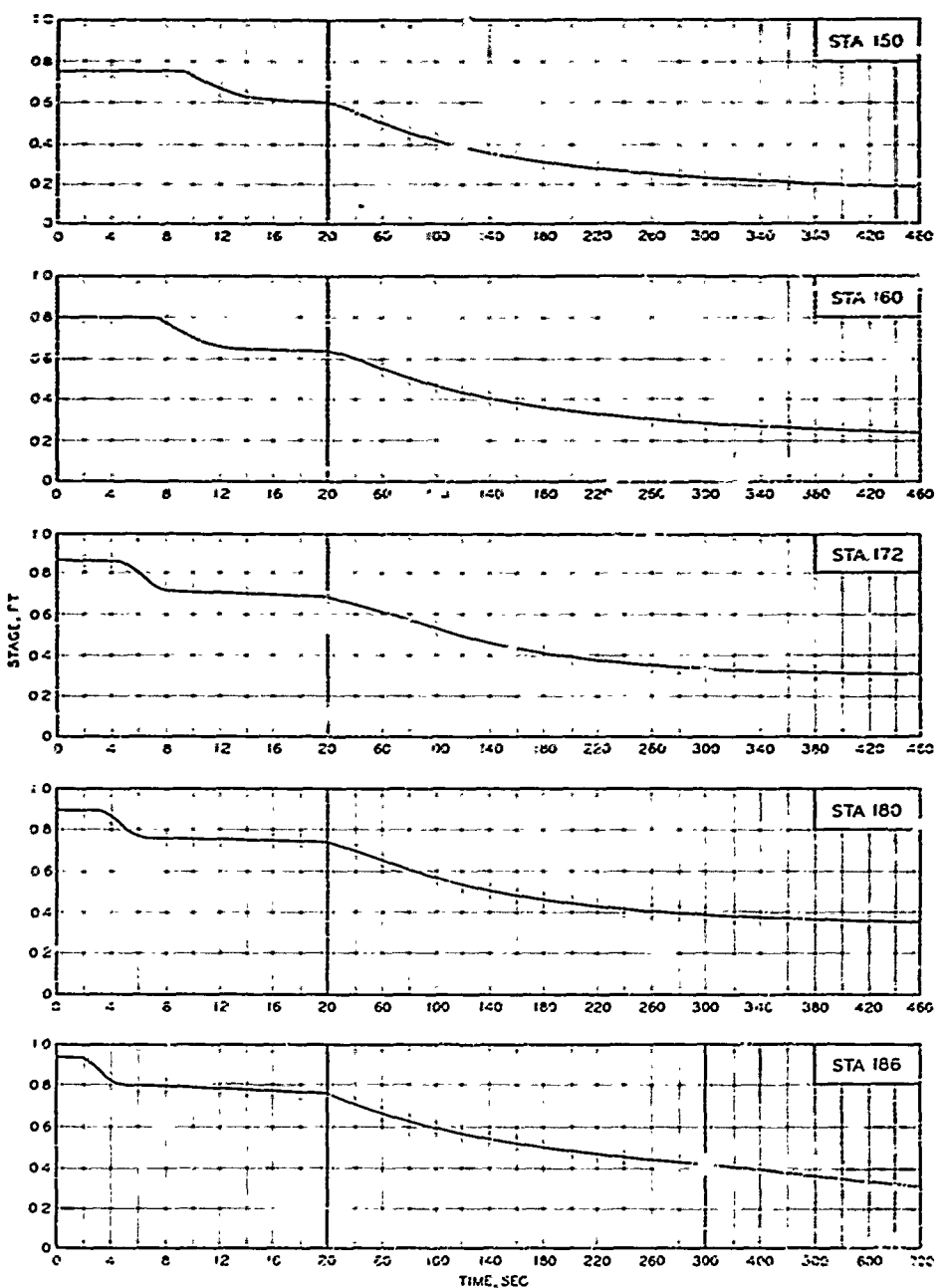


STAGE-TIME HYDROGRAPHS  
STATIONS 200, 225, 280, AND 350  
TEST CONDITION 8.2

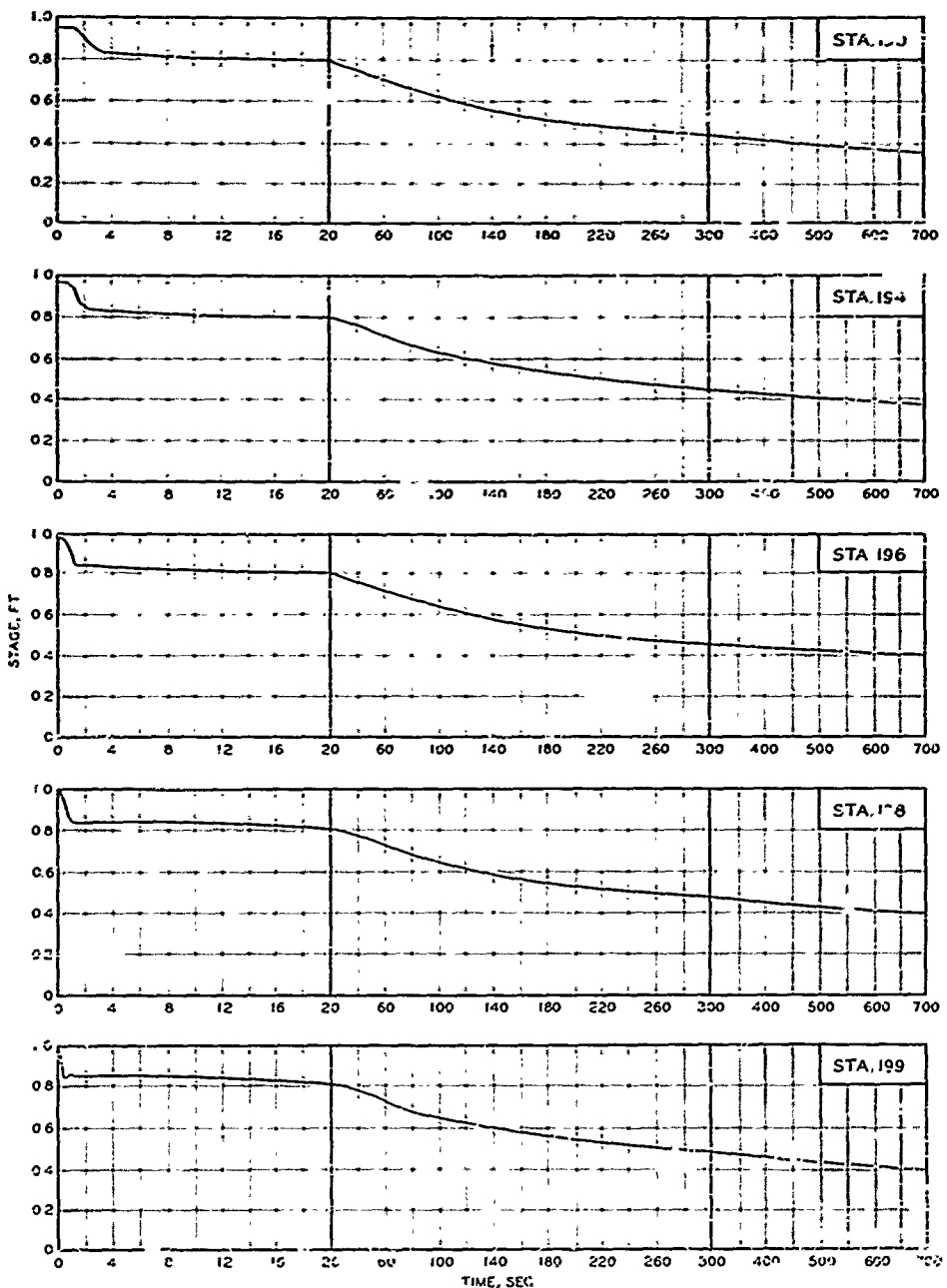
PLATE 26



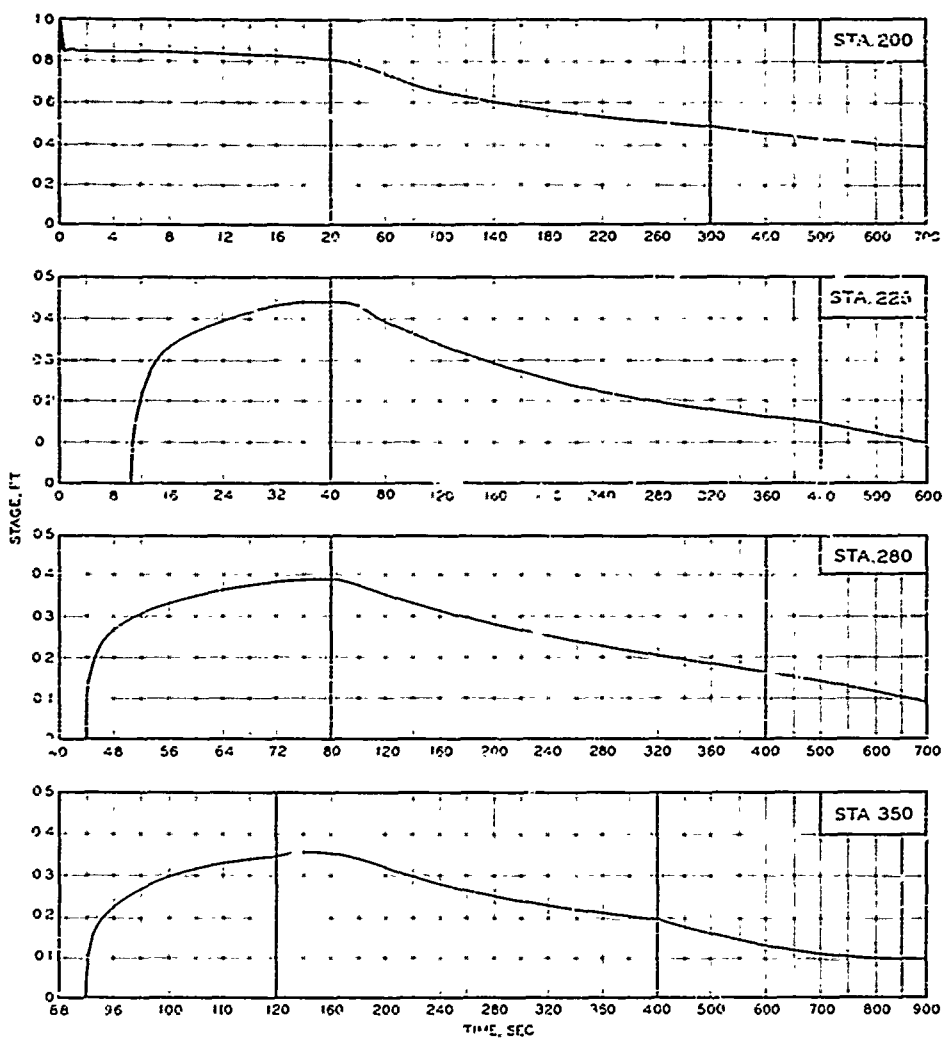
STAGE-TIME HYDROGRAPHS  
STATIONS 40, 70, 100, 120, AND 140  
TEST CONDITION II.2



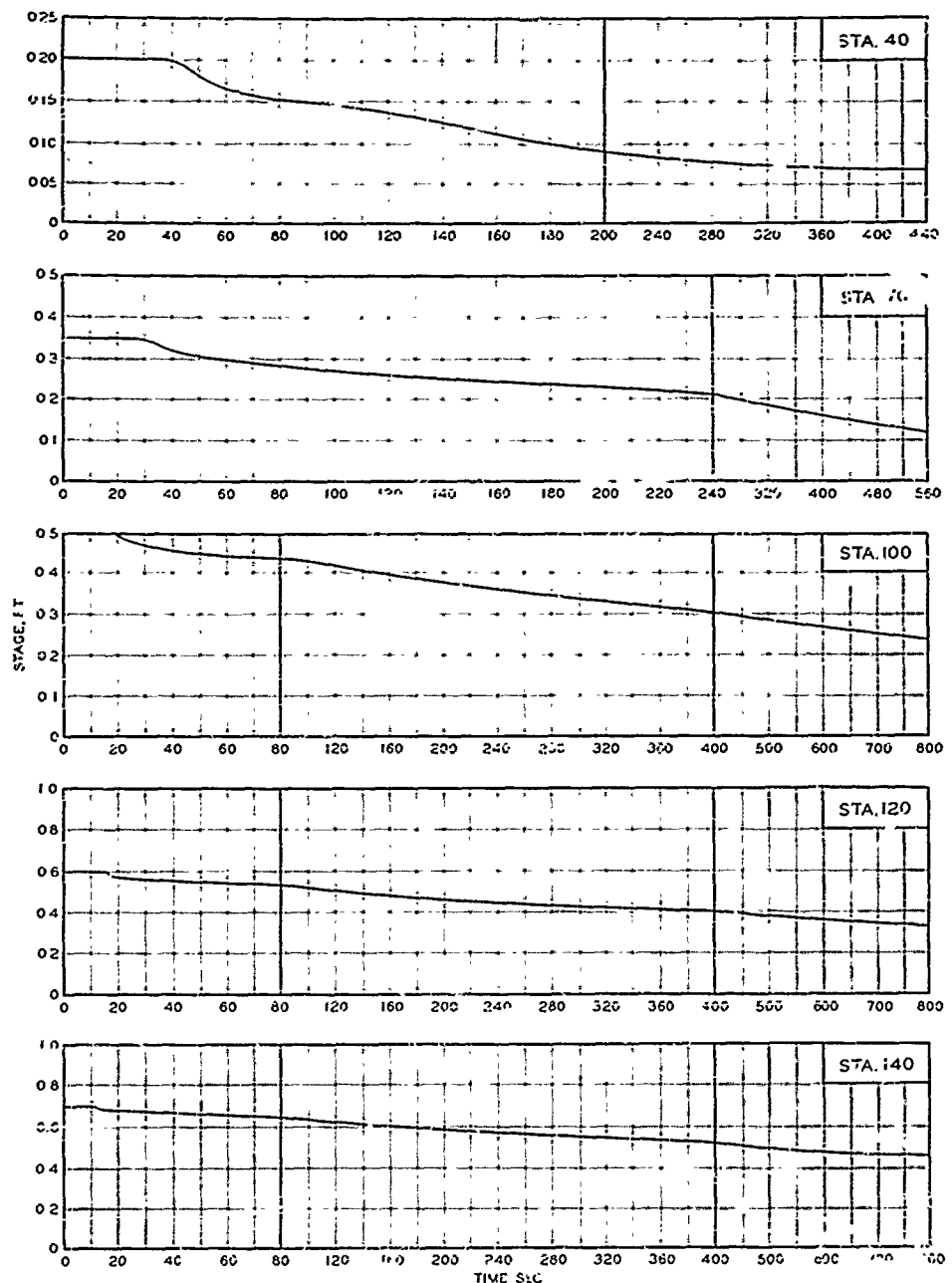
STAGE-TIME HYDROGRAPHS  
STATIONS 150, 160, 172, 180, AND 186  
TEST CONDITION II.2



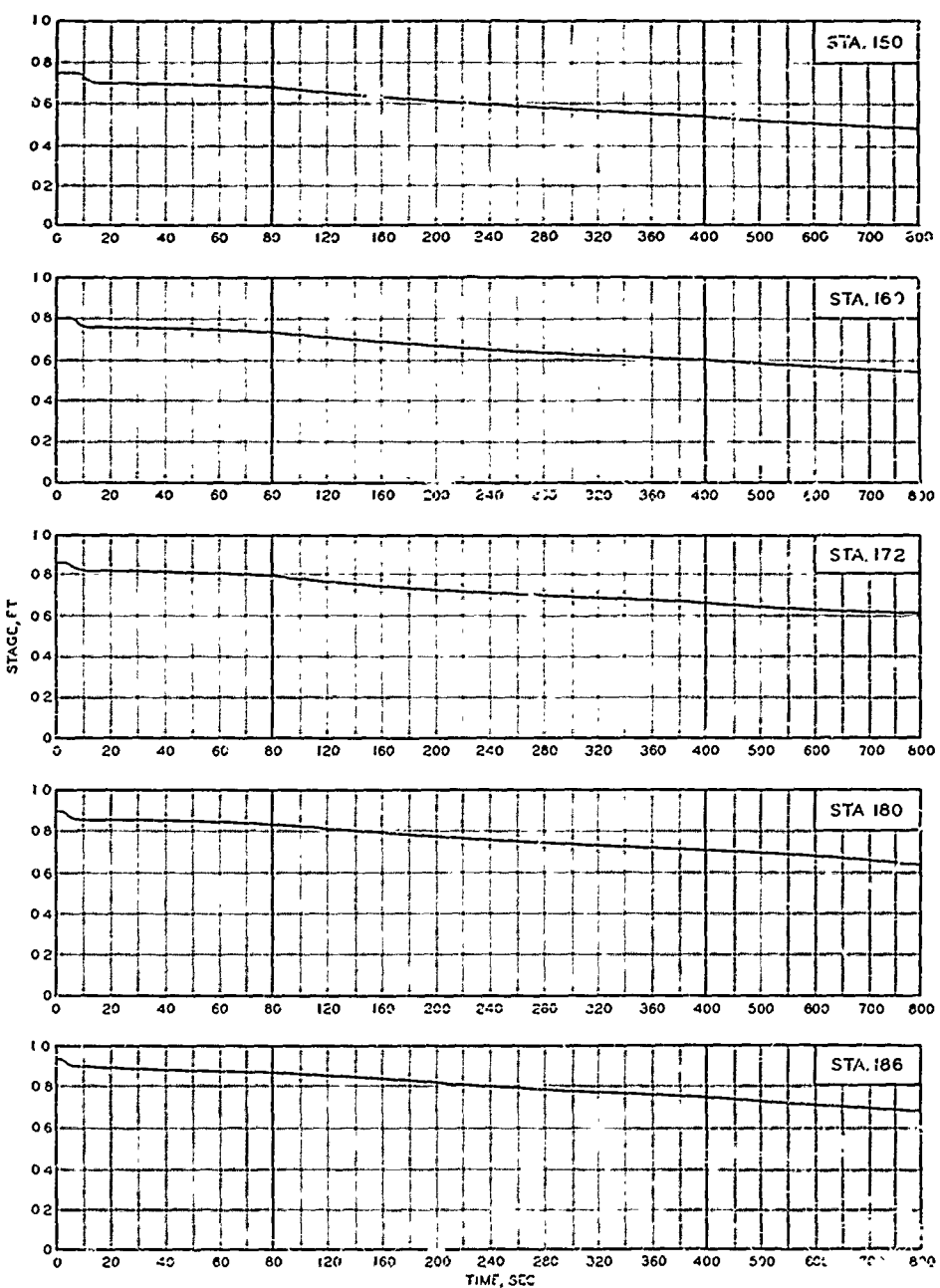
STAGE-TIME HYDROGRAPHS  
STATIONS 190, 194, 196, 198, AND 199  
TEST CONDITION 11.2



STAGE-TIME HYDROGRAPHS  
STATIONS 200, 225, 280, AND 350  
TEST CONDITION 11.2



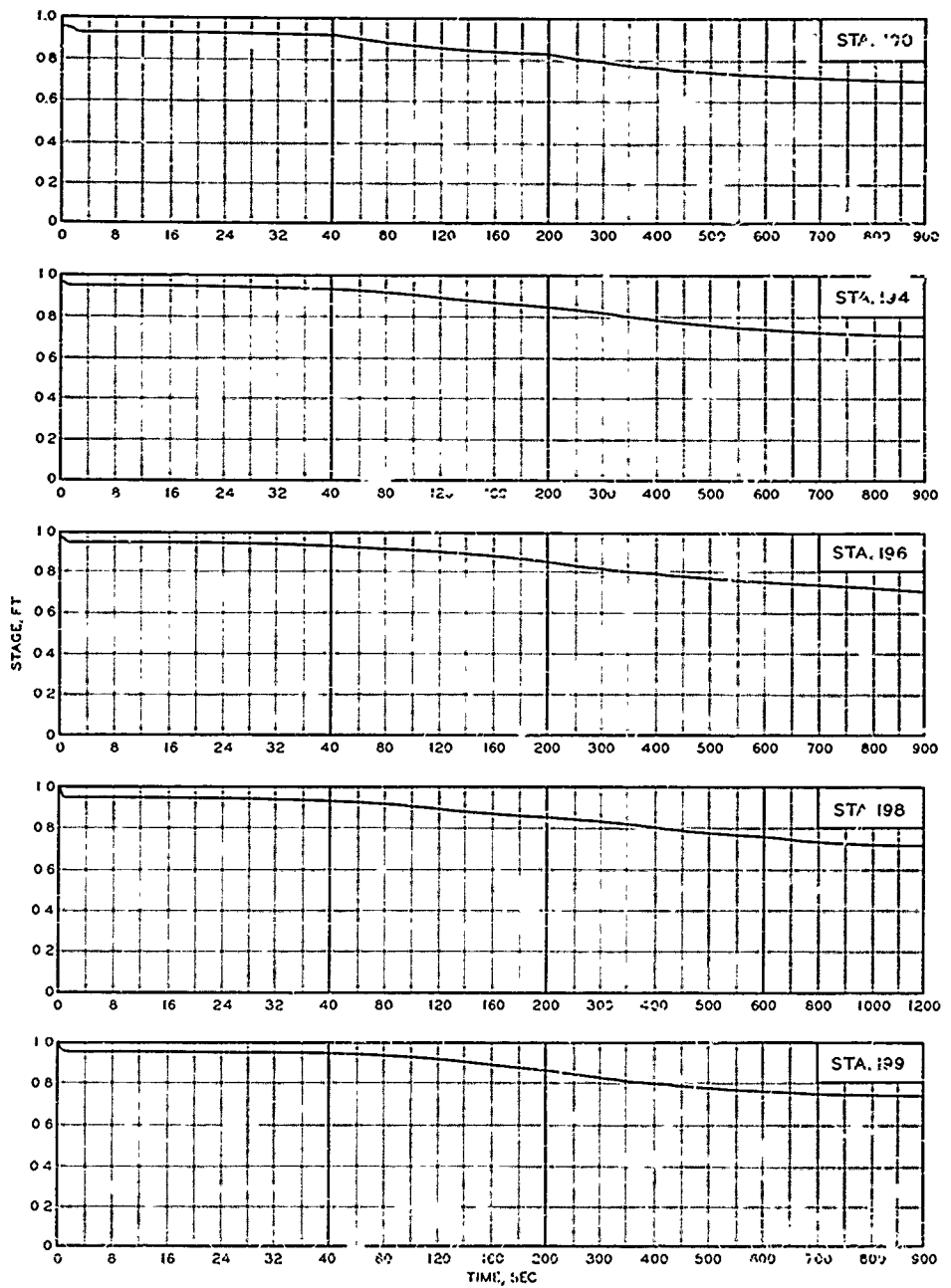
STAGE-TIME HYDROGRAPHS  
STATIONS 40, 70, 100, 120, AND 140  
TEST CONDITION 12.2



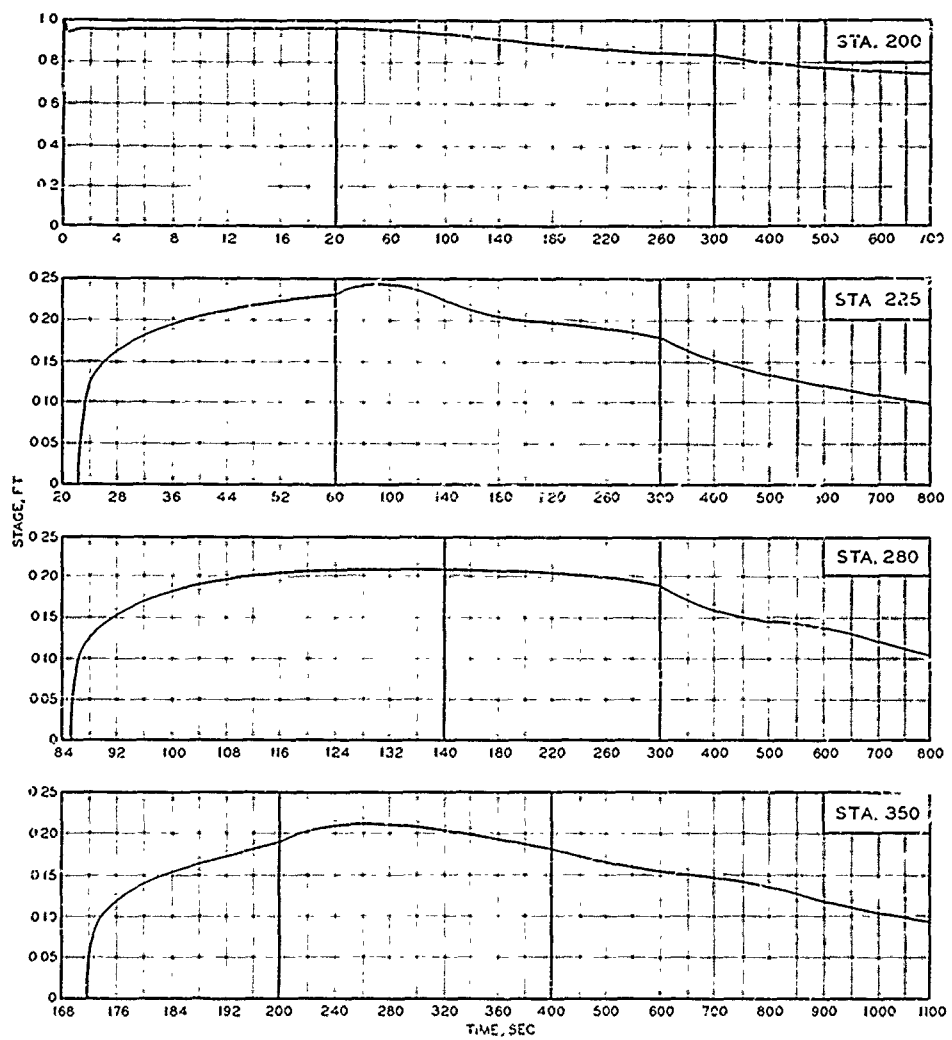
#### STAGE-TIME HYDROGRAPHS

STATIONS 150, 160, 172, 180, AND 186

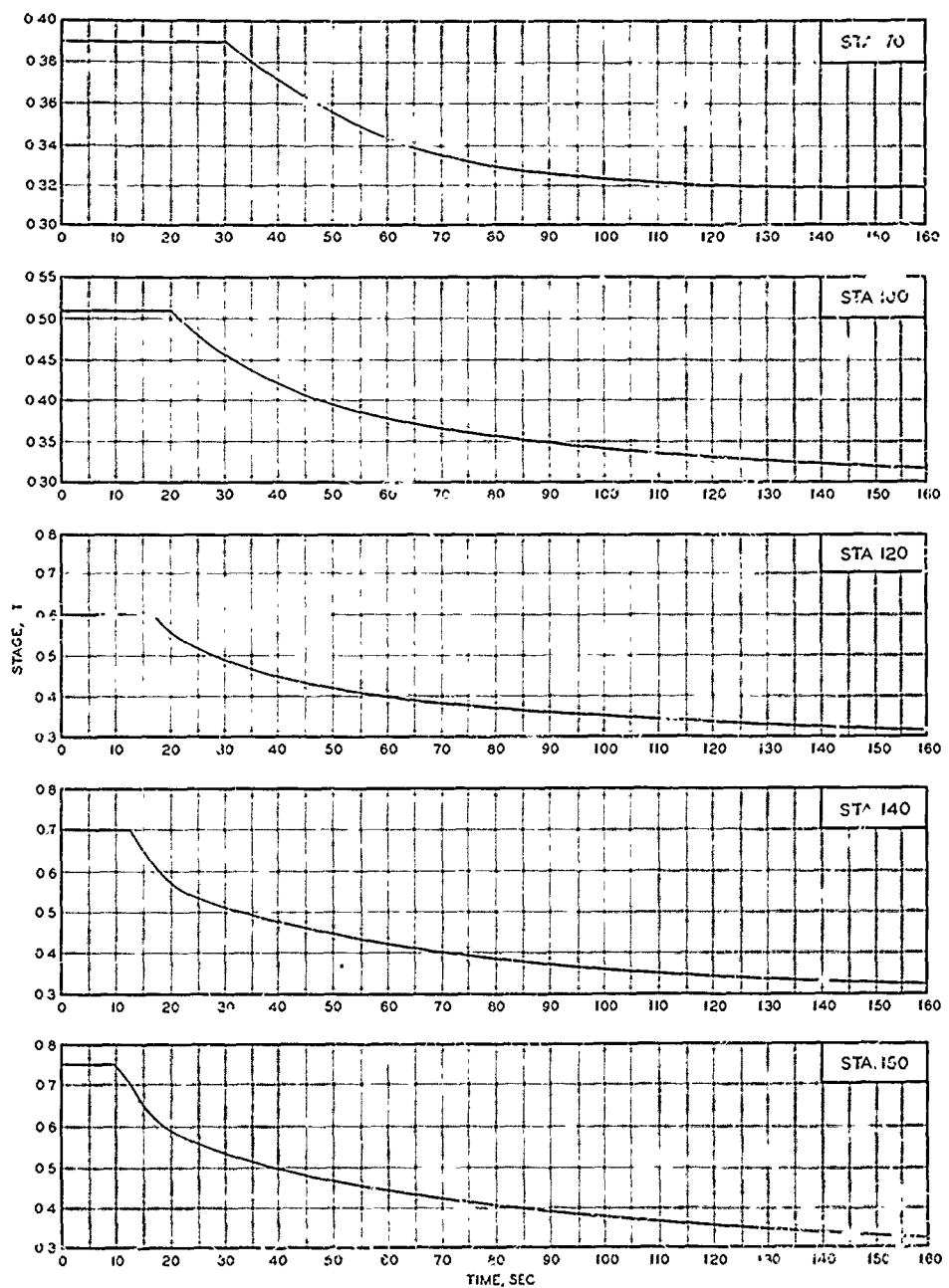
TEST CONDITION 12.2



STAGE-TIME HYDROGRAPHS  
STATIONS 190, 194, 196, 198, AND 199  
TEST CONDITION 12.2

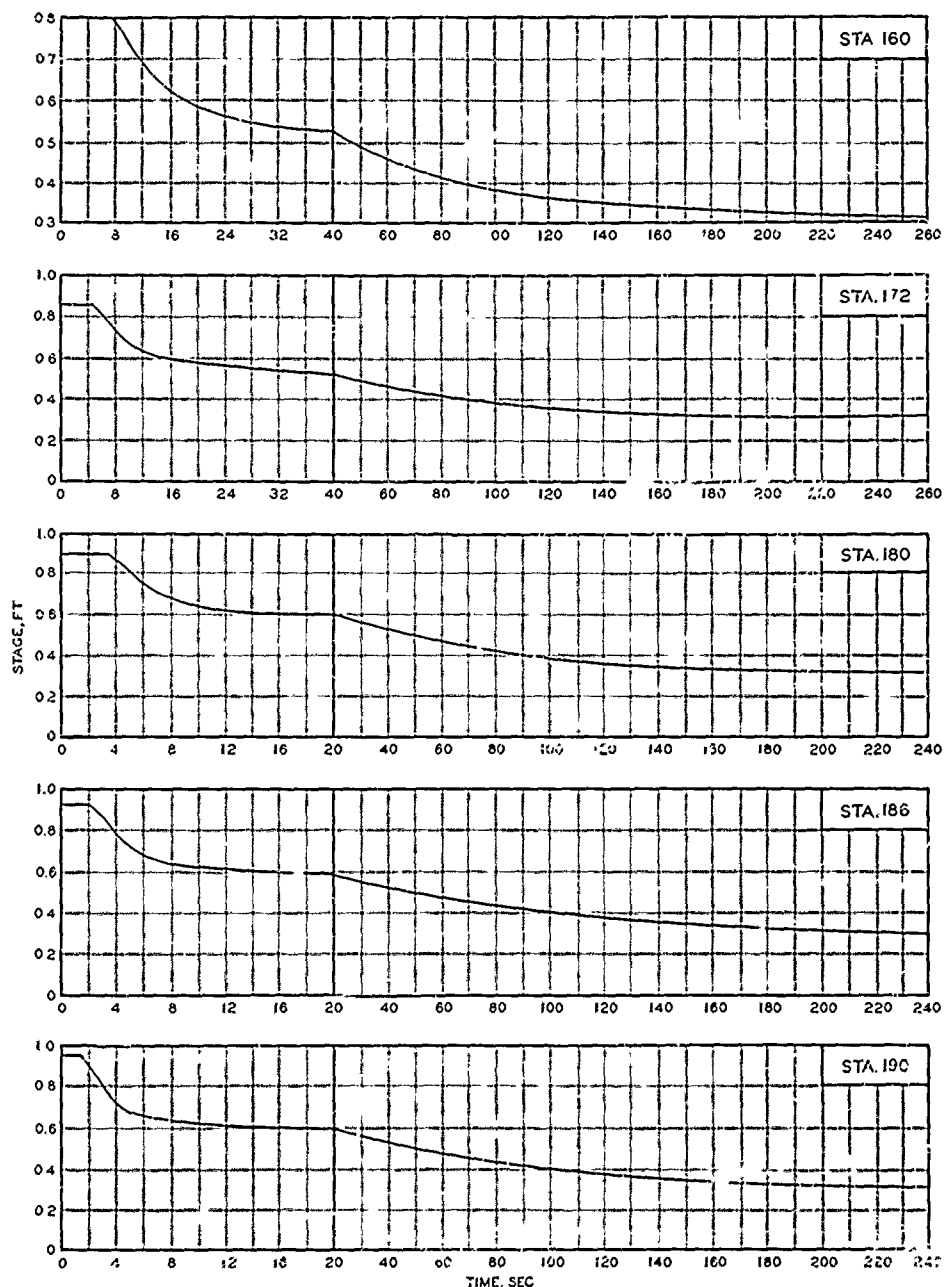


STAGE-TIME HYDROGRAPHS  
STATIONS 200, 225, 280, AND 350  
TEST CONDITION 12.2

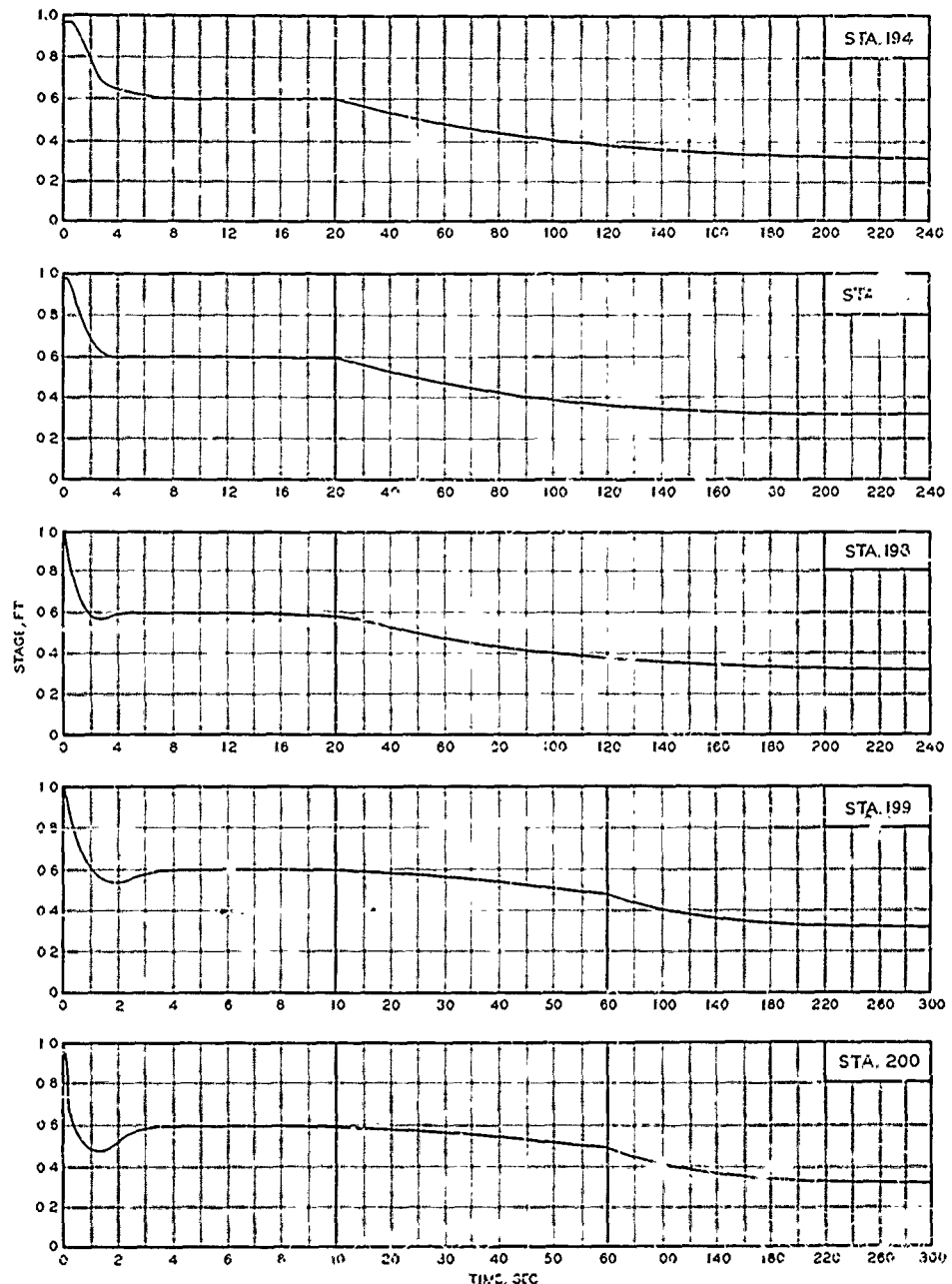


### STAGE - TIME HYDROGRAPHS

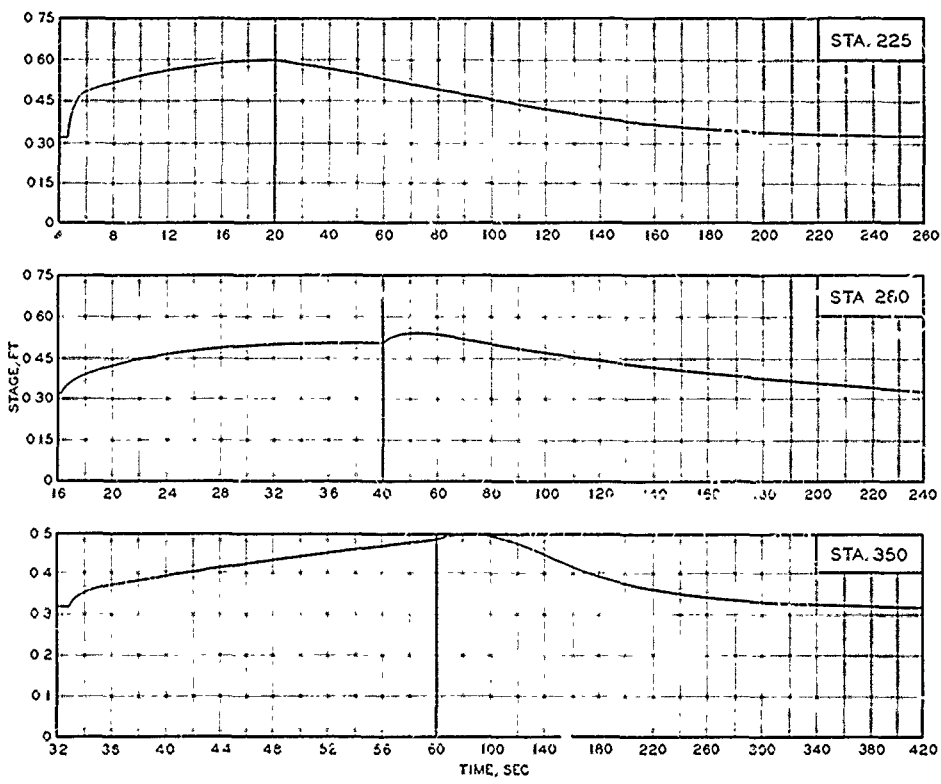
STATIONS 70, 100, 120, 140, AND 150  
TEST CONDITION 1.2(32)



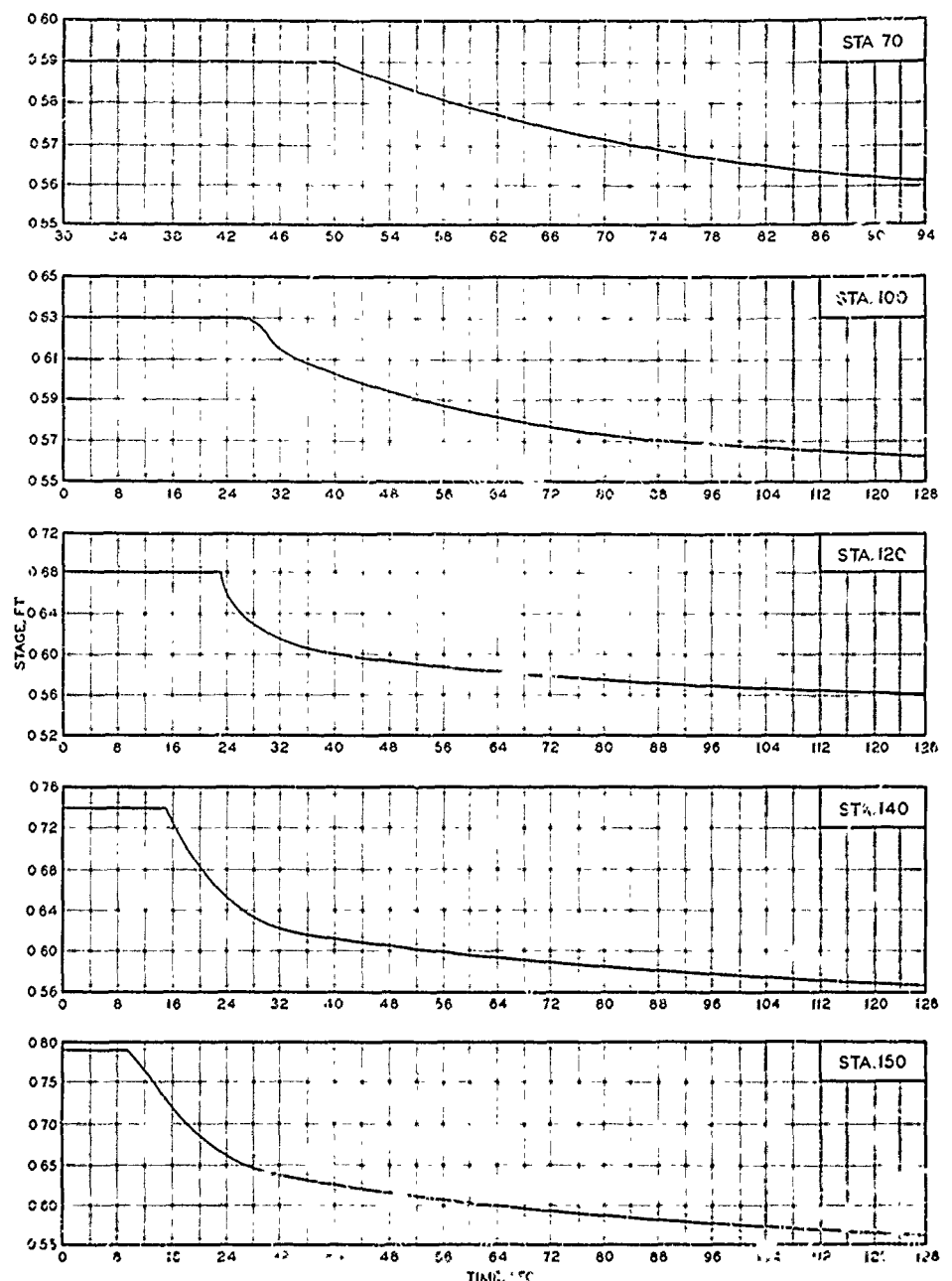
STAGE- TIME HYDROGRAPHS  
STATIONS I60, I72, I80, I86, AND I90  
TEST CONDITION 1.2 (32)



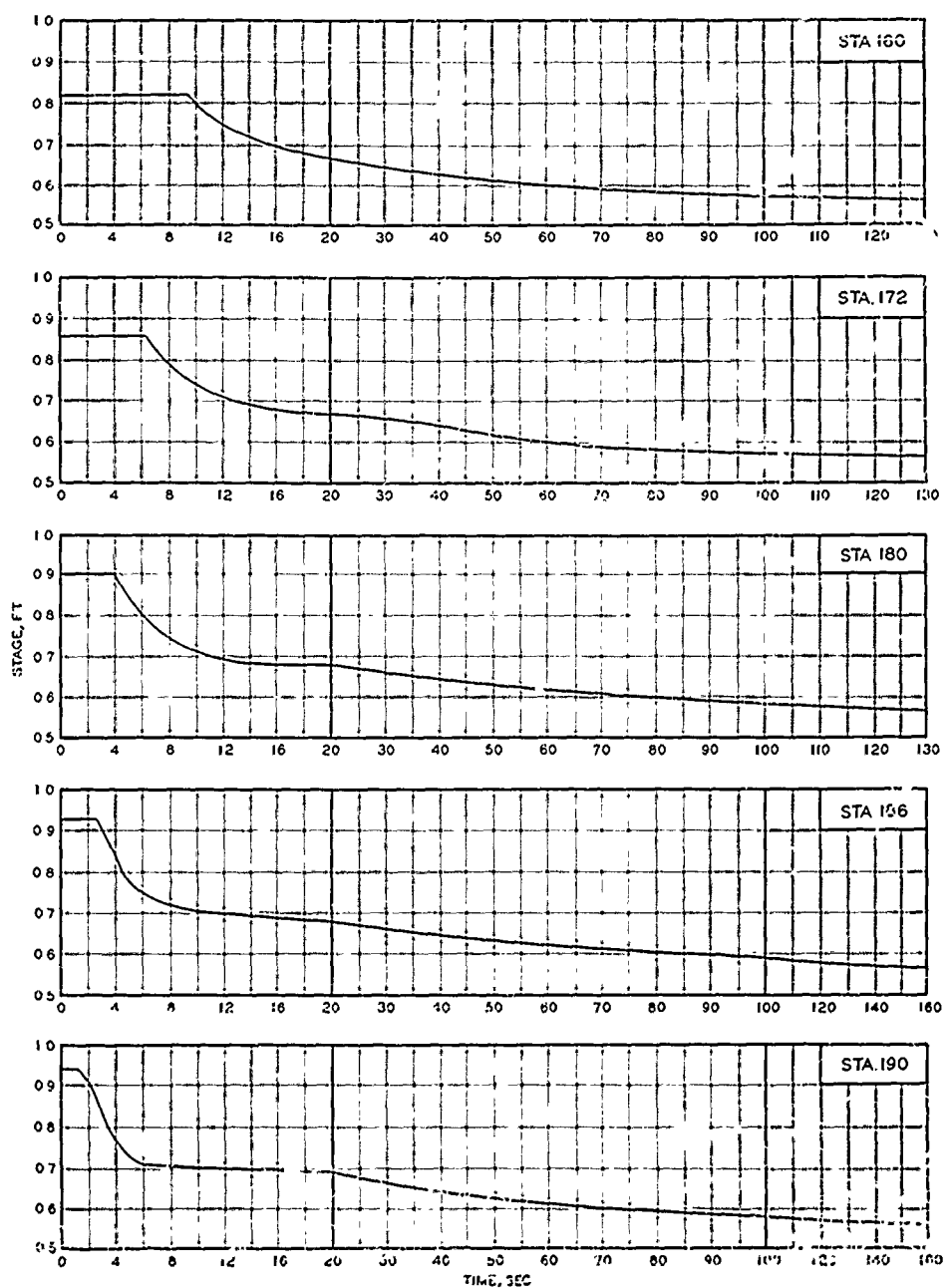
STAGE - TIME HYDROGRAPHS  
STATIONS 194, 196, 198, 199, AND 200  
TEST CONDITION I.2 (32)



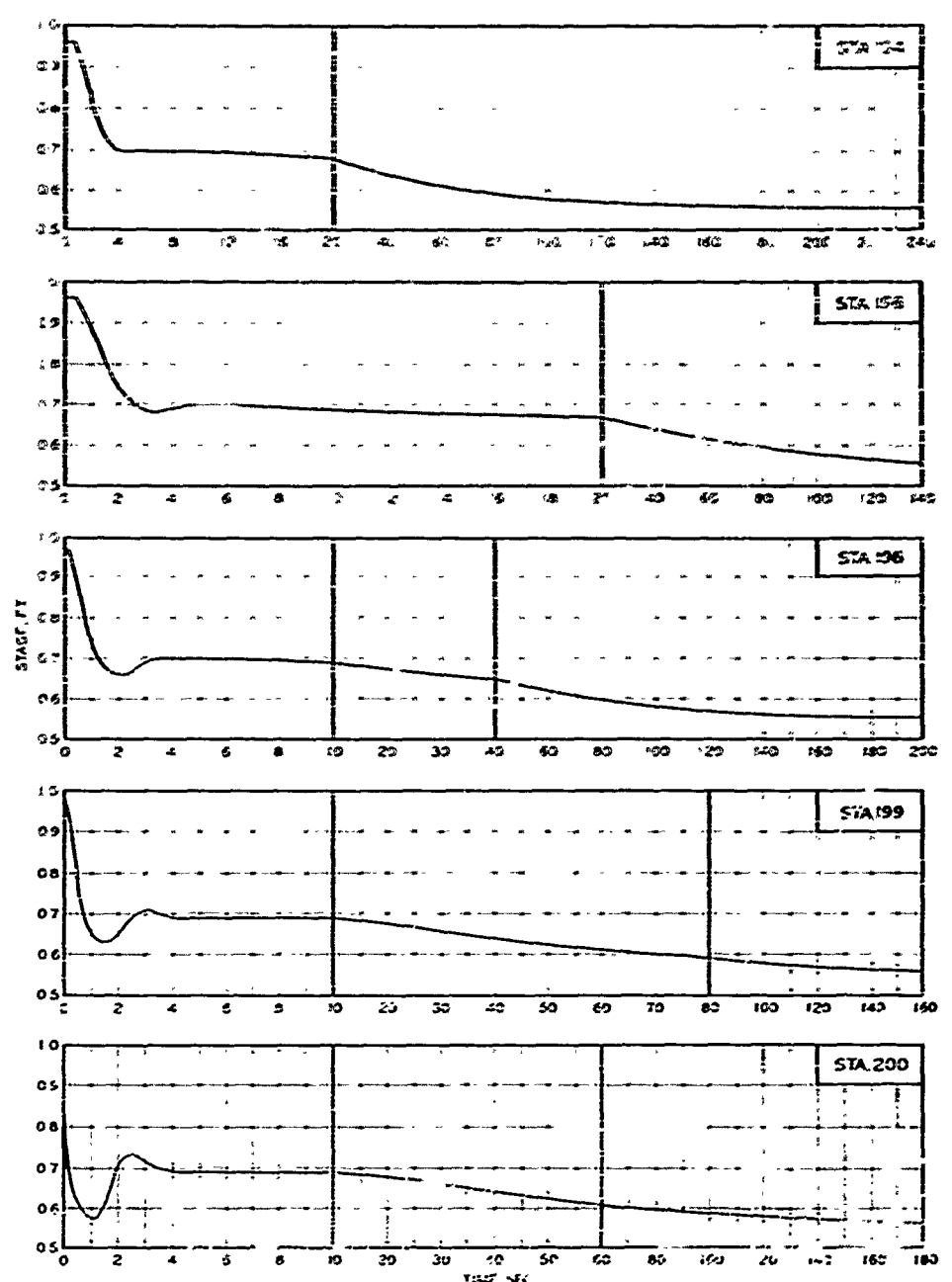
STAGE-TIME HYDROGRAPHS  
STATIONS 225, 280, AND 350  
TEST CONDITION I.2 (32)



STAGE - TIME HYDROGRAPHS  
STATIONS 70, 100, 120, 140, AND 150  
TEST CONDITION I.2(56)



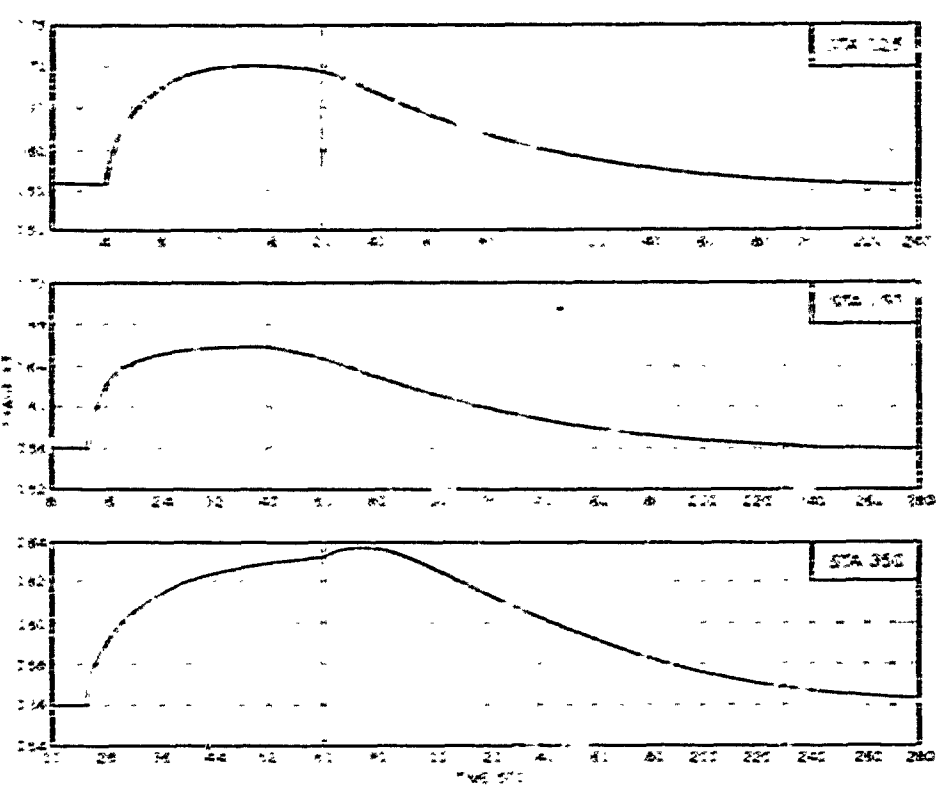
STAGE-TIME HYDROGRAPHS  
STATIONS 160, 172, 180, 156, AND 190  
TEST CONDITION 1.2 (56)



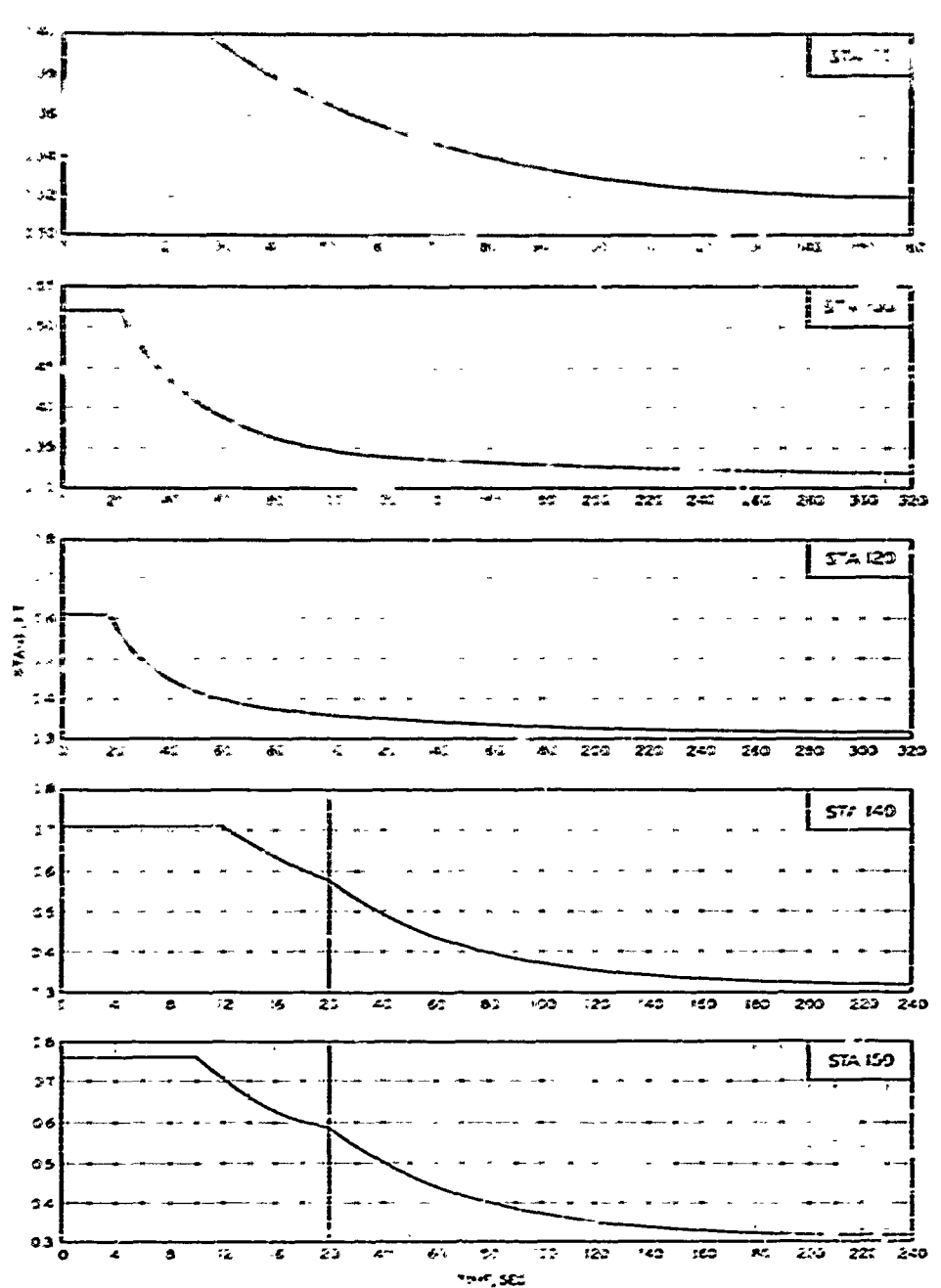
### STAGE - TIME HYDROGRAPHS

STATIONS 194, 196, 198, 199, AND 200

TEST CONDITION I.2 (56)



STAGE-TIME HYDROGRAPHS  
STATIONS 225, 280, AND 350  
TEST CONDITION 1.2(56)



STAGE-TIME HYDROGRAPHS  
STATIONS 70, 100, 120, 140, AND 150  
TEST CONDITION 2.2(32)

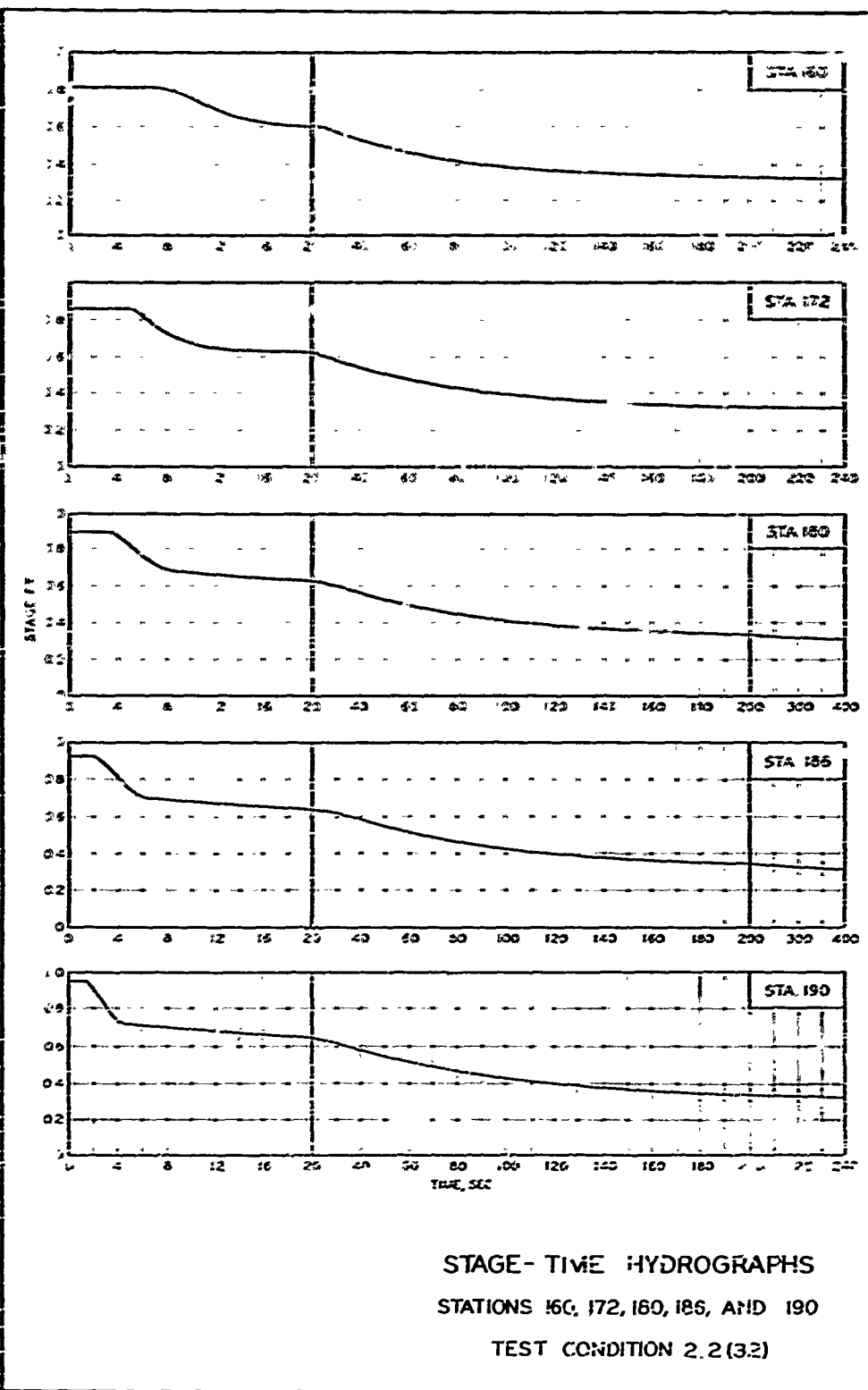
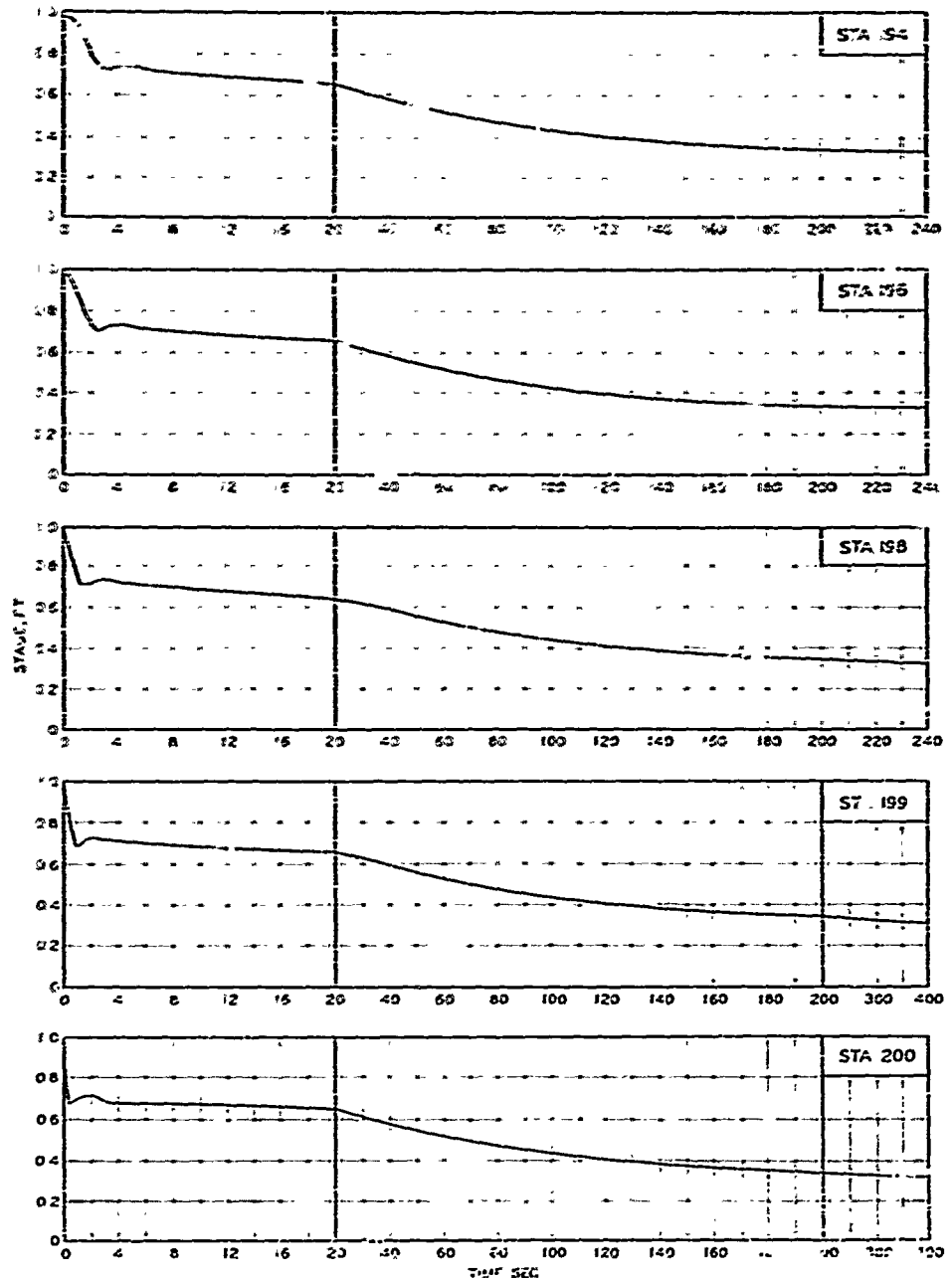
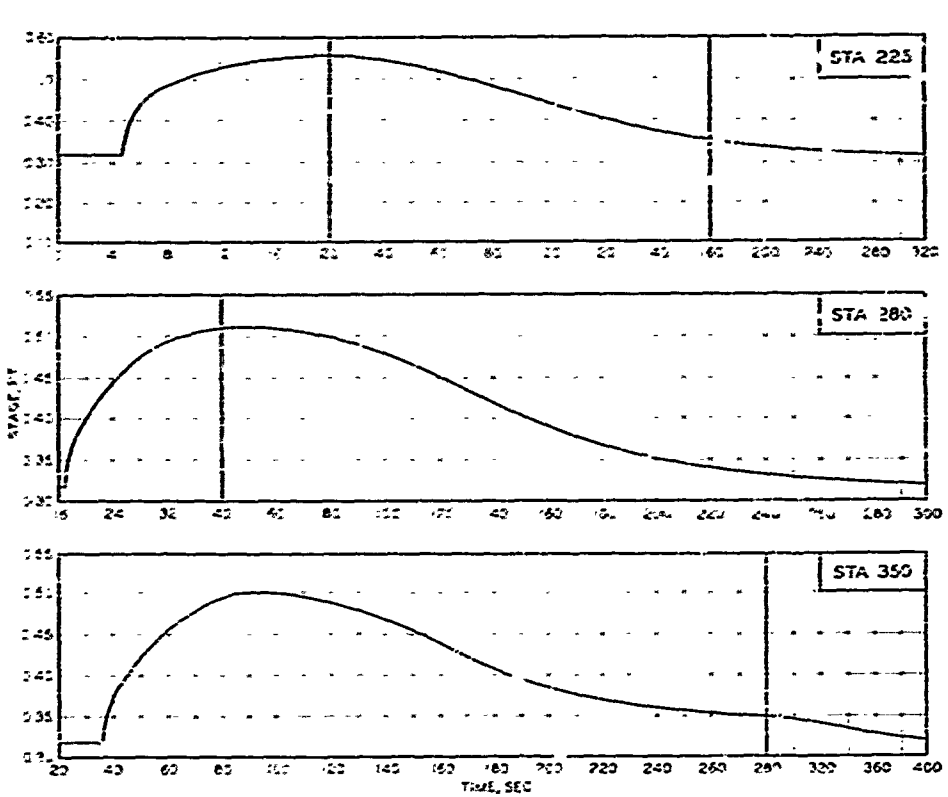


PLATE 46

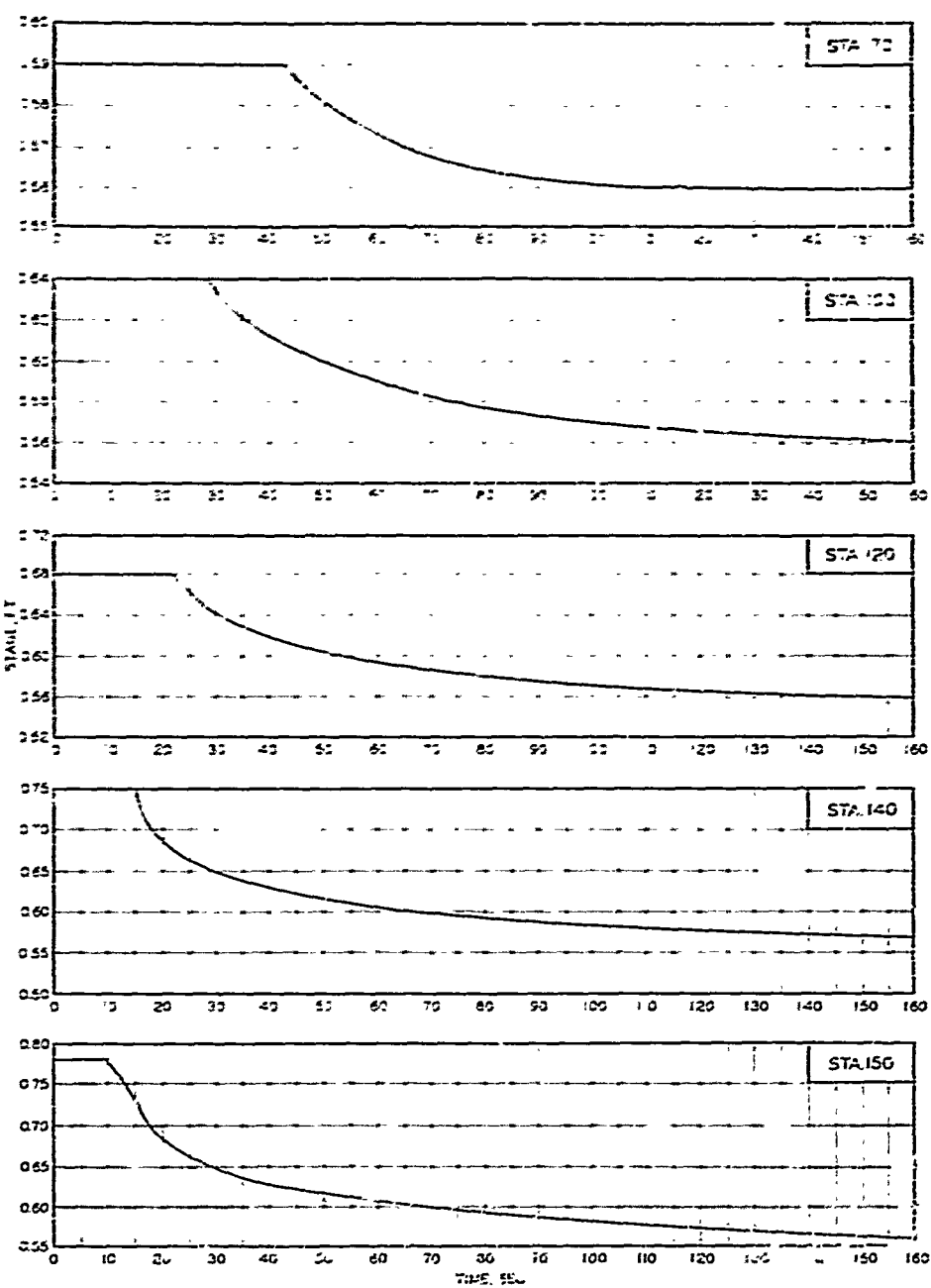


STAGE - TIME HYDROGRAPHS  
STATIONS 194, 196, 198, 199, AND 200  
TEST CONDITION 2.2(32)

PLATE 47



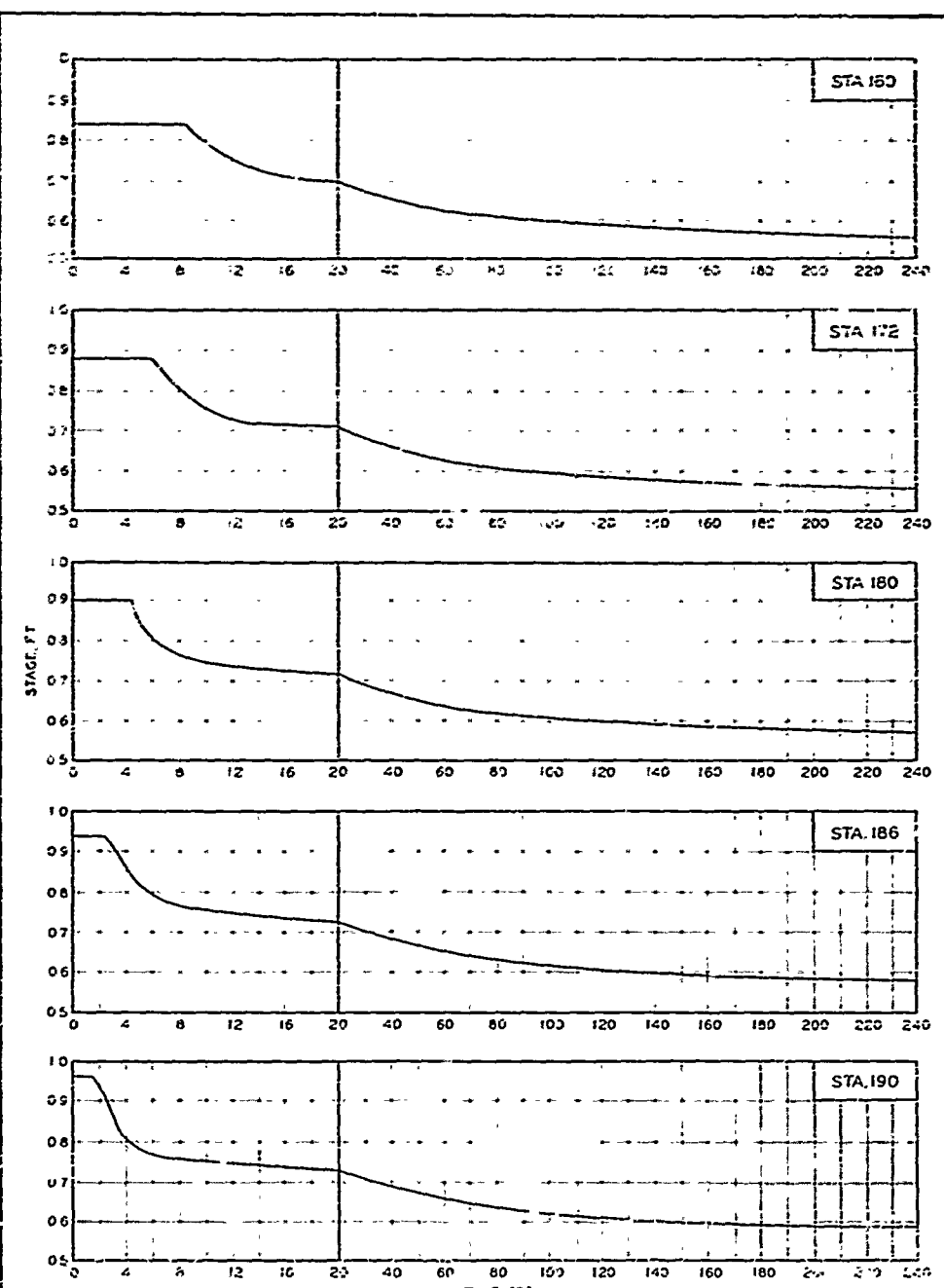
STAGE-TIME HYDROGRAPHS  
STATIONS 225, 280, AND 350  
TEST CONDITION 2.2(32)



### STAGE - TIME HYDROGRAPHS

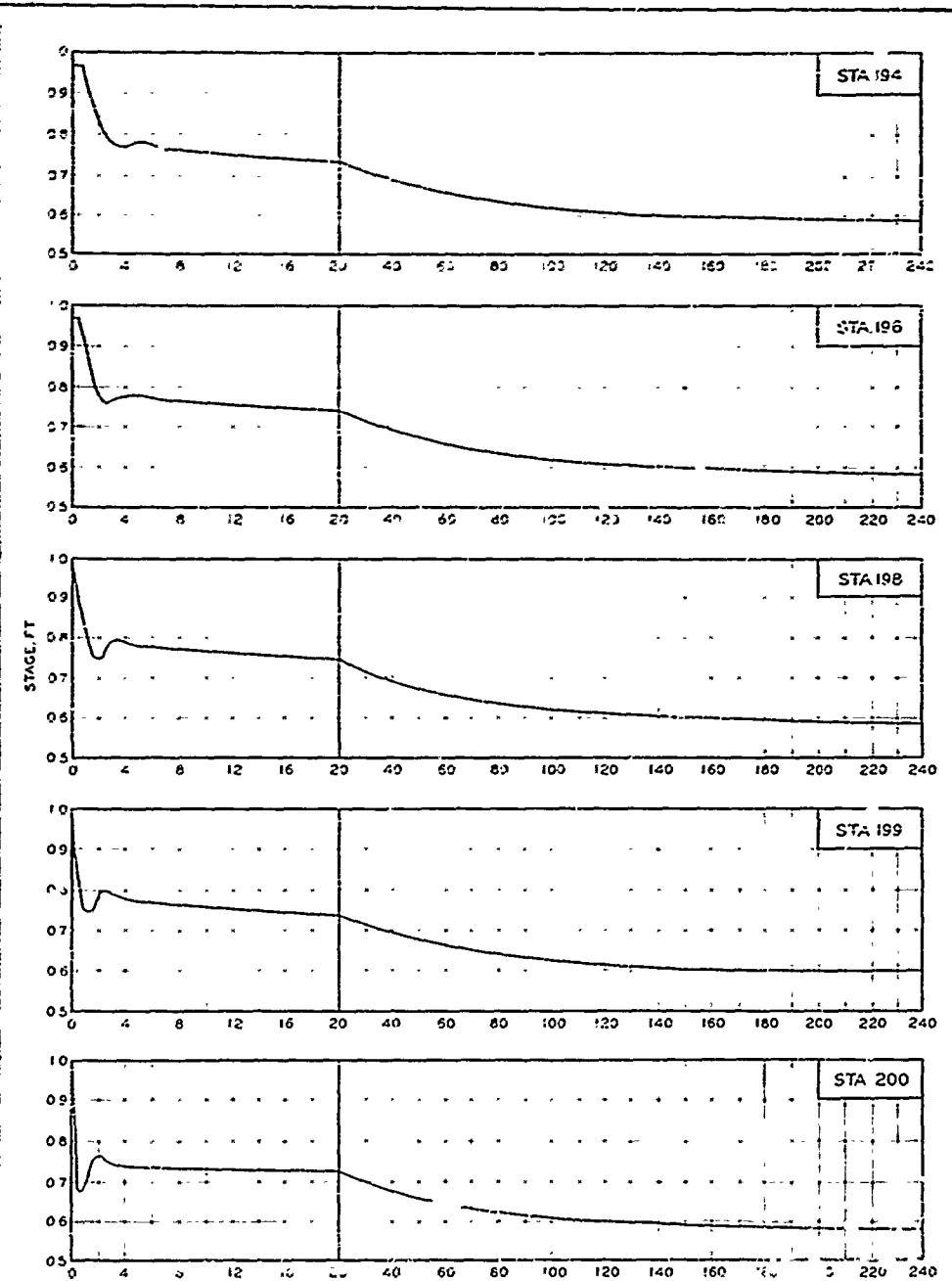
STATIONS 70, 100, 120, 140, AND 150

TEST CONDITION 2.2 (56)

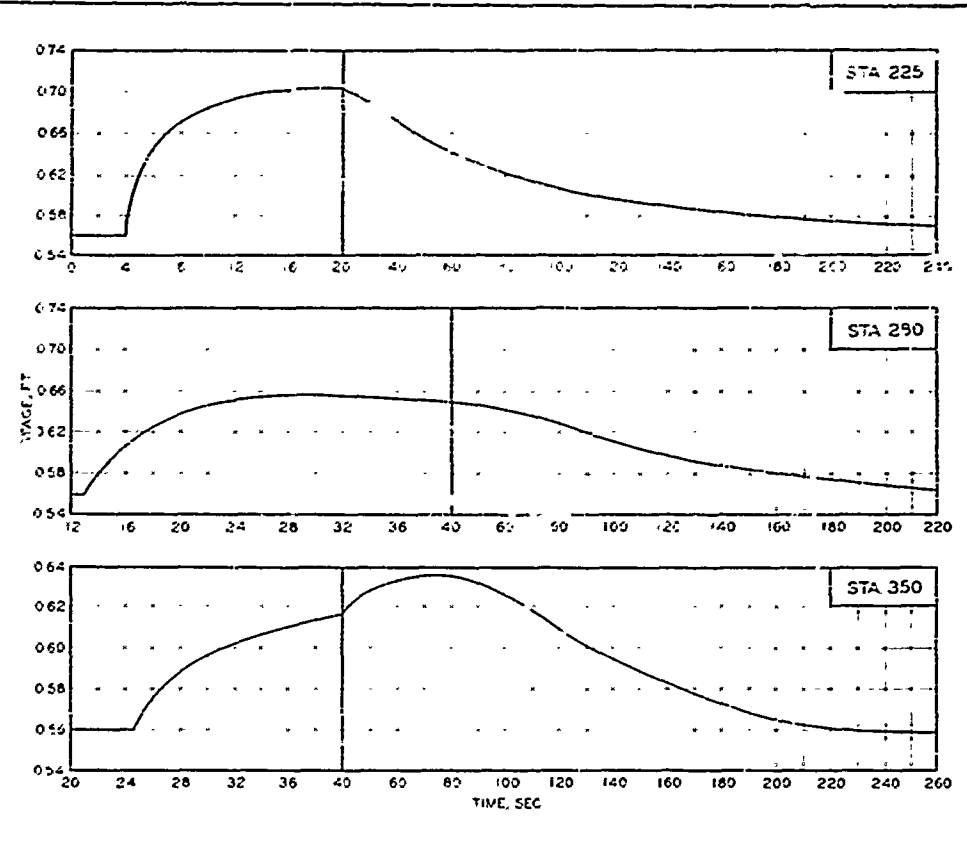


STAGE-TIME HYDROGRAPHS  
STATIONS 160, 172, 180, 186, AND 190  
TEST CONDITION 2.2 (56)

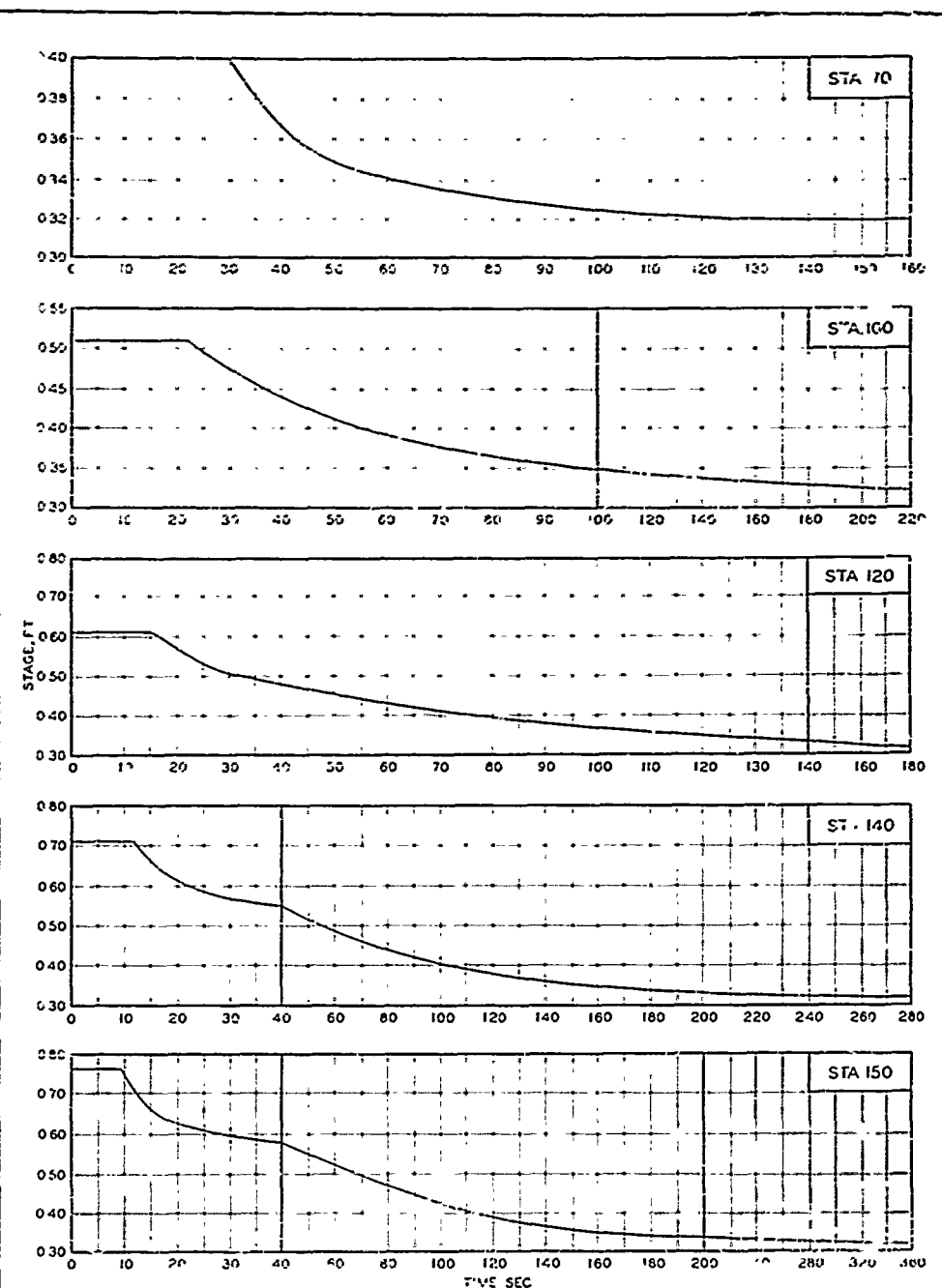
PLATE 50



STAGE - TIME HYDROGRAPHS  
STATIONS 194, 196, 198, 199, AND 200  
TEST CONDITION 2.2 (56)

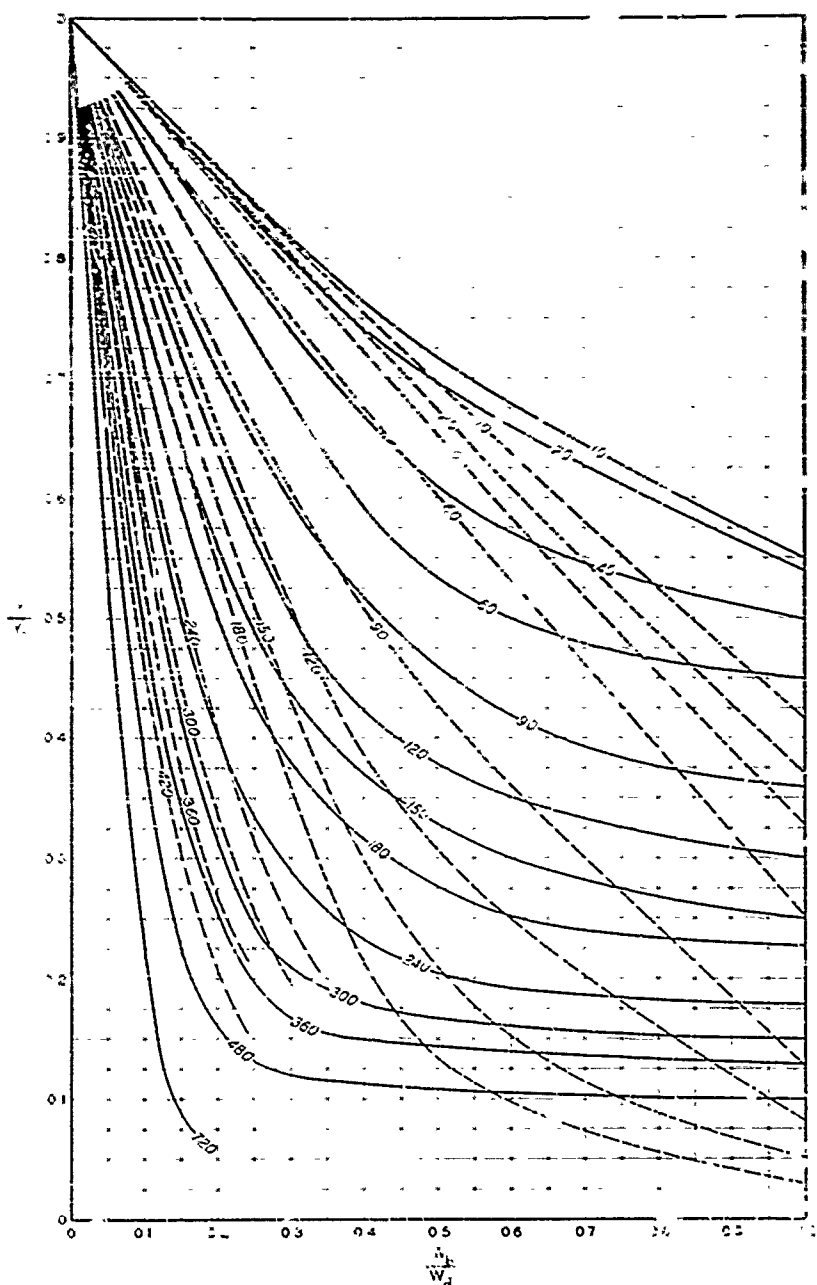


STAGE-TIME HYDROGRAPHS  
STATIONS 225, 280, AND 350  
TEST CONDITION 2.2 (56)



STAGE - TIME HYDROGRAPHS

STATIONS 70, 100, 120, 140, AND 150  
TEST CONDITION 3.2 (32)

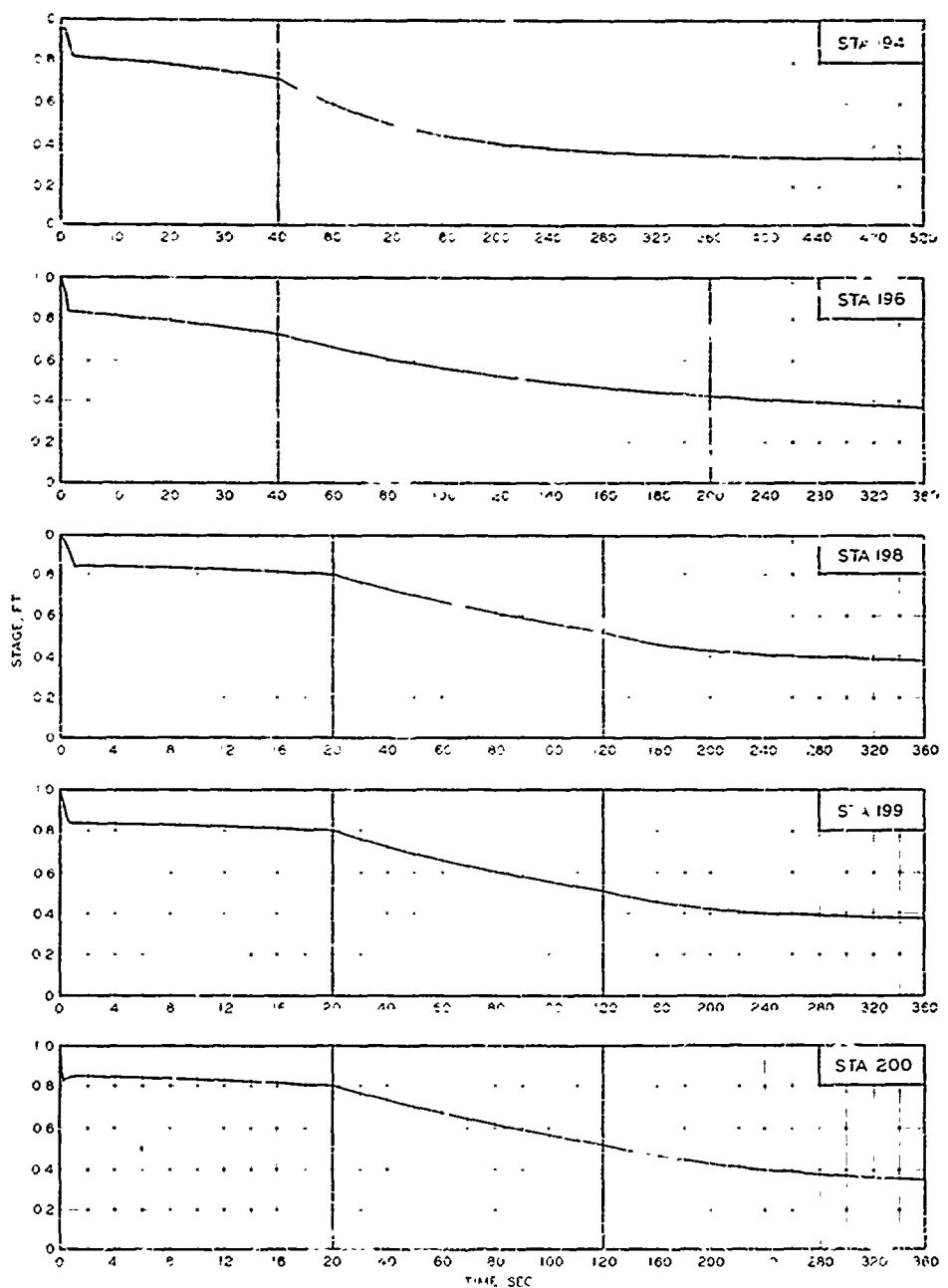


NOTE: NUMERICAL VALUE ON EACH CURVE  
INDICATES TIME IN SECONDS AFTER DAM BREACH

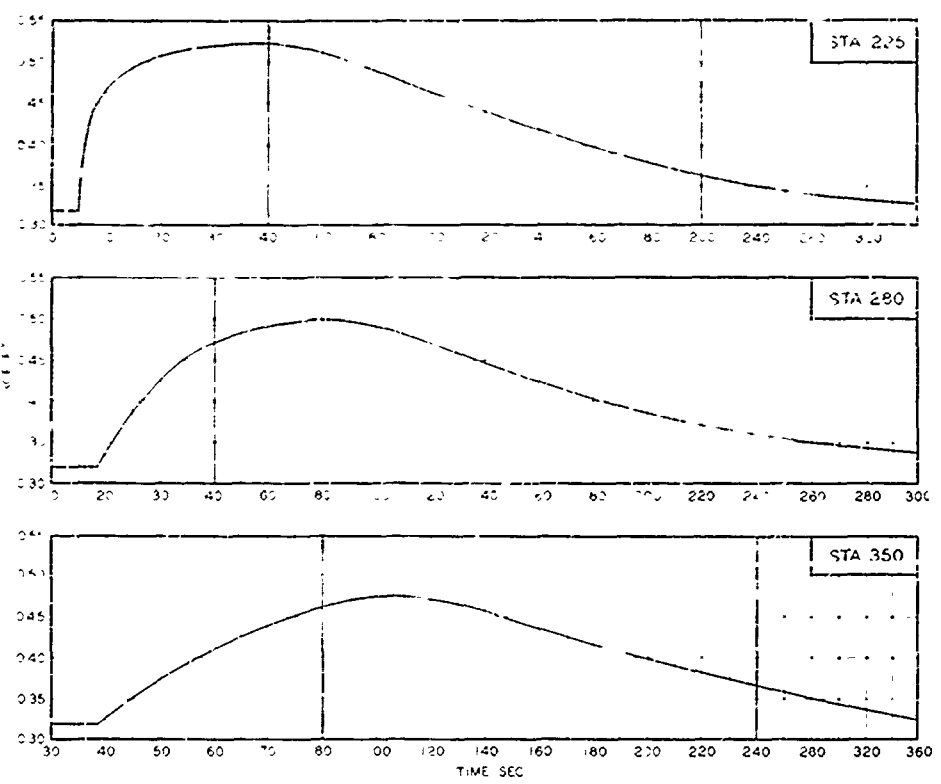
— FIRST SERIES OF TESTS  
— SECOND SERIES OF TESTS

### EFFECT OF BREACH WIDTH ON OUTFLOW DEPTH AT THE DAM

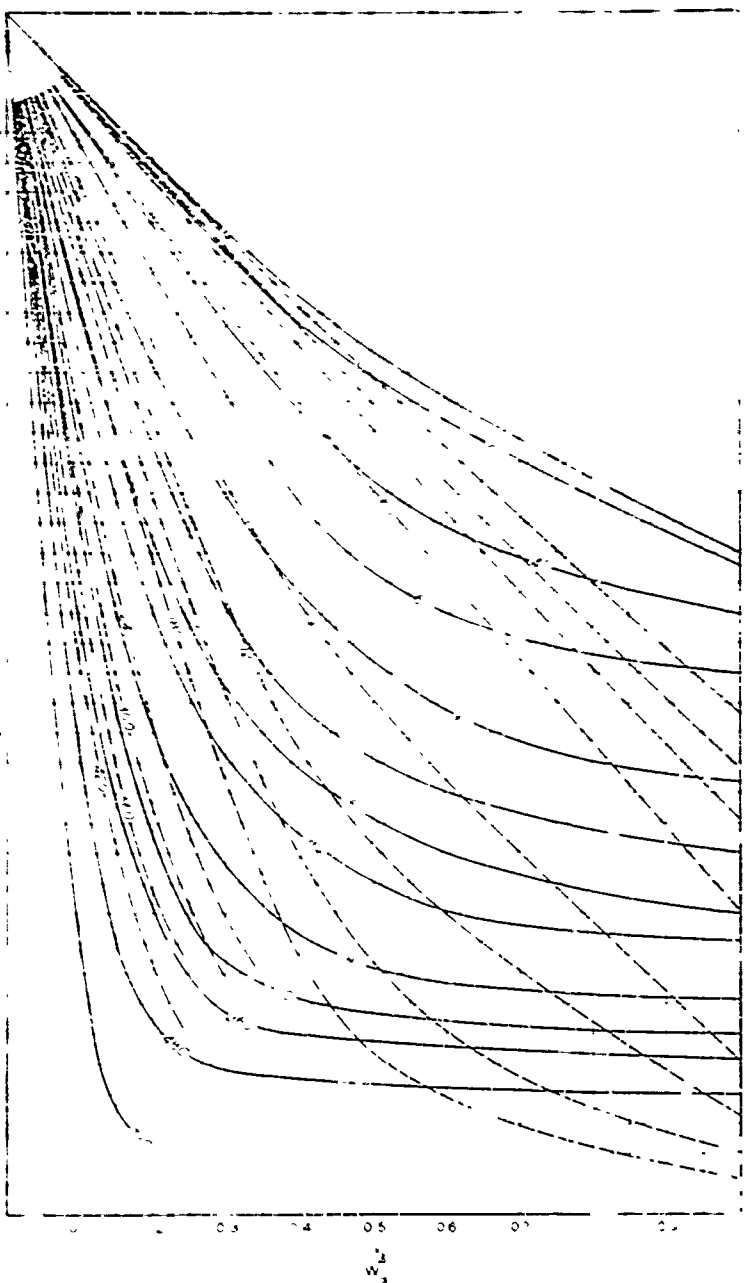
$$D_b / Y_0 = 1$$



STAGE - TIME HYDROGRAPHS  
STATIONS I94, I96, I98, I99, AND 200  
TEST CONDITION 3.2(32)



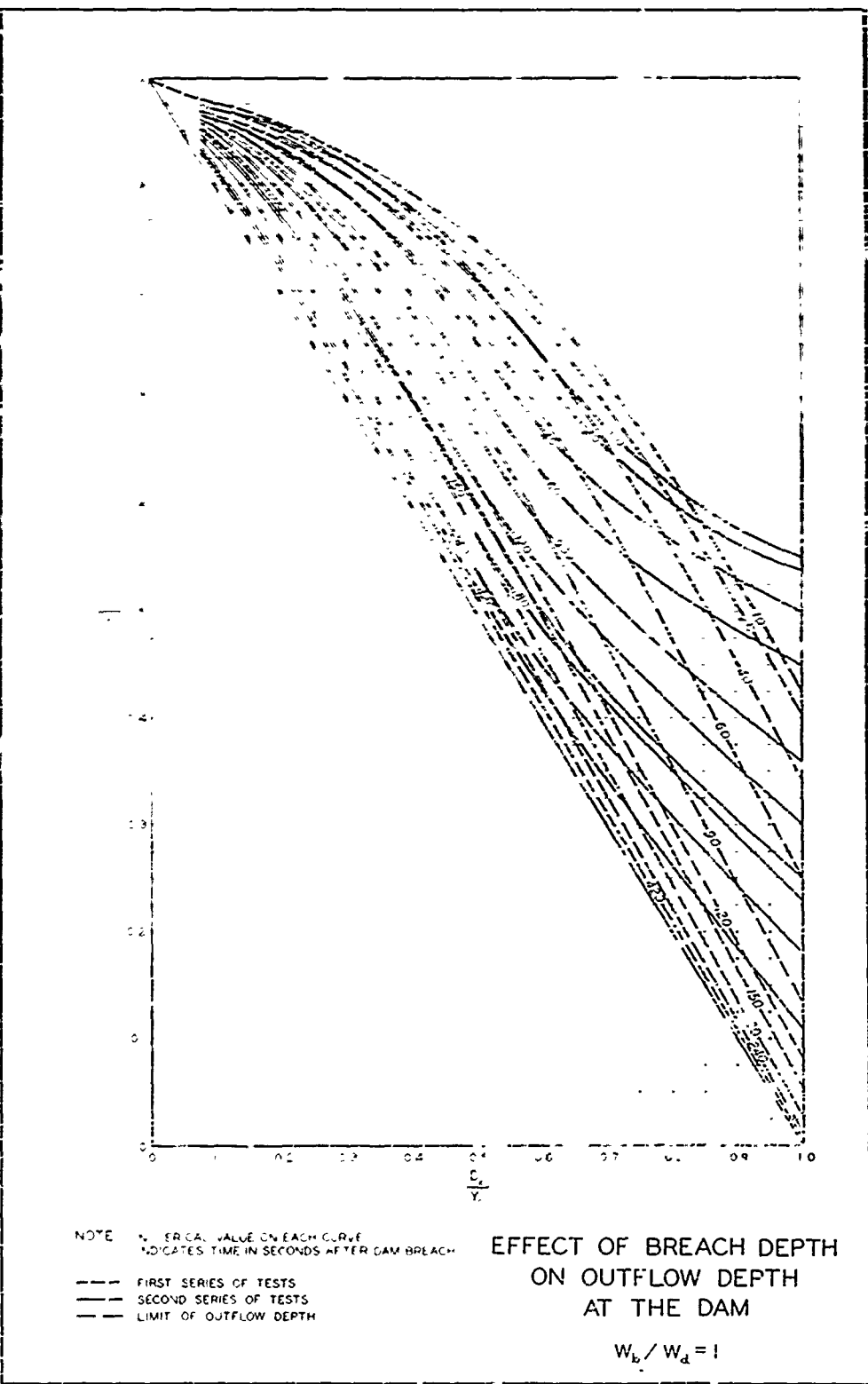
STAGE-TIME HYDROGRAPHS  
STATIONS 225, 280, AND 350  
TEST CONDITION 3.2 (32)

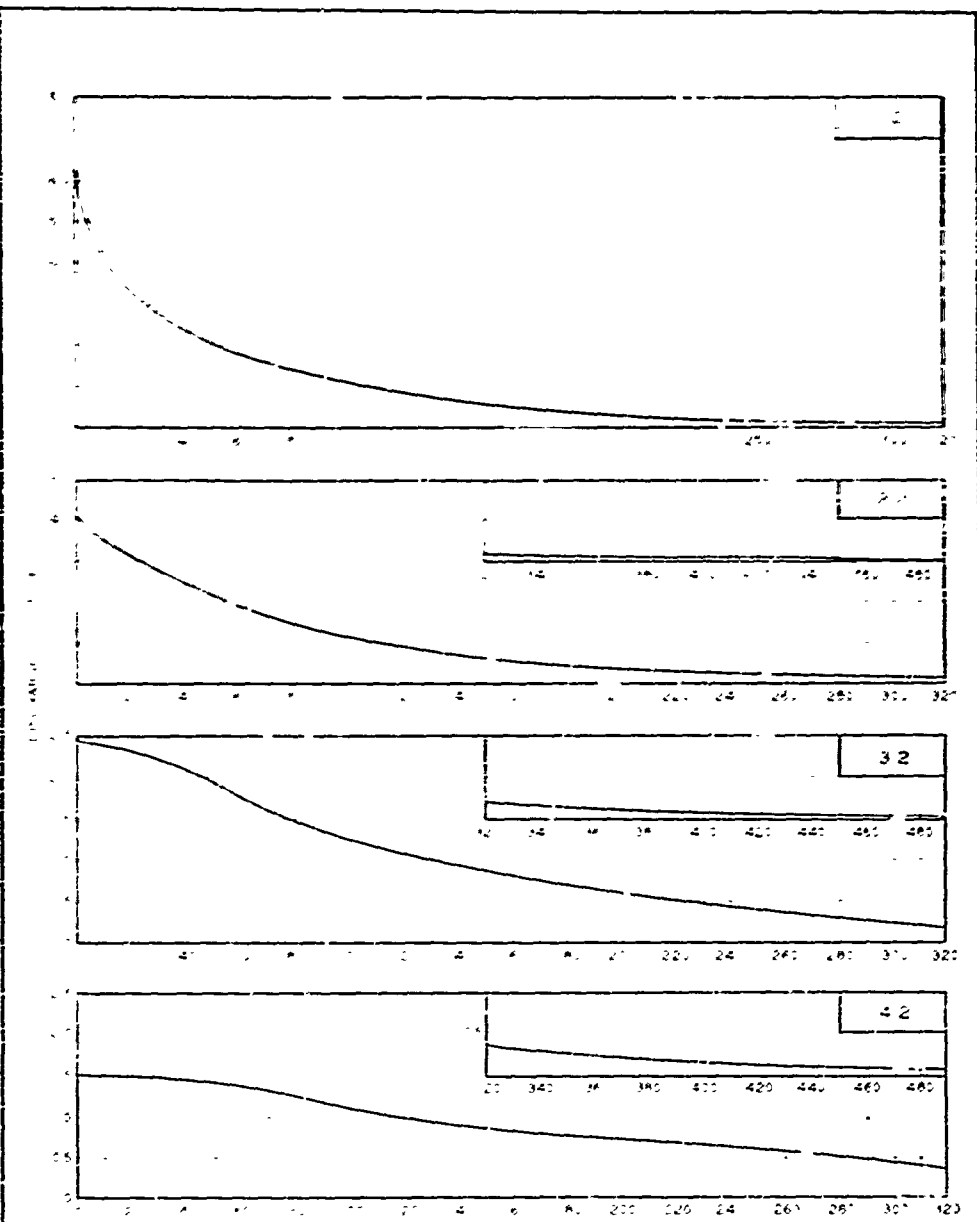


NOTE: NUMBER A IS THE BREACH RVE  
IN FEET TIME N IS THE ACTUAL BREACH  
— — — FIRST SERIES OF TESTS  
— — — SECOND SERIES OF TESTS

EFFECT OF BREACH WIDTH  
ON OUTFLOW DEPTH  
AT THE DAM

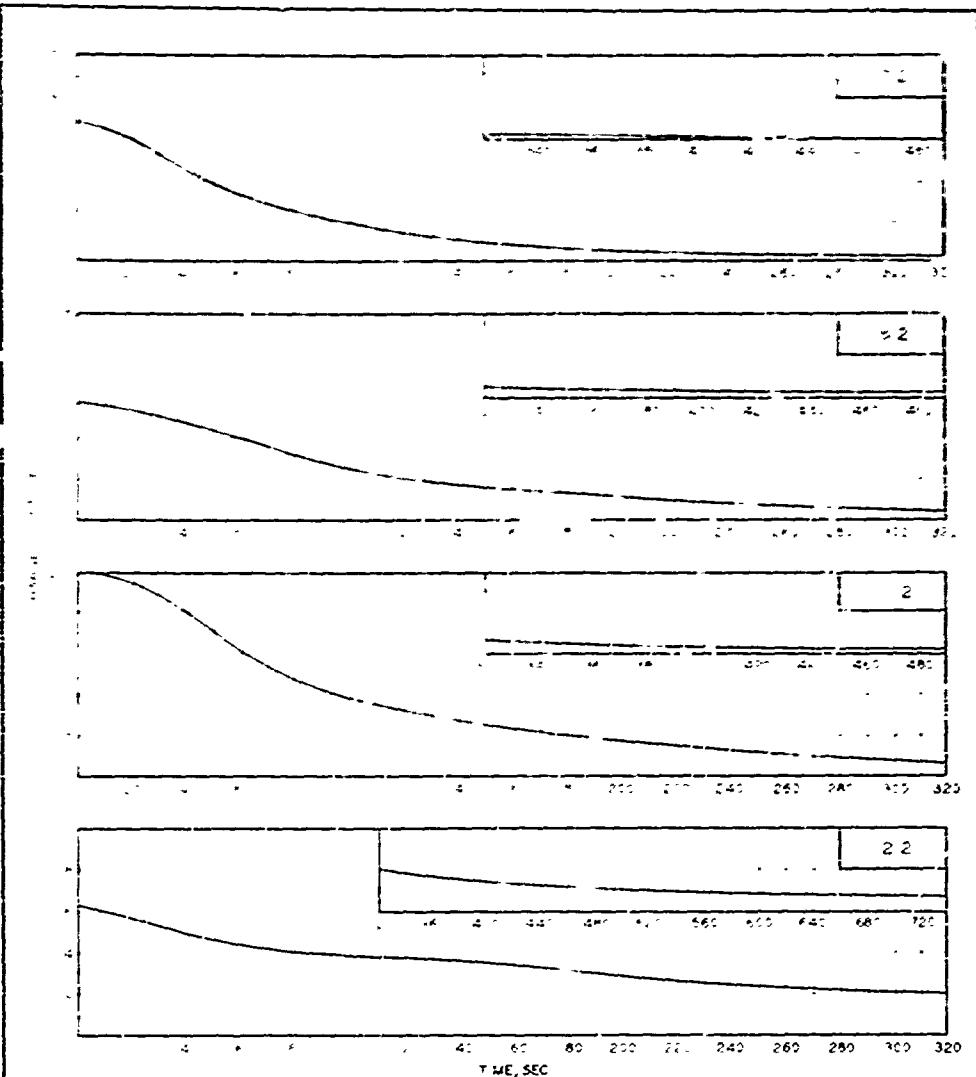
$$D_b / Y_o = I$$





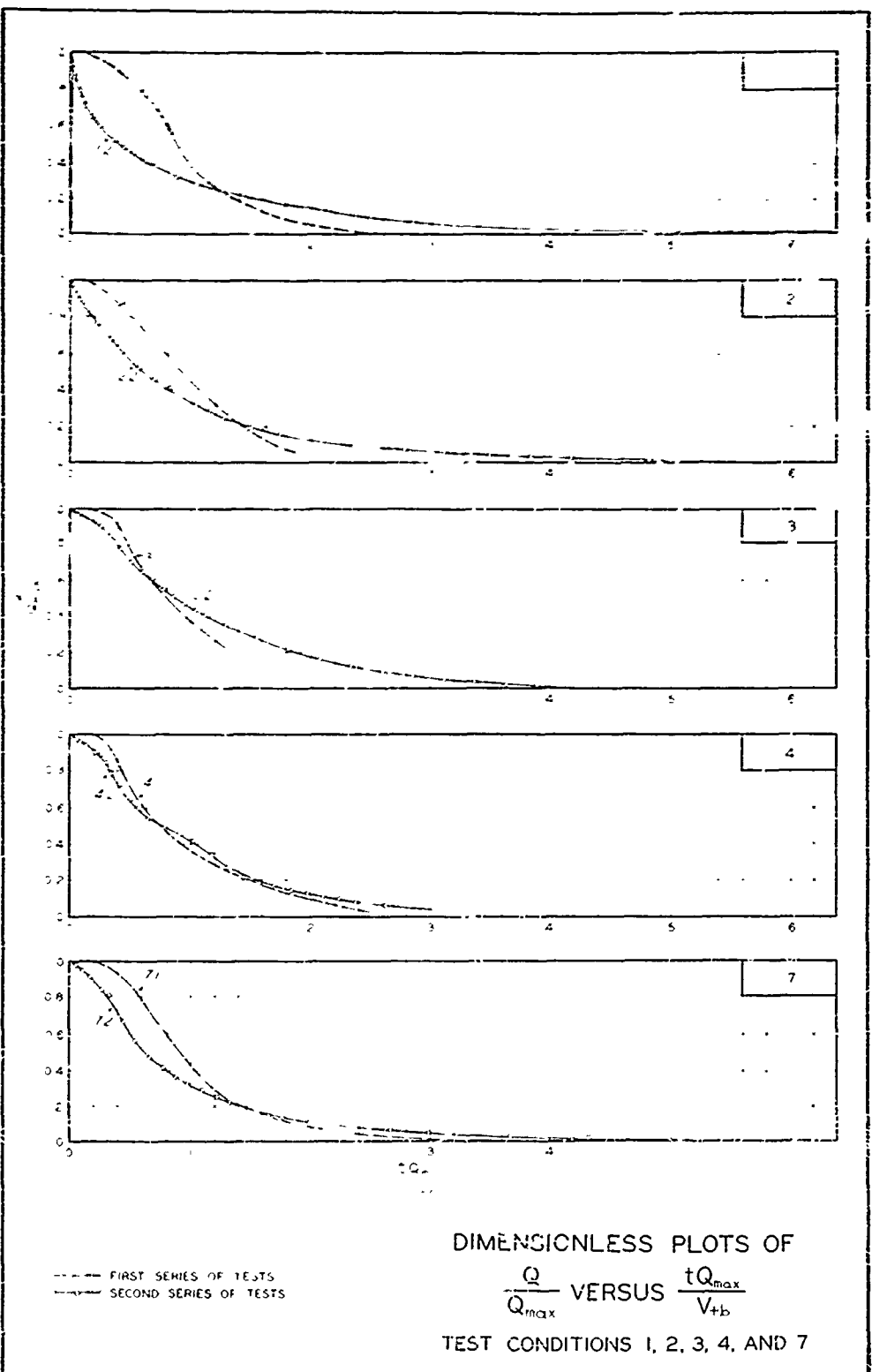
DISCHARGE-TIME HYDROGRAPH  
AT STATION 200

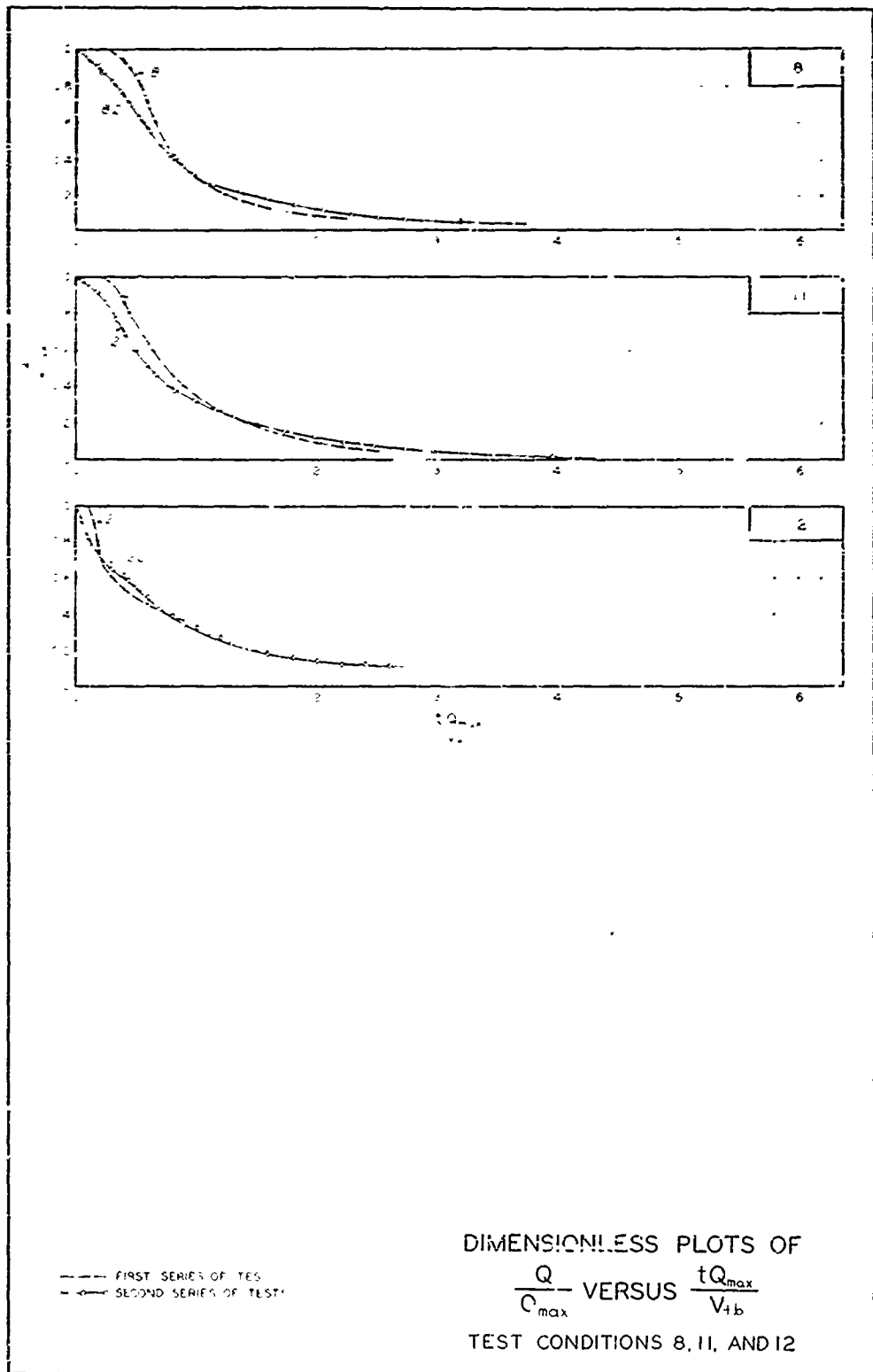
TEST CONDITIONS 12, 22, 32, AND 42

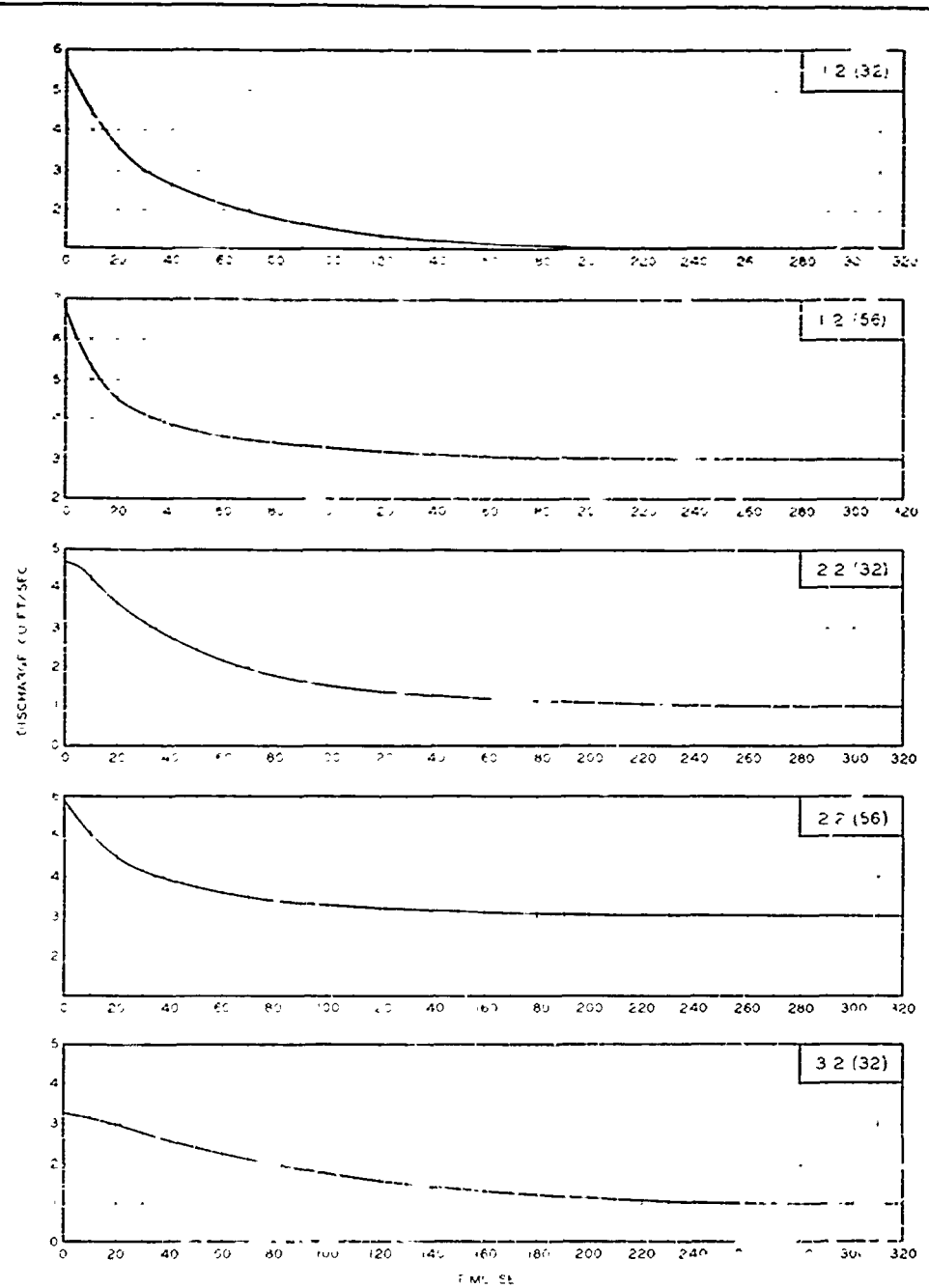


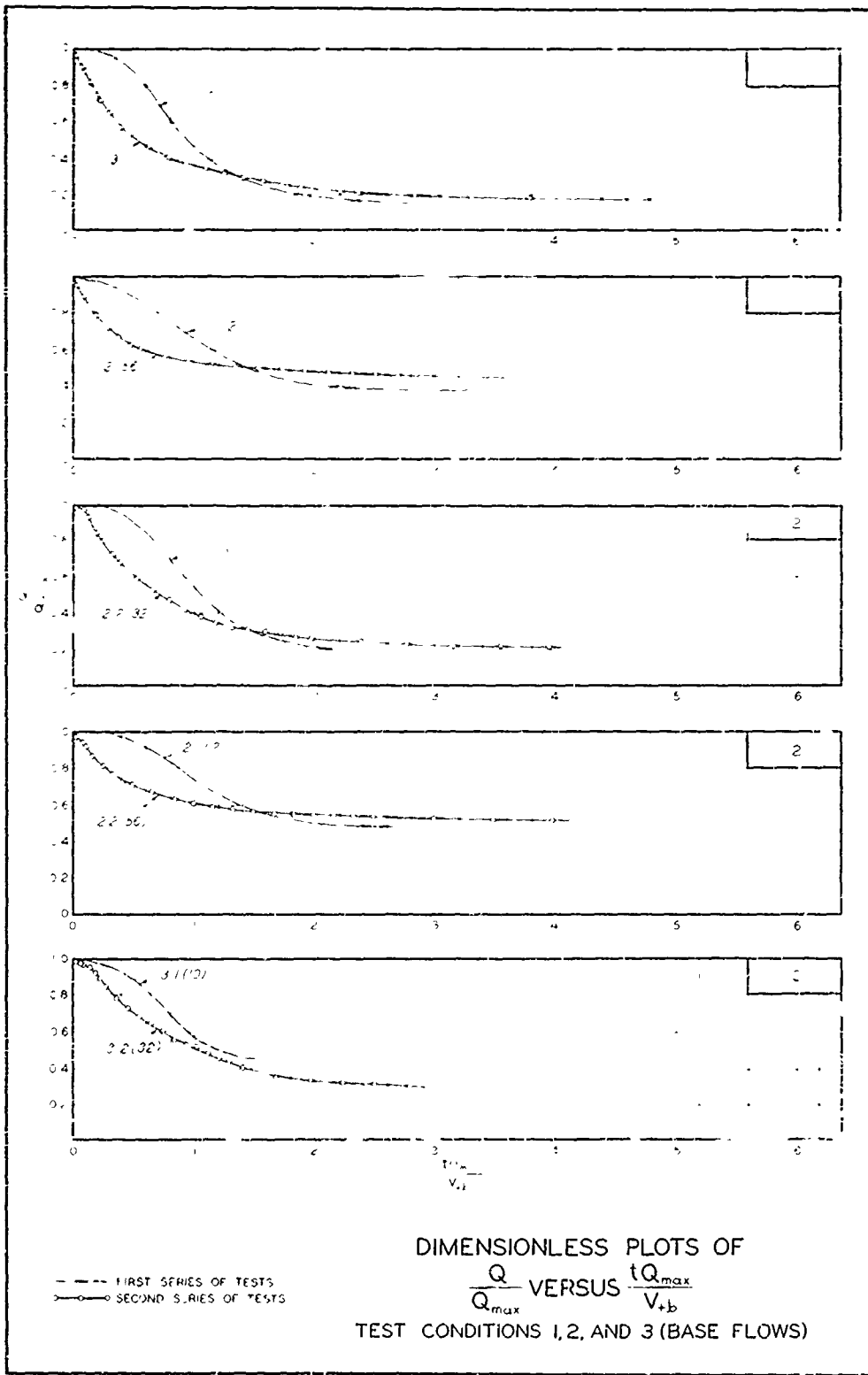
DISCHARGE-TIME HYDROGRAPH  
AT STATION 200

TEST CONDITIONS 72, 82, 112, AND 122









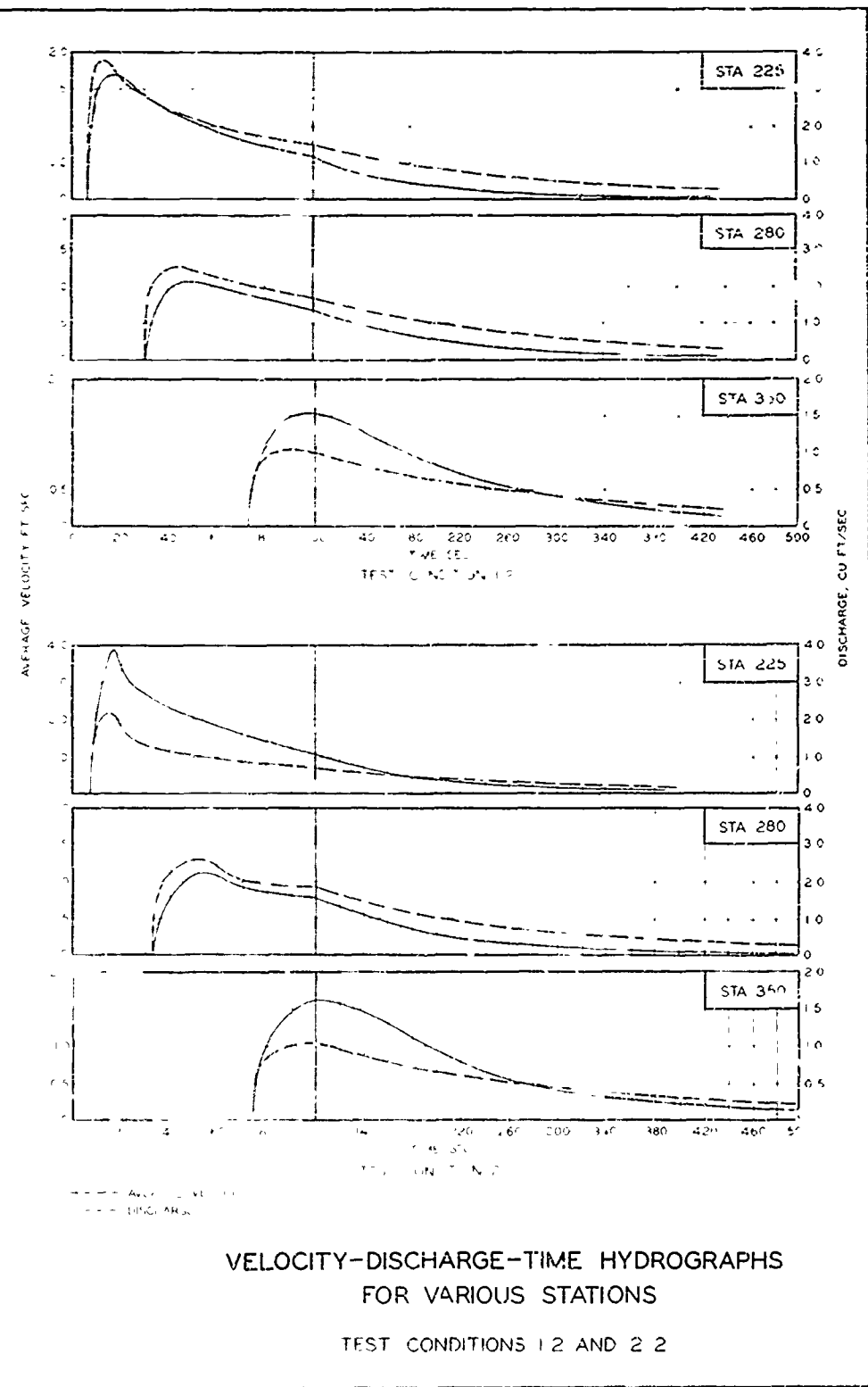


PLATE 65

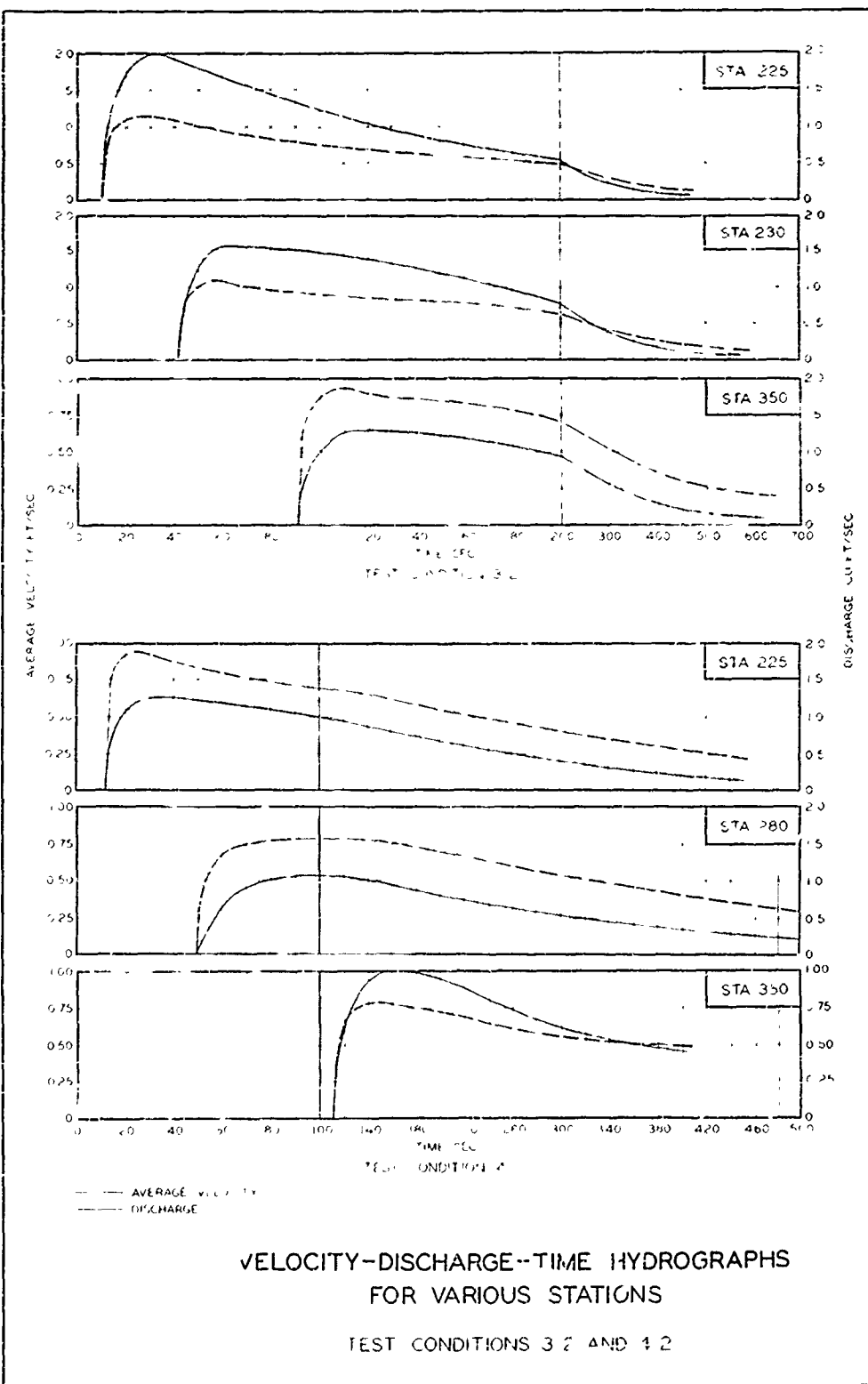
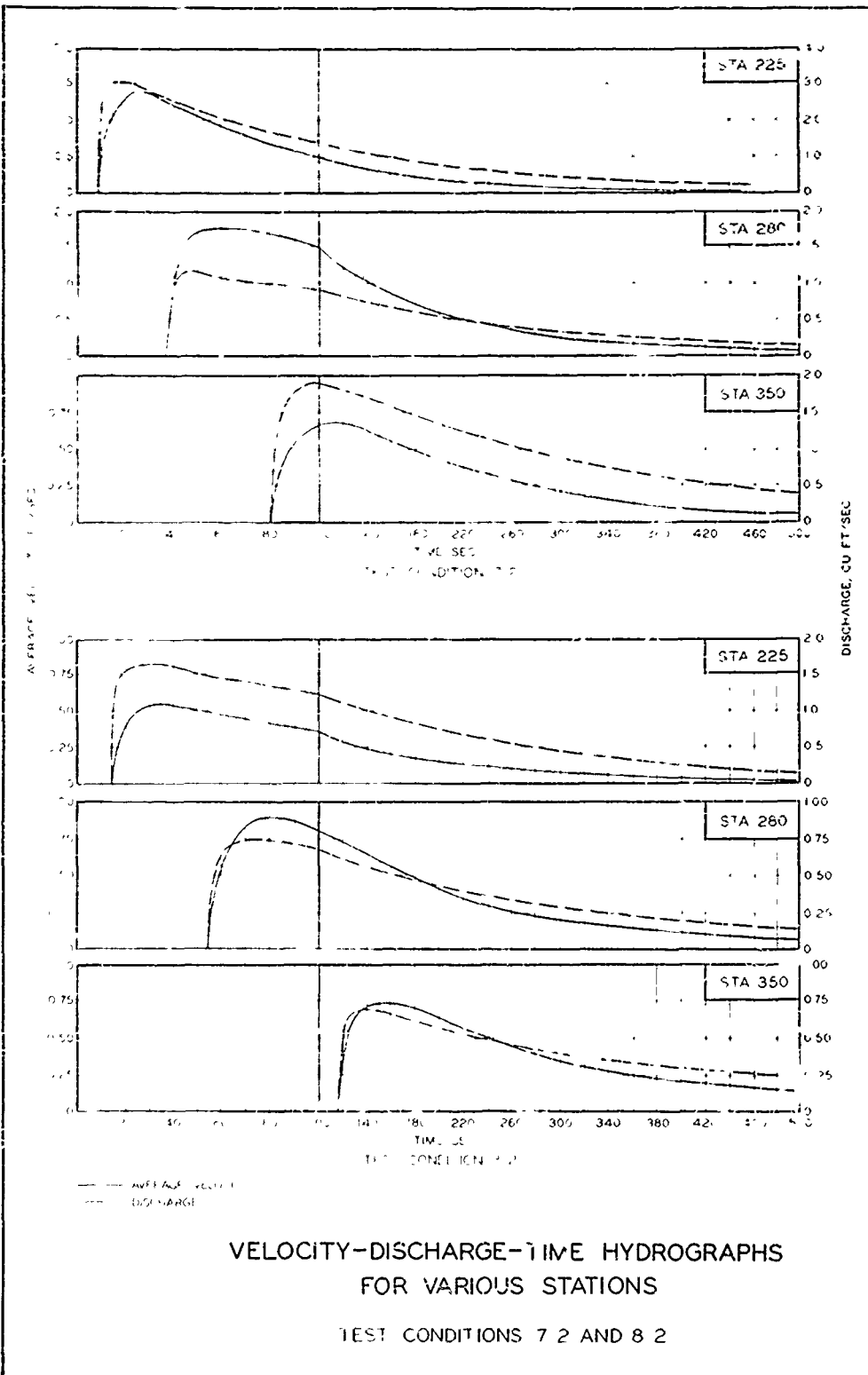
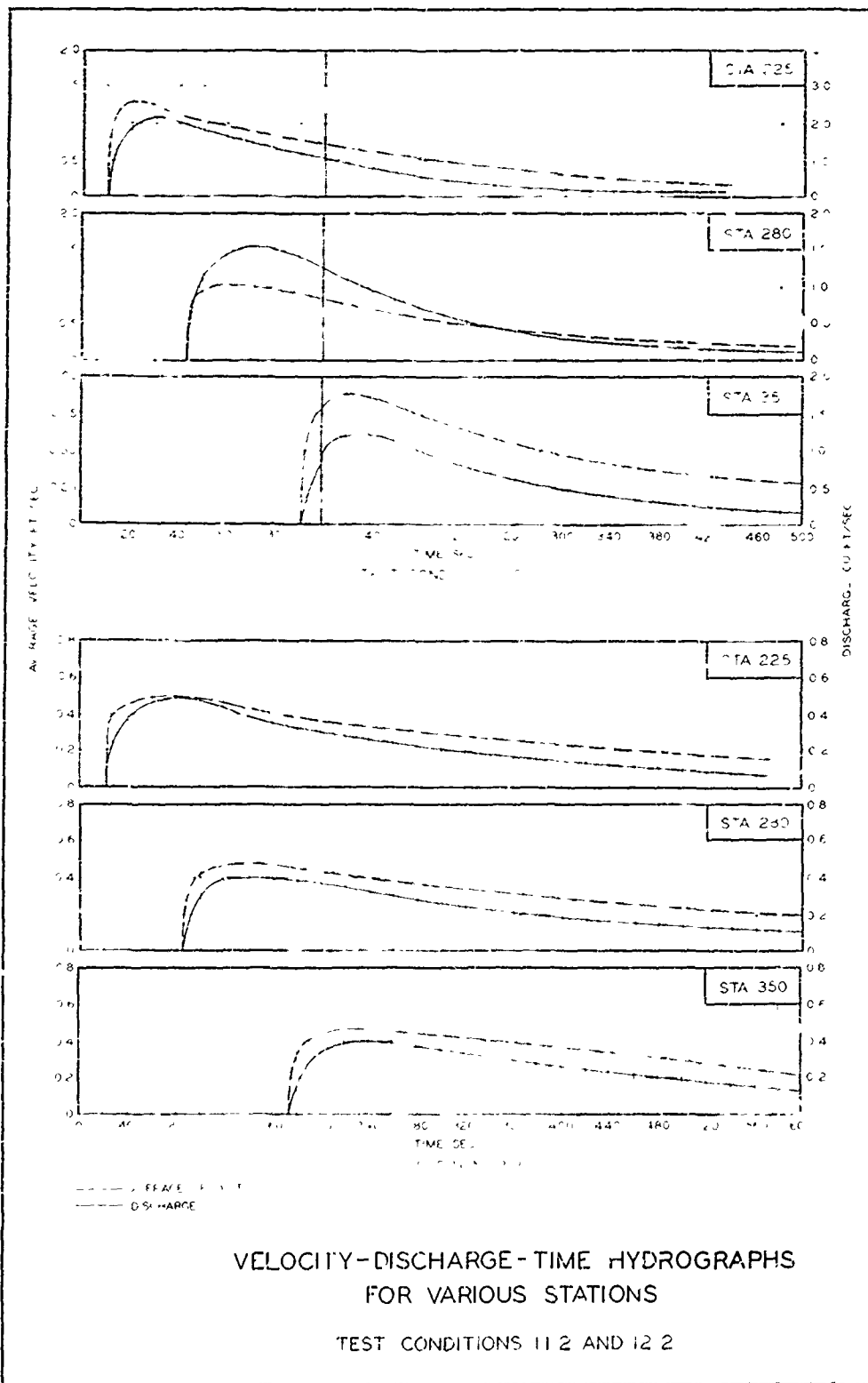
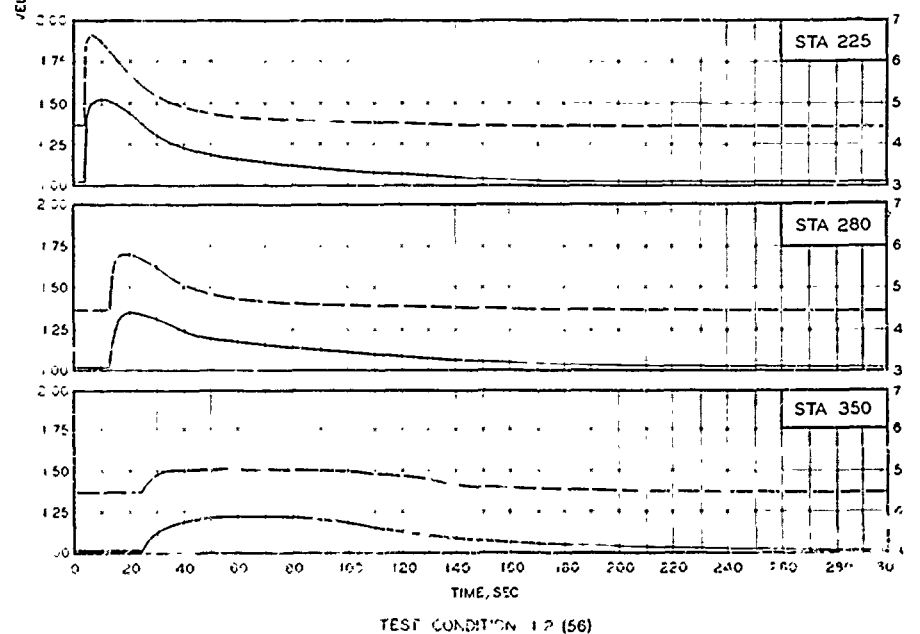
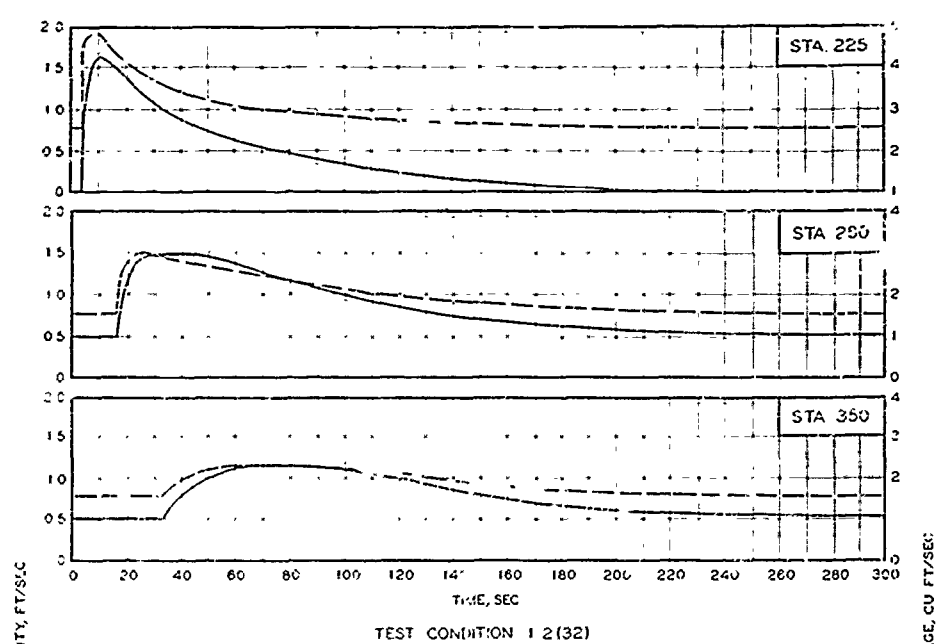


PLATE 66



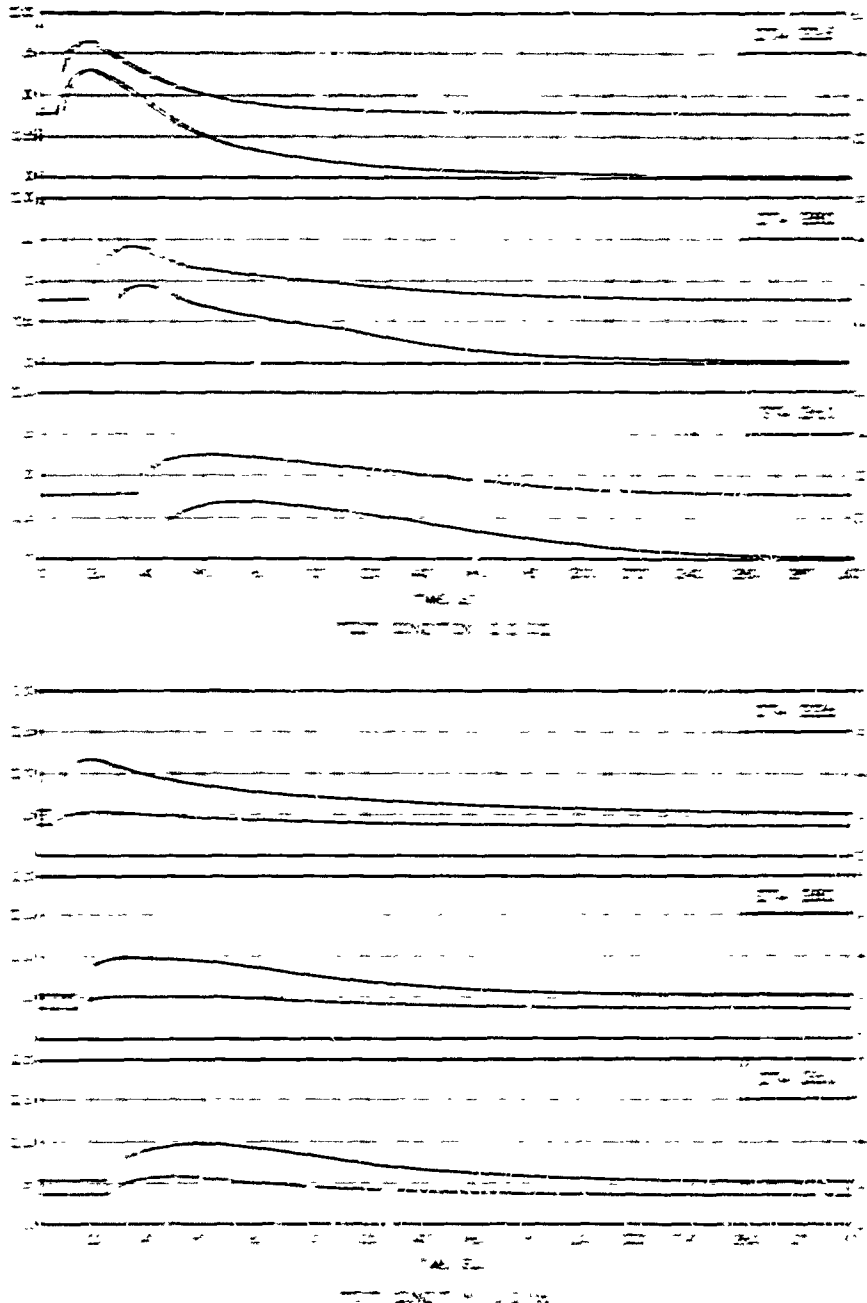




VELOCITY-DISCHARGE-TIME HYDROGRAPHS  
FOR VARIOUS STATIONS

TEST CONDITIONS 1.2(32) AND 1.2(56)

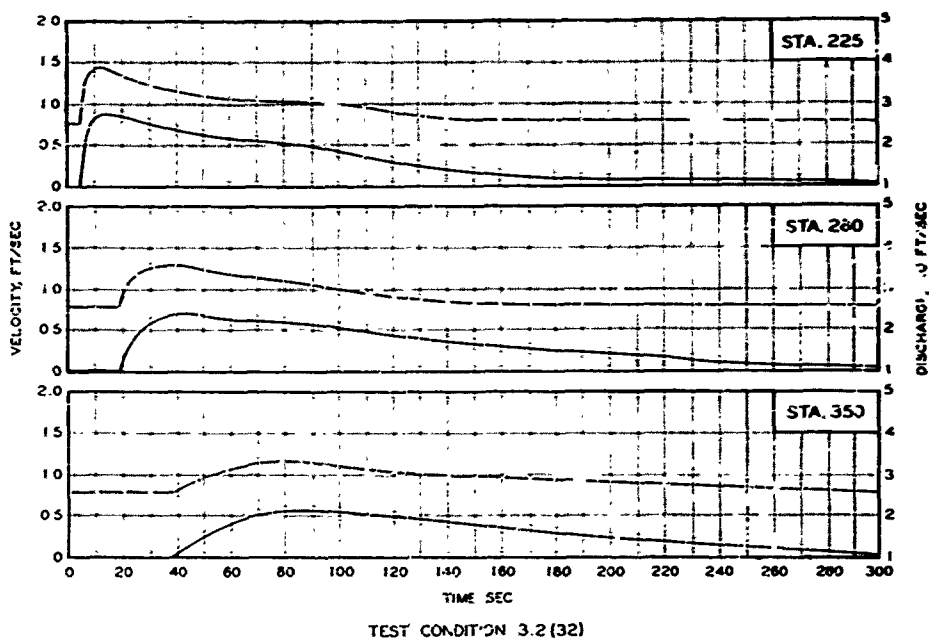
— VELOCITY  
— DISCHARGE



**SELECT-DISCHARGE-TIME - DROGUE TYPE  
FOR VARIOUS STATIONS**

FOR CONDITIONS EEE32 AND EEE50

SDT

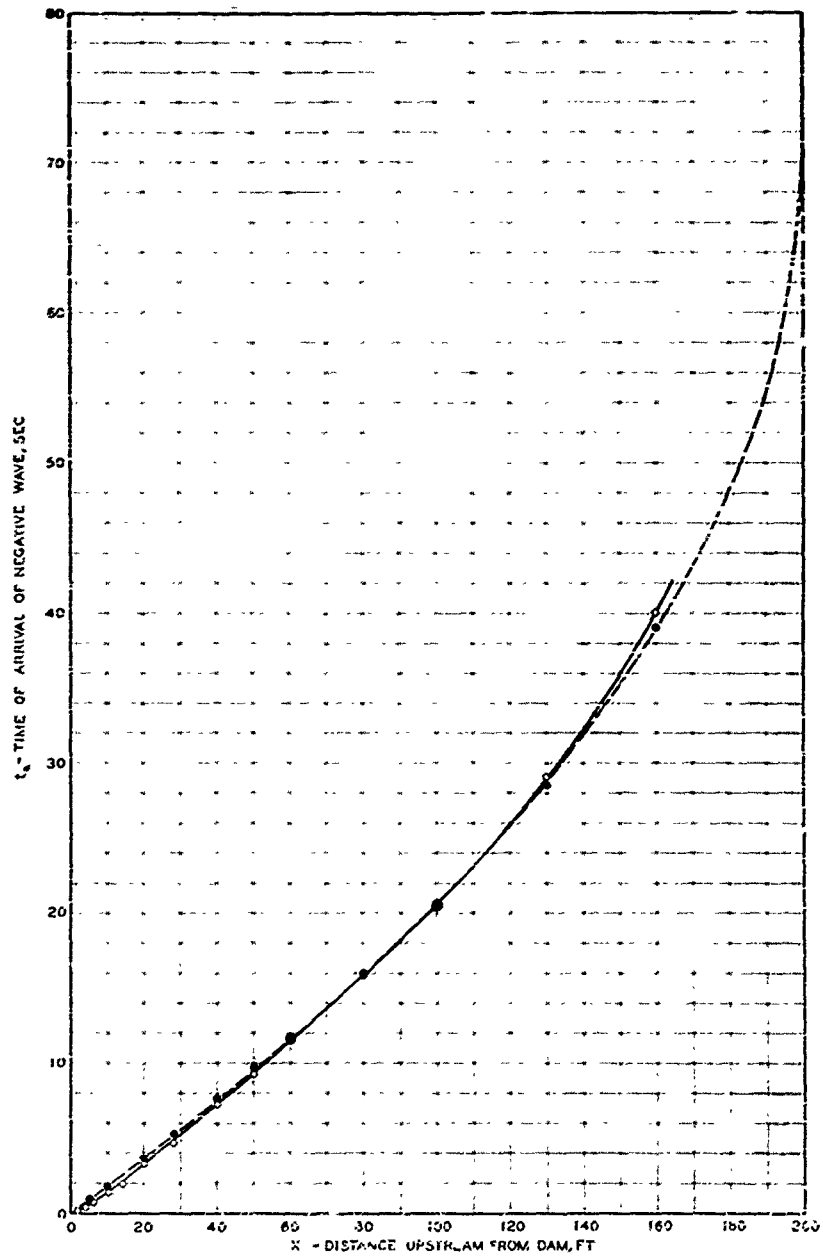


TEST CONDITION 3.2 (32)

VELOCITY-DISCHARGE-TIME HYDROGRAPHS  
FOR VARIOUS STATIONS

TEST CONDITION 3.2 (32)

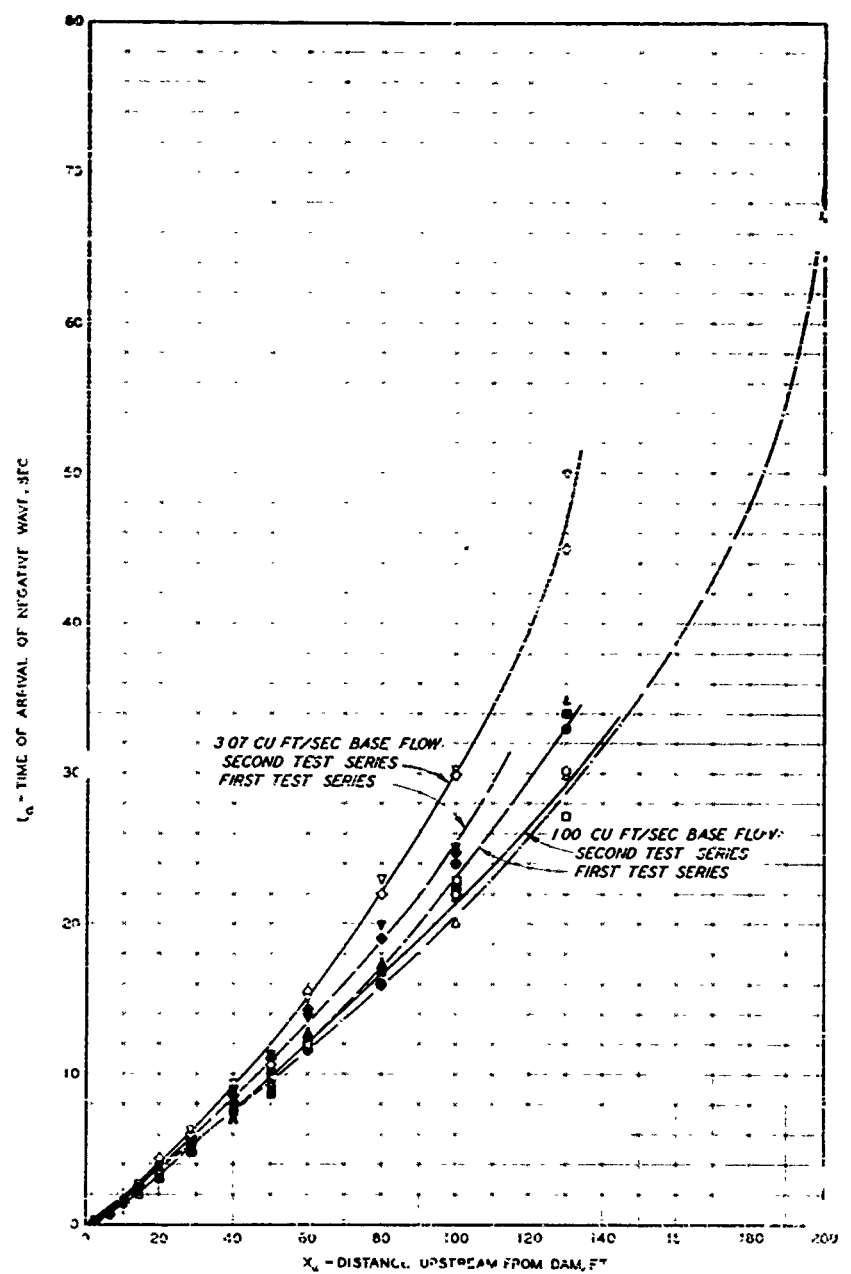
— VELOCITY  
— DISCHARGE



- FIRST SERIES OF TESTS
- SECOND SERIES OF TESTS
- THEORETICAL TIME:

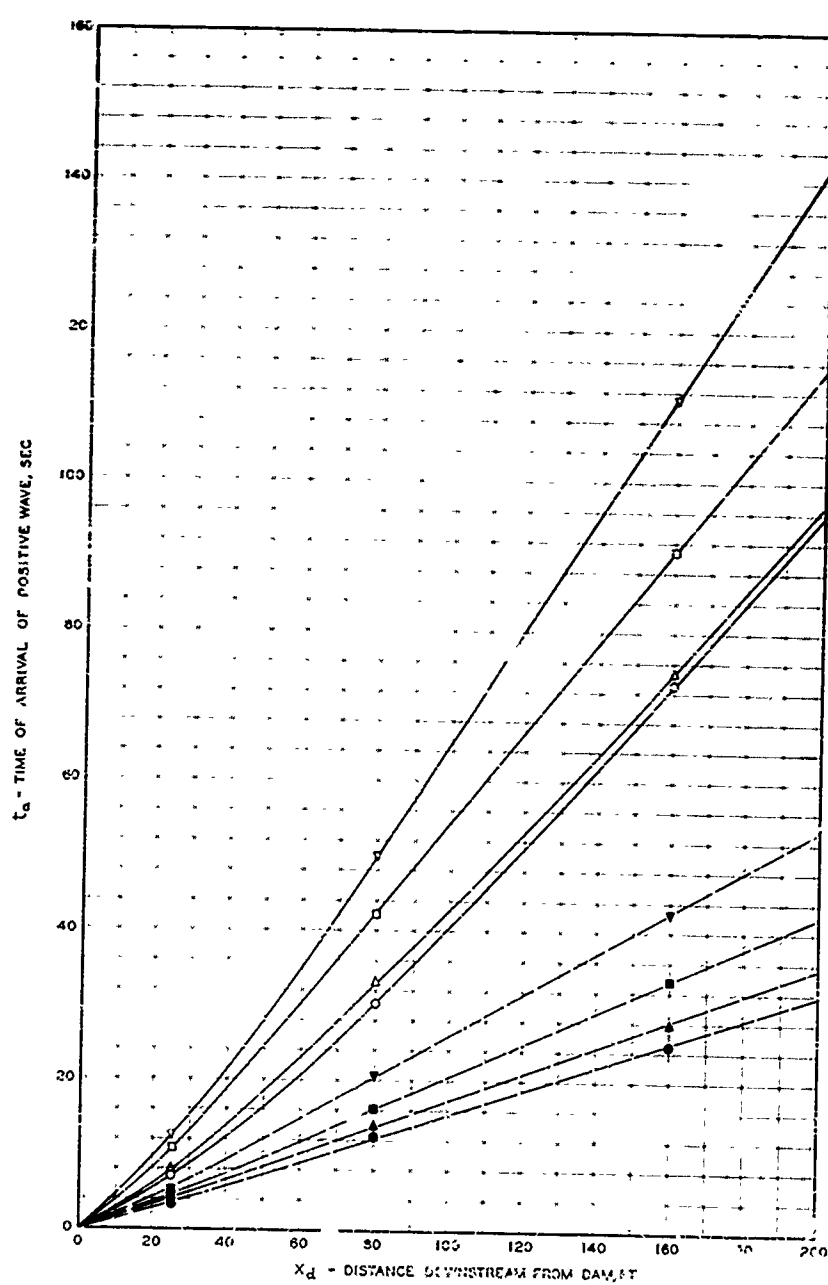
$$t_a = -70.6 \left[ (1 - 0.005 X_a)^{1/2} - 1 \right]$$

AVERAGE ARRIVAL TIME  
OF NEGATIVE WAVE  
NON-BASE-FLOW TESTS



TEST CONDITIONS	
1ST SERIES	2ND SERIES
▲ 11(10)	△ 12 (32)
▼ 11(20)	▽ 12 (56)
■ 21(10)	□ 22 (32)
◆ 21(20)	◇ 22 (56)
● 31(10)	○ 32 (32)
— THEORETICAL TIME (NON-BASE FLOW)	

ARRIVAL TIME OF NEGATIVE WAVE  
BASE-FLOW TESTS

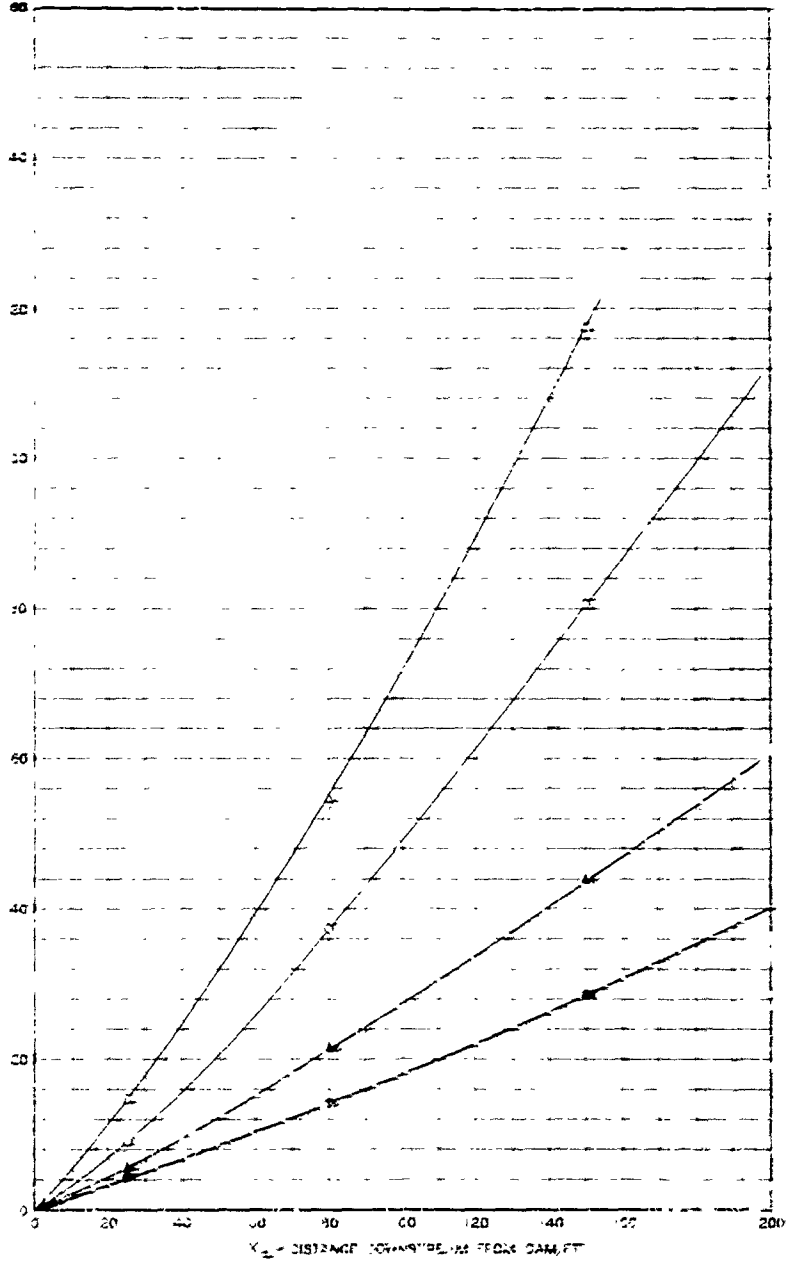


TEST CONDITIONS	
FIRST SERIES	SECOND SERIES
• 11	○ 12
▲ 21	△ 22
■ 31	□ 32
▼ 41	▽ 42

ARRIVAL TIME OF POSITIVE WAVE  
NON-BASE-FLOW TESTS

$$\frac{D_b}{Y_0} = 1$$

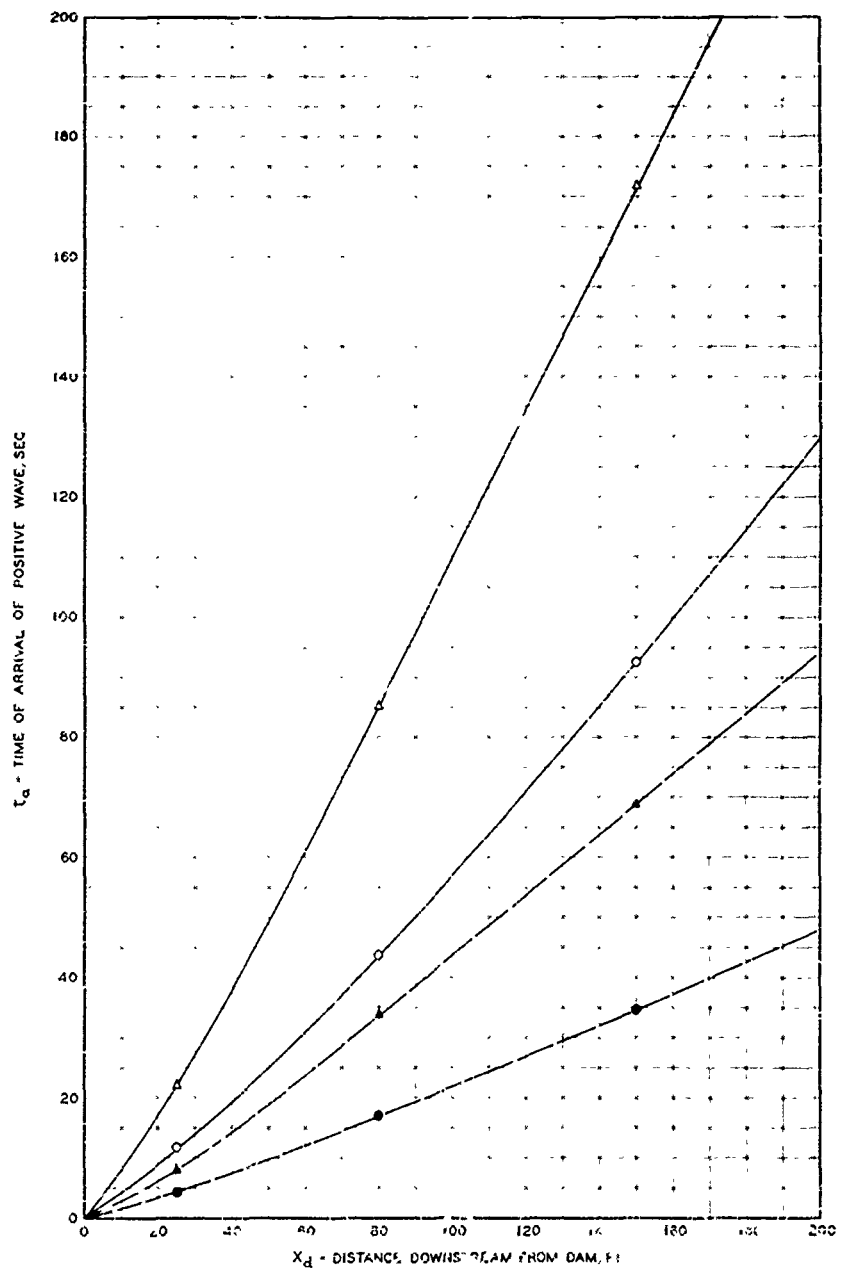
Fig. 11. Arrivals of positive wave.



TEST CONDITIONS	
FIRST SERIES	SECOND SERIES
7	12
85	32

ARRIVAL TIME OF POSITIVE WAVE  
NON-BASE FLOW TESTS

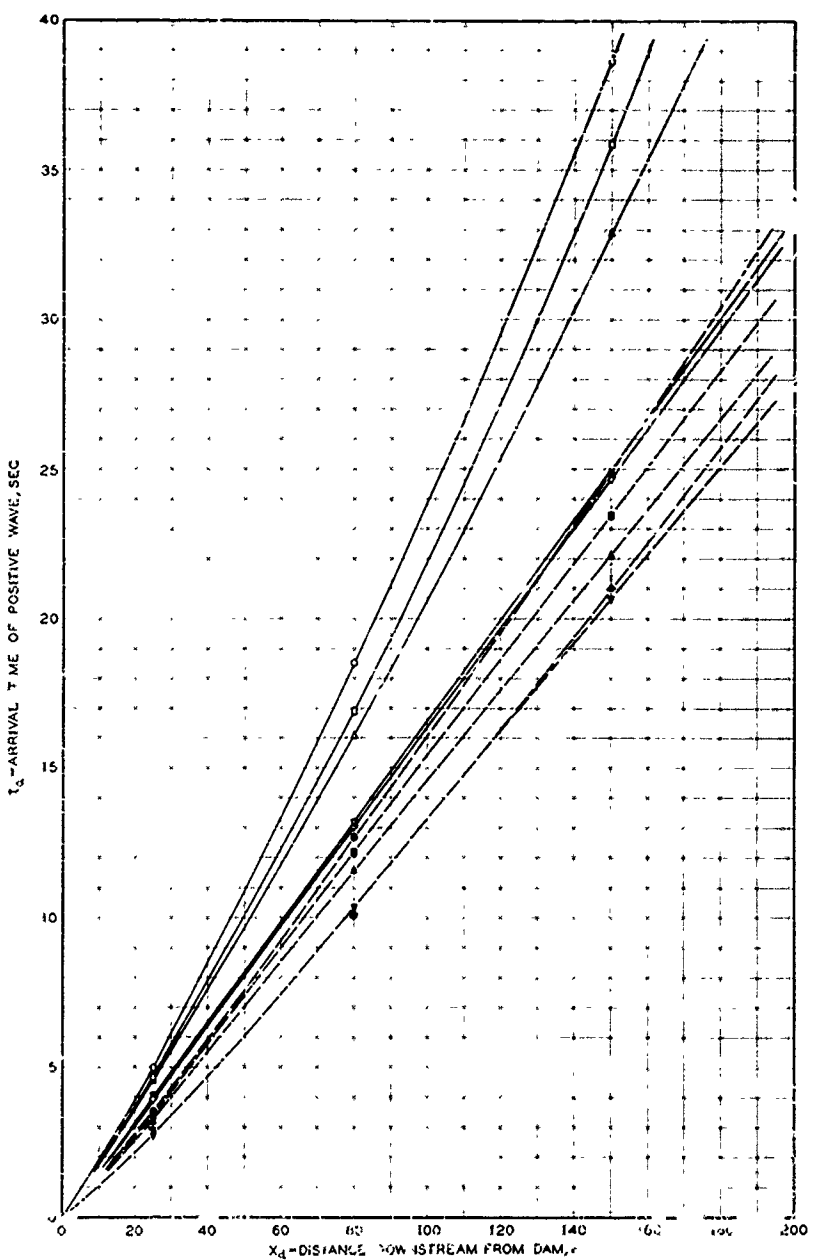
$$\frac{W_b}{W_s} = 1$$



TEST CONDITIONS  
 FIPS, SERIES      SECOND SERIES  
 ● 11.1            ○ 11.2  
 ▲ 12.1            △ 12.2

### ARRIVAL TIME OF POSITIVE WAVE NON-BASE-FLOW TESTS

$$\frac{D_b}{Y_o} = \frac{W_b}{W_d}$$



TEST CONDITIONS	
FIRST SERIES	SECOND SERIES
▲ - 11 (10)	△ - 12 (32)
▼ - 11 (20)	▽ - 12 (56)
■ - 21 (10)	□ - 22 (32)
◆ - 21 (20)	◇ - 22 (56)
● - 31 (10)	○ - 32 (32)

ARRIVAL TIME  
OF POSITIVE WAVE  
BASE-FLOW TESTS

**DISTRIBUTION LIST**

<u>Address</u>	<u>No. of Copies</u>
<u><b>Army</b></u>	
Chief of Research and Development, DA, Washington 25, D. C. ATTN: Atomics, Air Defense & Missile Division	1
Chief of Engineers, DA, Washington 25, D. C. ATTN: ENGTO-P ENGRD-S ENGMC-EB ENGTO-O ENGCW-E, Mr. Booth	1 2 1 1 1
Commanding General, U. S. Continental Army Command, Ft. Monroe, Va.	1
President, Board #4, Headquarters, U. S. Continental Army Command, Ft. Bliss, Tex.	1
Commandant, Command & General Staff College, Ft. Leavenworth, Kans. ATTN: ALLS (AS)	1
Secretary, The U. S. Army Air Defense School, Fort Bliss, Tex. ATTN: Major George L. Alexander, Dept. of Tactics and Combined Arms	1
Director, Special Weapons Development Office, Headquarters, U. S. Continental Army Command, Ft. Bliss, Tex.	1
Commanding General, Research & Engineering Command, Army Chemical Center, Md.      ATTN: Deputy for RW & Non-Toxic Material	1
Commanding General, Aberdeen Proving Ground, Aberdeen, Md. ATTN: Director, Ballistics Research Lab	1
Commanding General, The Engineer Center, Ft. Belvoir, Va. ATTN: Asst Commandant, Eng School	2
Commanding Officer, Engineer Research and Development Laboratory, Ft. Belvoir, Va.      ATTN: Chief, Technical Support Branch Technical Library	1 1
Commanding Officer, Picatinny Arsenal, Dover, N. J. ATTN: ORDBB-TK	1
Commanding Officer, Chemical and Radiological Lab., Army Chemical Center, Md.      ATTN: Tech Library	1
Commanding Officer, Transportation R&D Command, Ft. Eustis, Va. ATTN: Special Projects Division	1
Director, Technical Documents Center, Evans Signal Lab., Belmar, N. J.	1
Board of Engineers for Rivers & Harbors, Tempo C Building, 2nd & Q Sts, SW, Washington 25, D. C.      ATTN: Mr. R. L. Irwin	1

Address	No. of Copies
<u>Army (Continued)</u>	
Director, Operations Research Office, Johns Hopkins University, 7100 Connecticut Avenue, Chevy Chase, Md., Washington 15, D. C.	1
Chief of Ordnance, DA, Washington 25, D. C. ATTN: ORDTX-AR	1
Army Map Service, 6500 Brooks Lane, Washington 25, D. C. ATTN: Mr. Fred B. Barkalow	1
Division Engineer, U. S. Army Engineer Division, North Pacific, 210 Custom House, Portland 9, Oreg. ATTN: Mr. Oliver Johnson	1
<u>Navy</u>	
Chief of Naval Operations, DN, Washington 25, D. C. ATTN: OP-36	2
Chief of Naval Operations, DN, Washington 25, D. C. ATTN: OP-03EG	1
Director of Naval Intelligence, DN, Washington 25, D. C. ATTN: OF-922V	1
Chief, Bureau of Ordnance, DN, Washington 25, D. C.	1
Chief, Bureau of Aeronautics, DN, Washington 25, D. C.	1
Chief, Bureau of Ships, DN, Washington 25, D. C. ATTN: Code 348	1
Code 423	1
Chief, Bureau of Yards and Docks, DN, Washington 25, D. C. ATTN: D-400	1
D-440	1
Chief of Naval Research, DN, Washington 25, D. C. ATTN: Code 811	1
Commander-in-Chief, U. S. Pacific Fleet, FPO, San Francisco, Calif.	1
Commander-in-Chief, U. S. Atlantic Fleet, U. S. Naval Base, Norfolk 11, Va.	1
Commandant of the Marine Corps, DN, Washington 25, D. C. ATTN: Code AO3H	4
President, U. S. Naval War College, Newport, R. I.	1
Superintendent, U. S. Naval Postgraduate School, Monterey, Calif.	1
Commanding Officer, U. S. Naval Schools Command, U. S. Naval Station, Treasure Island, San Francisco, Calif.	1
Commanding Officer, U. S. Fleet Training Center, Naval Base, Norfolk 11, Va. ATTN: Special Weapons School	1
Commanding Officer, U. S. Fleet Training Center, Naval Station, San Diego, Calif. ATTN: SPWP School	2

~~DoD~~  
DoD

4000000000000000

Navy (Continued)

Commanding Officer, U. S. Naval Damage Control Training Center,  
Naval Base, Philadelphia, Pa. ~~AMMUN~~ CMC Defense Course

Commanding Officer, U. S. Naval Ordnance Technical Center  
Army Chemical Training Center, Ft. Monmouth, N.J.

Commander, U. S. Naval Ordnance Laboratory, White Oak,  
Silver Spring, Md. ~~AMMUN~~ CMC

RE

E

Commanding Officer, Air Development Squadron Five, NAS China Lake,  
Calif.

Commanding Officer and Director, U. S. Naval Civil Engineering  
Laboratory, Fort Belvoir, Va. ~~AMMUN~~ Code 732

Director, U. S. Naval Research Laboratory, Washington 25, D. C.

Commanding Officer and Director, U. S. Navy Electronics Lab.,  
San Diego 35, Calif. ~~AMMUN~~ Code 4221

Commanding Officer, U. S. Naval Research and Defense Laboratory,  
San Francisco, Calif. ~~AMMUN~~ Navy Civil Division

Commanding Officer & Director, David W. Taylor Model Basin,  
Washington 4, D. C. ~~AMMUN~~ Library

Commander, Norfolk Naval Supply, Portsmouth, Va.  
~~AMMUN~~ Code 271

Commander-in-Chief Pacific, Pearl Harbor, HI. E.

Air Force

Director of Plans, Headquarters, USAF, Washington 25, D. C.  
~~AMMUN~~ Air Plans Division

Director of Research & Development, Headquarters, USAF,  
Washington 25, D. C. ~~AMMUN~~ Science Components Division

Director of Requirements, Headquarters, USAF, Westover A. F. B., Mass.  
~~AMMUN~~ AFPR-34/N

Director of Personnel, Headquarters, USAF, Washington 25, D. C.  
~~AMMUN~~ AFPR-13

Commander-in-Chief, Strategic Air Command, Offutt AFB, Neb.  
~~AMMUN~~ Spec. of Vice Admiral, Inspector Civil, Inspection General

Commander, Technical Air Command, Langley AFB, Va.  
~~AMMUN~~ Document Security Br.

<u>Address</u>	<u>No. of Copies</u>
<u>Air Force (Continued)</u>	
Commander, Air Material Command, Wright-Patterson AFB, Ohio	2
Commander, Air Research and Development Command, Andrews AFB, Washington 25, D. C. ATTN: RDDN	1
Director, Air University Library, Maxwell AFB, Ala.	2
Commander, Wright Air Development Center, Wright-Patterson AFB, Ohio ATTN: WCOSI	1
Commander, AF Cambridge Research Center, L. G. Hanscom Field, Bedford, Mass. ATTN: CRQST-2	1
Commander, AF Special Weapons Center, Kirtland AFB, N. Mex. ATTN: Library	1
Commandant, USAF Institute of Technology, Wright-Patterson AFB, Ohio ATTN: Resident College	1
Commander, Western Development Division, P. O. Box 262, Inglewood, Calif.	1
The RAND Corporation, 1700 Main Street, Santa Monica, Calif. (For Nuclear Energy Division)	1
Assistant Chief of Staff, Civil Engineering, Headquarters, USAF, Washington 25, D. C. ATTN: AFOCE-E	1
Civil Engineering Center, Headquarters, AFIT, Wright-Patterson AFB, Ohio	1
<u>Other DOD Agencies</u>	
Assistant Secretary of Defense (Research and Development), Washington 25, D. C. ATTN: Tech Library	1
U. S. Documents Officer, Office of the United States National Military Representative, SHAPE, AFO 55, New York, N. Y.	1
Director, Weapons Systems Evaluation Group, OSD, Washington 25, D. C.	1
Commandant, Armed Forces Staff College, Norfolk 11, Va. ATTN: Secretary	1
Commander, Field Command, DASA, P. O. Box 5100, Albuquerque, N. Mex.	1
Commander, Field Command, DASA, P. O. Box 5100, Albuquerque, N. Mex. ATTN: Training Division	2
Chief, Defense Atomic Support Agency, Washington 25, D. C.	15
ASTIA, Document Service Center, Arlington Hall Station, Arlington 12, Va. ATTN: TIPDR	10

<u>Address</u>	<u>No. of Copies</u>
<u>Others</u>	
Los Alamos Scientific Laboratory, I. C. Box 1663, Los Alamos, N. Mex. ATTN: Report Librarian (For Dr. Alvin C. Graves, J-Division)	1
National Advisory Committee for Aeronautics, 1512 H Street, NW, Washington 25, D. C. ATTN: Mr. Eugene B. Jackson, Chief, Div of Research Information	1
Assistant Director of Research, Langley Aeronautical Lab., National Advisory Committee for Aeronautics, Langley Field, Va. ATTN: Mr. John Stack	1
Chief, Classified Technical Library, Technical Information Service, U. S. Atomic Energy Commission, 1901 Constitution Avenue, NW Washington 25, D. C. ATTN: Mrs. Jean O'Leary (For Dr. Paul C. Fine)	1
Chief, Classified Technical Library, Technical Information Service, U. S. Atomic Energy Commission, 1901 Constitution Avenue, NW, Washington 25, D. C. ATTN: Mrs. Jean M. O'Leary	1
Forestal Research Center Library, Aeronautical Sciences Building, Princeton University, Princeton, N. J. ATTN: Maurice H. Smith, Librarian (For Dr. Walker Bleakney)	1
Manager, Albuquerque Operations Office, U. S. Atomic Energy Commission, P. O. Box 5400, Albuquerque, N. Mex.	1
Forest Service, U. S. Department of Agriculture, Washington 25, D. C. ATTN: Mr. A. A. Brown, Chief, Division of Forest Fire Research	1
Rensselaer Polytechnic Institute, Mason House, Troy, N. Y. ATTN: Security Officer (For Dr. Clayton Oliver Dohrenwend)	1
Massachusetts Institute of Technology, Director, Division of Defense Laboratories, Lincoln Laboratory, Cambridge 19, Mass. (For Dr. Robert J. Hansen)	1
The University of Michigan, University Research Office, Lobby 1, East Engineering Building, Ann Arbor, Mich. (For Dr. B. Johnson)	1
Sandia Corporation, Sandia Base, Albuquerque, N. Mex. ATTN: Classified Document Division (For Dr. Walter A. MacNair)	1
Superintendent, Eastern Experiment Station, U. S. Bureau of Mines, College Park, Md. ATTN: Dr. Leonard Gurt	1
The University of Illinois, Civil Engineering, Room 207 Talbot Lab, Urbana, Ill. (For Dr. N. M. Newmark)	1

<u>Address</u>	<u>No. of Copies</u>
<u>Others (Continued)</u>	
Massachusetts Institute of Technology, Dept. of Civil and Sanitary Engineering, Cambridge 39, Mass.	
ATTN: Dr. C. H. Norris	1
Dr. R. V. Whitman	1
Dr. J. B. Wilbur	1
Amherst College, Dept. of Physics, Amherst, Mass.	1
ATTN: Dr. A. B. Arons	
Stanford Research Institute, Menlo Park, Calif.	1
ATTN: Dr. R. B. Vaile	